eman ta zabal zazu

Universidad del País Vasco
Euskal Herriko Unibertsitatea

REGULATION OF MACROPHAGE AND PREADIPOCYTE PROLIFERATION AND MIGRATION BY C1P

DOCTORAL THESIS

Asier Domínguez Herrera

February 2022

Acknowledgements

This Doctoral Thesis was carried out in the Department of Biochemistry and Molecular Biology of the University of the Basque Country under the supervision of Dr. Antonio Gómez Muñoz and Dr. Arkaitz Carracedo Pérez, and it was supported by the predoctoral fellowship "Programa Predoctoral, de formación de Personal Investigador No Doctor" awarded by the Basque Government.

En primer lugar quisiera agradecer a Anton por haberme dado la oportunidad de formar parte de un gran equipo de investigación. Gracias por haberme guiado en este trabajo, por haberme dado la posibilidad de asistir a congresos internacionales, por haber tenido la ocasión de publicar en diferentes revistas científicas, etc., pero, por encima de todo, gracias por haberme apoyado en los momentos más difíciles. Sin esos ánimos este trabajo no habría sido posible. Por todo ello, considero que has sido mucho más que un director de tesis y, a pesar de que nuestros caminos ahora se separen, aquí siempre tendrás a un amigo. Muchas gracias también a Arkaitz por estar siempre dispuesto a ayudar, sugerir, proponer nuevos retos, etc. con el objetivo de mejorar este trabajo.

En segundo lugar, me gustaría nombrar a todxs lxs compañerxos de este viaje. Empezando por Natalia; muchas gracias por haberme transmitido todos tus conocimientos. Gracias a ti sé cómo funciona un laboratorio. Tu ayuda ha sido fundamental. A Cris, Benoit, Juanma, Nagore, Jabi, Laura, Unai, Ugo y Marta gracias por todos los momentos compartidos. Entre todxs vosotrxs me habéis enseñado a trabajar en equipo.

Eta amaitzeko, eskerrik asko Ama, Aita eta Oihane beti nire ondoan egoteagatik, erortzen ez uzteagatik. Honaino iritsi banaiz zuei esker izan da. Lan hau zuena da ere bai. Familia osoari, lagun guztiei eta maite ditudan pertsona orori eskerrik asko nondik gatozen gogoratzeagatik. Gauden tokian gaudela, beti batera egongo garelako! Maite zaituztet!

Index

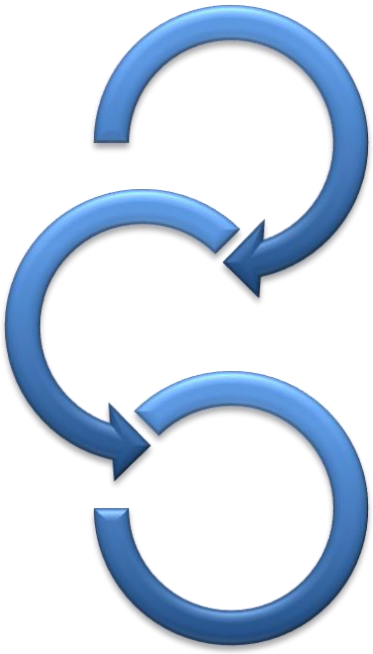

Index

Abstract

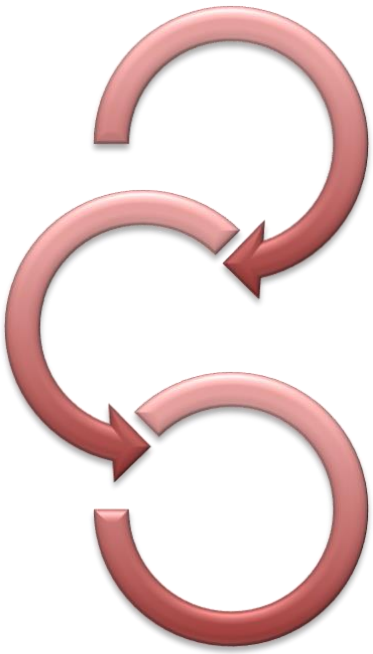

Abstract

Chronic inflammatory diseases are the most significant cause of death in the world. Indeed, according to the World Health Organization (WHO), 3 out of 5 people die due to chronic inflammatory diseases such as stroke, chronic respiratory diseases, heart disorders, cancer, obesity or diabetes. It has been demonstrated that sphingolipid metabolism is altered in this type of disorders. Therefore, understanding the molecular mechanisms by which bioactive sphingolipids participate in the establishment or progression of those diseases may be useful for developing novel therapeutic strategies to control them. In the first chapter of this thesis, we demonstrate that the bioactive sphingolipid ceramide 1-phosphate (C1P) induces survival, proliferation and migration of preadipocytes through mechanisms that implicate the PI3K/Akt, MEK/ERK1-2 and JAK/STAT3 signaling pathways. These biological actions suggest a possible role of this phosphosphingolipid in fat accumulation and dysfunction of adipose tissue, which might lead to metabolic diseases, most notably, obesity. In the second chapter we show that exogenous C1P inhibits alveolar macrophage migration, an action that seems to be caused by dephosphorylation of important proteins that are involved in the regulation of cell migration, such as, PKB/Akt, ERK1-2, PAK1 and Paxillin. In addition, the latter study provides evidence that granular nanosized silica (SiO_2)-conditioned medium enhances alveolar macrophage migration through activation of PI3K/Akt signaling cascade and that C1P inhibits this action by blocking PKB/Akt phosphorylation. Taken together, the results of this thesis support the notion that C1P may have anti-inflammatory properties in lung cells.

Abbreviations

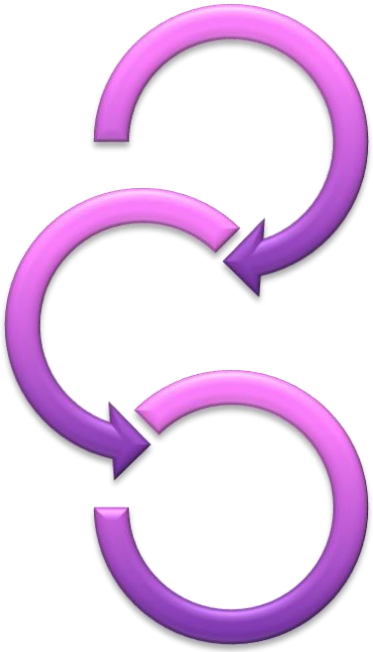

Abbreviations

AA	Arachidonic acid
AIM	Adipogenic induction medium
Arg-1	Arginase 1
AT	Adipose tissue
ATCC	American type culture collection
ATP	Adenosine triphosphate
BAT	Brown adipose tissue
BEAT	Beige adipose tissue
BMDM	Bone marrow-derived macrophages
BSA	Bovine serum albumin
C/EBP	CCAAT/enhancer binding protein
C1P	Ceramide 1-phosphate
C1PP	Ceramide 1-phosphate phosphatase
CAPK	Ceramide-activated protein kinase
CCM	Conditioned control medium
CDase	Ceramidase
Cer	Ceramide
CERK	Ceramide kinase
CerS	Ceramide synthase
CERT	Ceramide transfer protein
COPD	Chronic obstructive pulmonary disease
cPLA	Cytosolic phospholipase A
CPTP	Ceramide phosphate transfer protein

CTM	Conditioned treated medium
DAG	Diacylglycerol
DES	Desaturase
DMEM	Dulbecco´s modified Eagle´s medium
DMF	Dimethylformamide
DMSO	Dimethyl sulfoxide
DTT	Dithiothreitol
EDTA	Ethylenediaminetetraacetic acid
ELISA	Enzyme-linked immunosorbent assay
ER	Endoplasmatic reticulum
FA	Fatty acid
FBS	Fetal bovine serum
FFA	Free fatty acid
GAPDH	Glyceraldehyde 3-phosphate dehydrogenase
GM-CSF	Granulocyte-macrophage colony-stimulating factor
GPCR	Gi protein-coupled receptor
HK2	Hexokinase 2
HSL	Hormone sensitive lipase
IBMX	3-isobutyl-1-methylxanthine
iNOS	Inducible nitric oxide synthase
IR	Insulin resistance
JAK	Janus kinase
JNK/SAPK	c-Jun N-terminal kinase/stress-activated protein kinase
KSR	Kinase suppressor of Ras
LCB	Long-chain bases
LDHA	Lactate deshydorgenase A
LPL	Lipoprotein lipase

LPS	Lipopolysaccharide
MAM	Mitochondria-associated membrane
MAPK	Mitogen-activated protein kinase
MCE	Mitotic clonal expansion
MCP-1	Monocyte chemoattractant protein 1
MKK	MAP kinase kinase
MKKK	MAP kinase kinase kinase
MSC	Mesenchymal stem cell
mTOR	Mammalian target of rapamycin
MTS	3-(4,5-dimethylthiazole-2-yl)-5-(3-carboxymethoxyphenyl)-2-(4-sulfophenyl)-2H-tetrazolium
NCS	Newborn calf serum
PA	Phosphatidic acid
PAP	Phosphatidate phosphohydrolase
PBS	Phosphate-buffered saline
PC	Phosphatidylcholine
PH	Pleckstrin homology
PI3K	Phosphatidylinositol 3-kinase
PIC	Protease inhibitor cocktail
PIP2	Phosphatidylinositol (4, 5)-bisphosphate
PIP3	Phosphatidylinositol (3, 4, 5)-trisphosphate
PKB/Akt	Protein kinase B
PKM2	Pyruvate kinase M2
PMS	Phenazine methosulfate
PPAR	Peroxisome proliferator-activated receptor
Ptx	Pertussis toxin
S1P	Sphingosine 1-phosphate
S1PR	Sphingosine 1-phosphate receptor

SDS	Sodium dodecyl sulfate
SM	Sphingomyelin
SMase	Sphingomyelinase
SMS	Sphingomyelin synthase
Spa	Sphinganine
Sph	Sphingosine
SphK	Sphingosine kinase
SPPase	Sphingosine phosphatase
SPT	Serine palmitoyl transferase
STAT	Signal transducer and activator of transcription
T2D	Type II diabetes
TAG	Triacylglycerol
TBS	Tris-buffered saline
TNF	Tumor necrosis factor
UCP	Uncoupling protein 1
VLDL	Very low-density lipoprotein
WAT	White adipose tissue
WHO	World health organization

Introduction

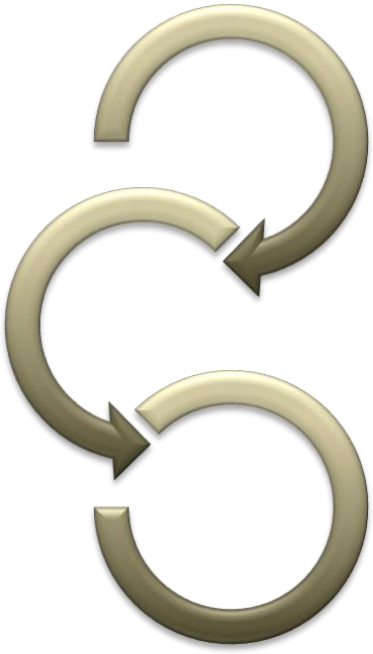

Introduction

1. Sphingolipids

Sphingolipids have been classically known as fundamental blocks of eukaryotic cell membrane architecture. Nevertheless, in the past few decades they have emerged as potent bioactive lipids and some of them have been shown to play critical roles in cell biology. In particular, sphingosine (Sph), ceramide (Cer) and their phosphorylated forms, sphingosine 1-phosphate (S1P) and ceramide 1-phosphate (C1P), were discovered to regulate key physiological functions and to be implicated in many pathological processes, by regulating different signal transduction pathways [1-3].

Sphingolipids are composed of a structurally related family of backbones termed sphingoid bases, which are sometimes referred to as Long-Chain Bases (LCB) (Figure1). LCBs are long-chain aliphatic amines, containing two or three hydroxyl groups, and often a distinctive *trans*-double bond in position 4. To be more precise, they are 2-amino-1,3-dihydroxy-alkanes or alkenes with (2*S*,3*R*)-*erythro* stereochemistry, often with various further structural modifications in the alkyl chain. In animal tissues and humans, the most common or abundant of sphingoid bases are sphingosine (Sph) and its saturated analogue dihydrosphingosine or sphinganine (Spa). Even if there are some patterns defining the association between specific components of these sphingoid bases, the long-chain base composition of individual lipids can vary markedly between species, tissues, organelles and even different membranes within a single organelle. This fact gives an idea of the potential number of combinations and of the complexity that these lipids can reach.

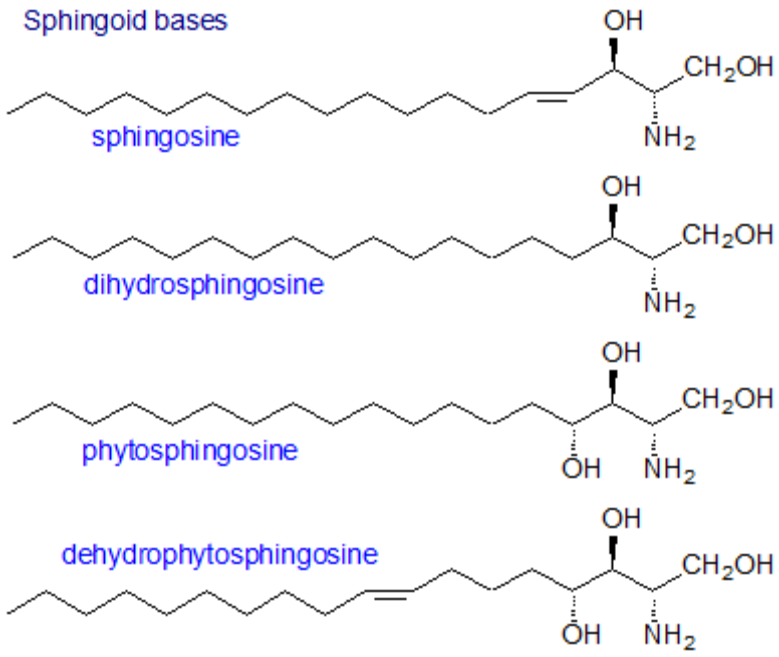

Figure 1. Structure of four different sphingoid bases or LCBs. Taken from LipidHome.

2. Metabolism of sphingolipids

Ceramide (Cer) is the central hub of sphingolipid metabolism and precursor of complex sphingolipids [1]. Structurally, ceramide is composed of a sphingosine backbone and a fatty acid (FA) of varying carbon chain lengths that is linked to the sphingosine moiety by and amide bond. There is a great variety of ceramides with differences in the length of their fatty acids and in the number of unsaturations. Furthermore, each organism or tissue can synthesize different ceramide species. Apart from being an essential part of the cell membrane structure it is also an important signaling molecule capable of regulating cell proliferation, differentiation, adhesion, migration and apoptosis.

Cer can be synthesized by at least three major pathways: the *de novo* pathway, through hydrolysis of complex lipids, especially sphingomyelin (sphingomyelinase pathway), and through the salvage pathway (Figure 2).

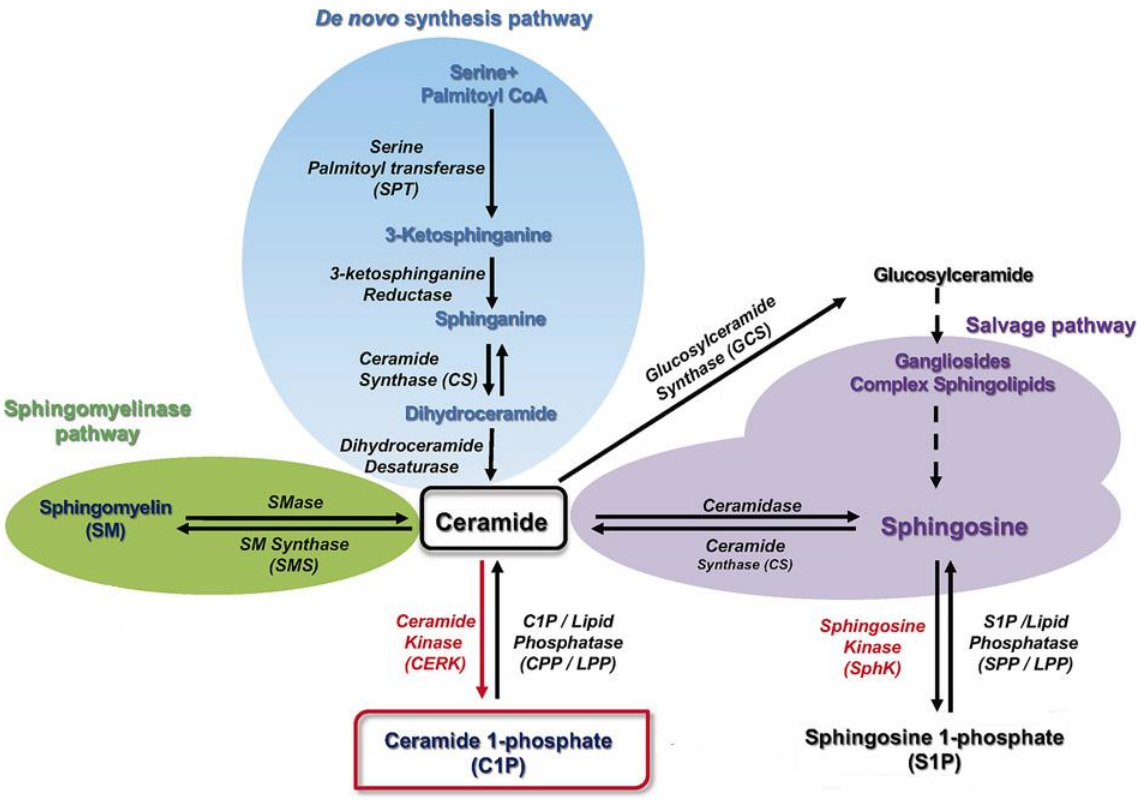

Figure 2. Metabolism of sphingolipids. Image modified from [4].

2.1. The *de novo* synthesis pathway

The de novo synthesis pathway is an anabolic pathway that takes place in the endoplasmic reticulum (ER) where serine and palmitoyl-CoA are condensed to form 3-ketosphinganine (3-dehydrosphingosine) in a reaction that is catalyzed by serine palmitoyl transferase (SPT), which is the major regulatory enzyme of this pathway. 3-ketosphinganine is then converted to sphinganine (dehydrosphingosine) through the action of 3-keto-sphingosine reductase. The next step involves the incorporation of a fatty acid (N-acylation) by sphinganine to render dihydroceramide in a reaction catalyzed by ceramide synthase activity (CerS). The last step of this pathway is catalyzed by a desaturase (DES) through introduction of a *trans* double bond between carbons 4 and 5 of dihydroceramide molecule to generate ceramide (Figure 2).

2.2. The sphingomyelinase (SMase) pathway

The second major pathway of Cer synthesis occurs through the hydrolysis of complex lipids, especially sphingomyelin (SM). This pathway is a catabolic pathway that takes place in the lysosomes and in the plasma membrane of cells and involves the stimulation of sphingomyelinase activity (SMase), which generates phosphocholine and ceramide directly from the breakdown of SM. The opposite reaction is catalyzed by SM synthase (SMS) which is an important enzyme due to its capacity of controlling ceramide and sphingomyelin levels in cells. Specifically, SMS catalyzes the transfer of phosphocholine from phosphatidylcholine (PC) to Cer, thereby releasing diacylglycerol (DAG) and lowering the levels of Cer to produce SM.

2.3. The salvage pathway

The third most important mechanism for generating Cer is the sphingosine salvage pathway, in which Sph produced from the metabolism of complex sphingolipids, is recycled to form Cer through the action of ceramide synthase (CerS). This pathway takes place in the ER and mitochondria-associated membranes (MAMs).

Once formed, Cer can undergo further processing to generate more complex sphingolipids, such as glycosylceramides or complex glycosphingolipids, which in turn, upon their breakdown by specific glucosidases and galactosidases, can once again generate Cer. Ceramides can also be metabolized by ceramidases (CDases), which remove the amide-linked fatty acid to give rise to Sph, and thus Sph can be available either for recycling into Cer or phosphorylation by one of the two Sph kinase enzymes (SphK). The product for this reaction, sphingosine 1-phosphate (S1P), can lose the phosphate group through the action of sphingosine phosphatases (SPPases) or be metabolized by S1P lyase for further conversion into other lipids. Finally, Cer can undergo phosphorylation by the action of ceramide kinase (CERK) to generate ceramide 1-phophate (C1P), and this last molecule can be transformed back into Cer by the action of ceramide 1-phosphate phosphatase (C1PP) (Figure 2).

A fourth pathway of ceramide synthesis was discovered in mitochondria where neutral ceramidase catalyzes the condensation of sphingosine and palmitoyl-CoA in a

two-step reaction. First, the fatty acyl-CoA chain is hydrolyzed in mitochondria to free FA (palmitate) and CoA by thioesterase activity, a reaction that is followed by condensation of palmitate and sphingosine to generate ceramide in a reversed ceramidase reaction [5].

3. Bioactive sphingolipids

The concept of bioactive lipids and its utility for understanding cell and organismal biology has evolved over the past several decades. Bioactive lipids are functionally defined as lipid species, levels of which respond to the action of specific stimuli. These lipids then regulate specific downstream effectors and targets, mediating diverse effects on cells. Thus, bioactive lipids are components of cellular regulatory circuits (such as signaling networks), which distinguishes them from other lipids that have structural and/or energetic functions.

Sphingolipids represent one of the major classes of eukaryotic lipids. Historically, they have been known as fundamental blocks of cell membrane architecture, but in the past few decades they have emerged as potent bioactive lipids. The main bioactive sphingolipids that have received the most attention are sphingosine (Sph), Cer, S1P and C1P.

3.1. Sphingosine (Sph)

Sphingosine (2-amino-4-trans-octadecene-1,3-diol) is an 18-carbon amino alcohol with an unsaturated hydrocarbon chain (Figure 3). Sph has been connected with cellular processes such as inducing cell cycle arrest and apoptosis, by controlling the activity of important enzymes involved in the regulation of metabolic and cell signaling pathways. For instance, Sph was first described as a potent inhibitor of PKC activity, when added to the cells exogenously [6], and also when generated intracellularly [7].

Subsequent studies showed that sphingosine also inhibited the Mg^{2+}-dependent and independent forms of phosphatidate phosphohydrolase (PAP) [8], and that it was a potent activator of PLD [9] and diacylglycerol kinase [10]. These actions of Sph produce low levels of diacylglycerol and elevated phosphatidic acid (PA) concentrations.

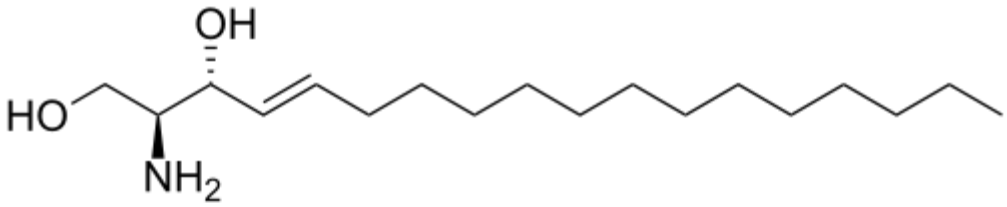

Figure 3. Sphingosine.

3.2. Sphingosine 1-phosphate (S1P)

Phosphorylation of Sph by sphingosine kinases 1 and 2 (SphK1 and SphK2) produces S1P [11] (Figure 4). In vertebrates, S1P is found to regulate an array of cellular responses, including cell migration, differentiation and survival [12]. As such, S1P plays fundamental roles in morphogenetic mechanisms, such as collective cell migration, tissue inductive events and biomechanical signaling. In line with this, recent studies have shown that S1P signaling plays crucial roles in development, for example during angiogenesis [13], cardiogenesis [14], limb development [15] and neurogenesis [16]. S1P can be produced intracellularly, and it is also present in serum at relatively high concentrations where it can be found attached to lipoproteins or albumin [17]. S1P and Sph are readily inter-convertible by specific intracellular S1P phosphatases [18, 19]. Although many of S1P's effects are exerted by intracellular action, a family of specific G-protein coupled receptors, S1P receptors (S1PR), have been described (Reviewed in [20]).

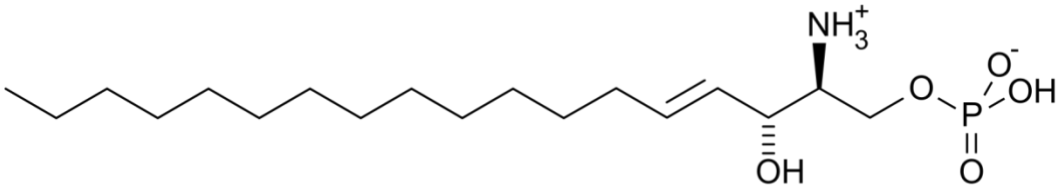

Figure 4. Sphingosine 1-phosphate.

3.3. Ceramide (Cer)

Ceramides (Cer) consist of a sphingosine backbone covalently linked to a fatty acid via an amide bond (Figure 5). Unlike the sphingoid precursors, ceramides are not soluble in water and are located in membrane compartments, including the plasma membrane, where they participate in raft formation.

This bioactive lipid has been mainly associated with cell cycle arrest and the induction of apoptosis in most cell types [21, 22]. Nevertheless, ceramides are also implicated in the regulation of cell growth, diabetes, insulin resistance, inflammation, autophagy, cell differentiation, neurodegenerative disorders, and atherosclerosis [23-25].

Cer can directly interact with and activate several intracellular target proteins. CAPK (ceramide-activated protein kinase) was the first identified ceramide-activated protein kinase and was described in 1991 [26]. This kinase is now often called KSR (kinase suppressor of Ras) and can initiate the JNK/SAPK (c-Jun N-terminal kinase/stress-activated protein kinase) signaling pathway resulting in induction of apoptosis [27]. Cer can also function through direct activation of protein phosphatases PP1A and PP2A, which can perform critical responses, such as cell apoptosis through inactivation of the antiapoptotic targets Akt and Bcl2, and activating pro-apoptotic proteins Bad and Bax [28]. It has also been shown that Cer directly activates the PKCζ atypical isoform by interacting with its cysteine-rich domain (CRD) [29, 30]. PKCζ activation suppresses activity of PKB/Akt, responsible for cell survival [31].

The process of ceramide production appears to be an important research area that could help to elucidate the subsequent bioactive sphingolipids derived from this

molecule and their cellular functions. Cer and its downstream metabolites have been suggested to play a decisive role in a number of pathological states, including obesity, cancer, neurodegeneration, diabetes, microbial pathogenesis, and inflammation.

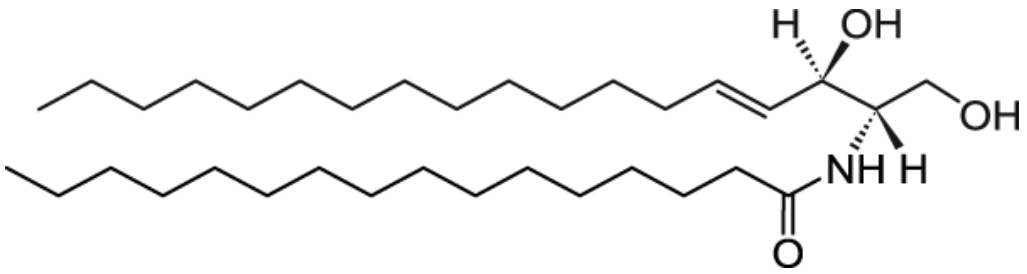

Figure 5. C16-Ceramide.

3.4. Ceramide 1-phosphate (C1P) and ceramide kinase (CERK)

C1P is a major metabolite of ceramide. The bioactivity of C1P was first demonstrated in 1995 as a potent stimulator of DNA synthesis and proliferation in rat fibroblasts [32, 33]. Later, C1P has been described as a pro-survival agent capable of stimulating cell growth of different cell types including primary bone marrow-derived macrophages (BMDM) [34], primary photoreceptor progenitors [35], C2C12 myoblasts [36], and different types of cancer cells such as A549 human lung adenocarcinoma [37], NCI-H358 human broncho-alveolar carcinoma [5], human neuroblastoma [38], MCF-7 breast cancer [5], RAW264.7 mouse leukemia [39], or Kaposi sarcoma [40], as well as inhibiting apoptosis [41-44]. Another major discovery concerning C1P biology was its implication in the regulation of cell migration. Initial studies from our group were carried out using different monocyte/macrophage cell lines, such as mouse RAW264.7 and J774.A1, and human THP-1 monocytes/macrophages, describing an association between cell migration and monocyte chemoattractant protein 1 (MCP-1) release [45, 46]. Moreover, initial work by Chalfant and co-workers showed that C1P promoted inflammation [47, 48]. This action involved translocation and activation of group IV cytosolic phospholipase A2 (cPLA2α) and subsequent generation of arachidonic acid (AA) and pro-inflammatory eicosanoids [49, 50].

C1P is synthesized in mammalian cells by the direct phosphorylation of ceramide by ceramide kinase (CERK) (Figure 6). At present, CERK is the only enzyme known to produce C1P in mammalian cells [51]. This enzyme was first observed in brain synaptic vesicles [52] as a calcium stimulated lipid kinase. After this initial finding, CERK was later found in human leukemia HL-60 cells [53].

The CERK protein sequence has 537 amino acids with two protein sequence motifs: an N-terminus that encompasses a sequence motif known as a pleckstrin homology (PH) domain (amino acids 32-121); and a C-terminal region containing a Ca^{2+}/calmodulin binding domain (amino acids 124-433). Using site-directed mutagenesis, it was found that leucine 10 in the PH domain is essential for its catalytic activity [54], and it was also reported that the interaction between this PH domain of CERK and 4,5- bisphosphate regulates plasma membrane targeting and C1P levels [55].

However, it has been reported that bone marrow-derived macrophages from CERK null mice (CERK-/- mice) still have significant levels of C1P, which suggests that there could be other metabolic pathways for generating C1P [56]. We have previously speculated that two alternative pathways for the generation of C1P in cells might be the transfer of a long acyl-CoA chain to S1P by a putative acyl transferase, or cleavage of SM by a PLD-like activity, similar to the existing arthropod or bacterial SMase D. Nevertheless, at the present time, CERK is considered to be the only C1P source in mammalian cells. Concerning enzyme regulation it has been clearly established that CERK is absolutely dependent on Ca^{2+} ions for activity, and more recently it has been proposed to be regulated by phosphorylation/dephosphorylation processes [57].

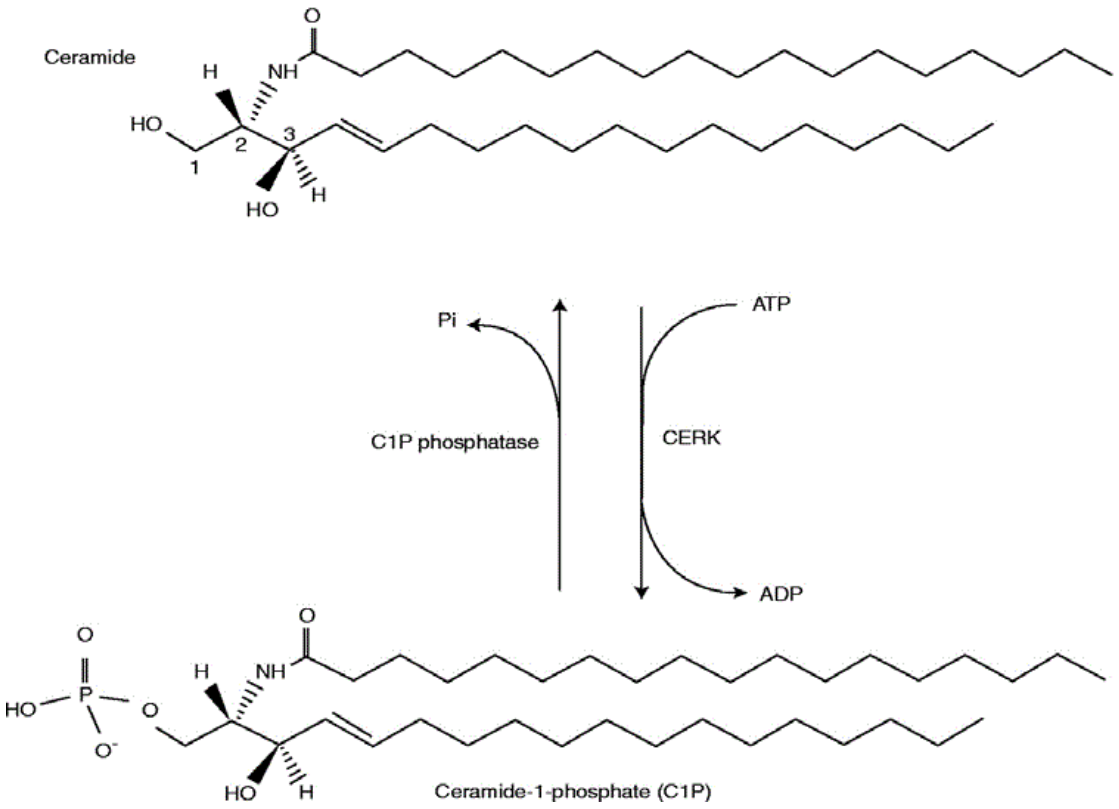

Figure 6. Conversion of ceramide in C1P by ceramide kinase enzymatic action. Taken from [58].

3.5. Transport of C1P

Cer generated in the endoplasmic reticulum (ER) are transported to the Golgi apparatus by a ceramide transfer protein (CERT). Cer can be phosphorylated by a CERK that resides in the Golgi to generate C1P. C1P is also found in perinuclear membranes. Once synthesized, C1P can be transported by a specific ceramide phosphate transfer protein (CPTP) to the plasma membrane, where it can act in signal transduction processes, and probably to other organelles [59, 60] (Figure 7).

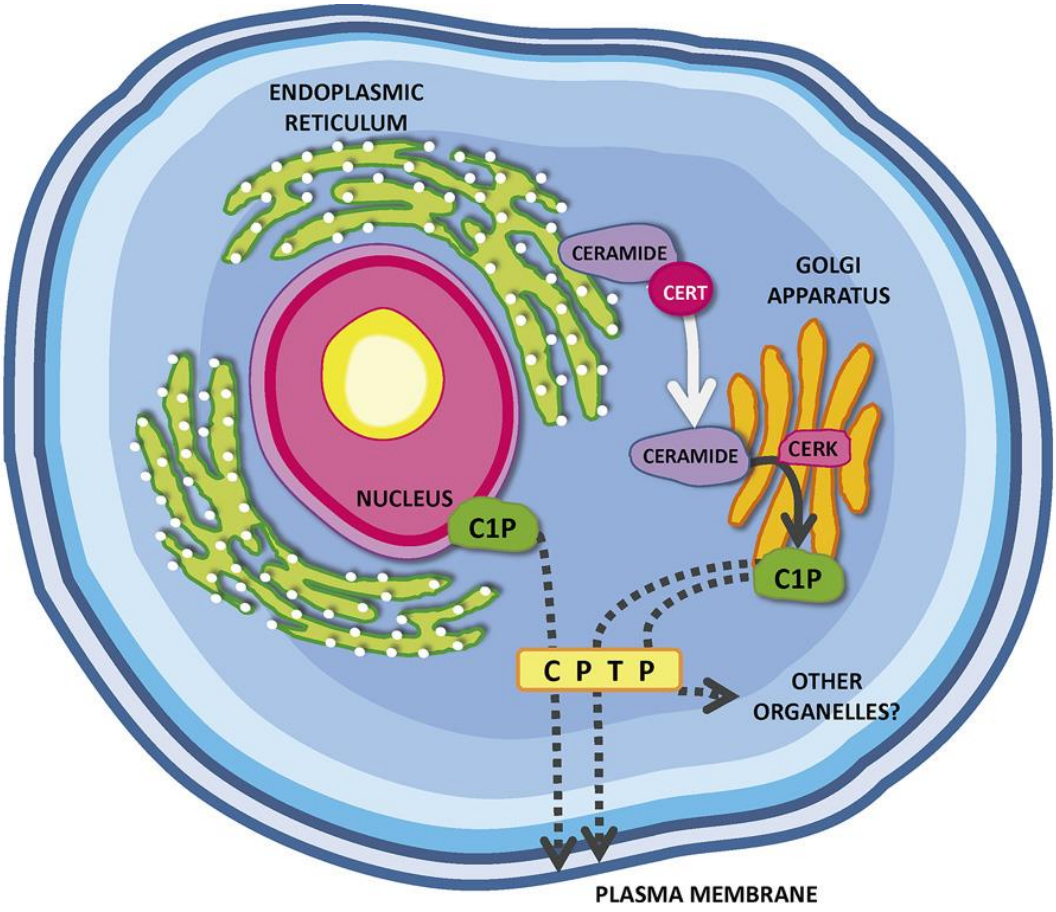

Figure 7. Biosynthesis and transport of C1P. C1P: ceramide 1-phosphate, CERT: ceramide transfer protein, CPTP: ceramide phosphate transfer protein, CERK: ceramide kinase. Taken from [4].

3.6. Putative receptor of C1P

It has been shown that not all of C1P's effects can be reproduced by increasing intracellular C1P levels. For instance, C1P can induce cell migration in RAW264.7 cells but it is not possible to stimulate chemotaxis by increasing intracellular C1P levels in these cells (i.e, with IL-1β or with the calcium ionophore A23187) [46]. This result suggests that there may be some kind of interaction between C1P and the plasma membrane that cannot be achieved intracellularly. In order to elucidate the existence of a possible C1P receptor binding experiments between C1P and cell membranes were performed. The receptor turned out to be a Gi protein-coupled receptor (GPCR) with low affinity for its substrate (Kd=7.8 μM) [46]. Later, we have also demonstrated that ligation of C1P to this receptor triggered ERK1-2 phosphorylation and stimulated

glucose uptake [61]. All of these effects were completely abolished by pretreatment of cells with pertussis toxin (Ptx), confirming that the receptor belongs to the Gi protein-coupled receptor family.

4. Sphingolipids and signaling pathways

Our group has pioneered the studies concerning the implication of C1P in cell biology. As mentioned above, it was first demonstrated that C1P stimulates cell proliferation in fibroblasts and macrophages [32-34], and it was also found to be a potent inhibitor of apoptosis [42, 43]. Some of the signaling pathways involved in these actions have already been described, and they are listed below.

4.1. Mitogen-activated protein kinase (MAPK) pathway

Mitogen-activated protein kinases (MAPKs) compose a family of protein kinases that respond to extracellular stimulus (mitogens, osmotic stress, heat shock and proinflammatory cytokines). MAPKs phosphorylate specific serine and threonine residues of target protein and regulate a variety of cellular activities including gene expression, mitosis, chemotaxis or programmed cell death. Because of the many important cellular functions controlled by MAPKs, they have been studied extensively to define their roles in physiology and human disease.

MAPKs are part of a phosphorelay system composed of three sequentially activated kinases, and, like their substrates, MAPKs are regulated by phosphorylation [62]. MAPKs serve as phosphorylation substrates for MAPK kinases (MKKs). MKK-catalyzed phosphorylation activates MAPKs and increases their activity to catalyze the phosphorylation of its own substrates. MAPK kinase kinases (MKKKs) are the third component of the phosphorelay system. MKKKs phosphorylate and activate specific MKKs. MKKKs have distinct motifs in their sequences that selectively confer their activation in response to different stimuli.

In multicellular organisms, there are four well characterized MAPK cascades, according to their MAPK components. These include the extracellular signal-regulated kinases 1 and 2 (ERK1-2), the c-Jun NH2-terminal kinases (JNK 1, JNK 2, and JNK 3), four p38 enzymes (p38α, p38β, p38γ, and p38δ) and ERK5.

The ERK1-2 cascade was the first MAPK pathway elucidated and is considered a prototype of these kinase cascades [63]. In most cases, the activation of membrane receptors is transmitted by several mechanisms to the small GTPase Ras, which is activated mainly at the plasma membrane. Ras activates a MKKK named Raf. Thereafter, the signal is transmitted to the MKKs, called MEK1 and MEK2 (MEK1-2) and finally these two kinases transmit their signal to ERK1 and ERK2 (ERK1-2) (Figure 8). When ERK1-2 is activated it can phosphorylate a number of substrates in many cellular locations, and these are responsible for the induction of ERK1-2-dependent cellular processes.

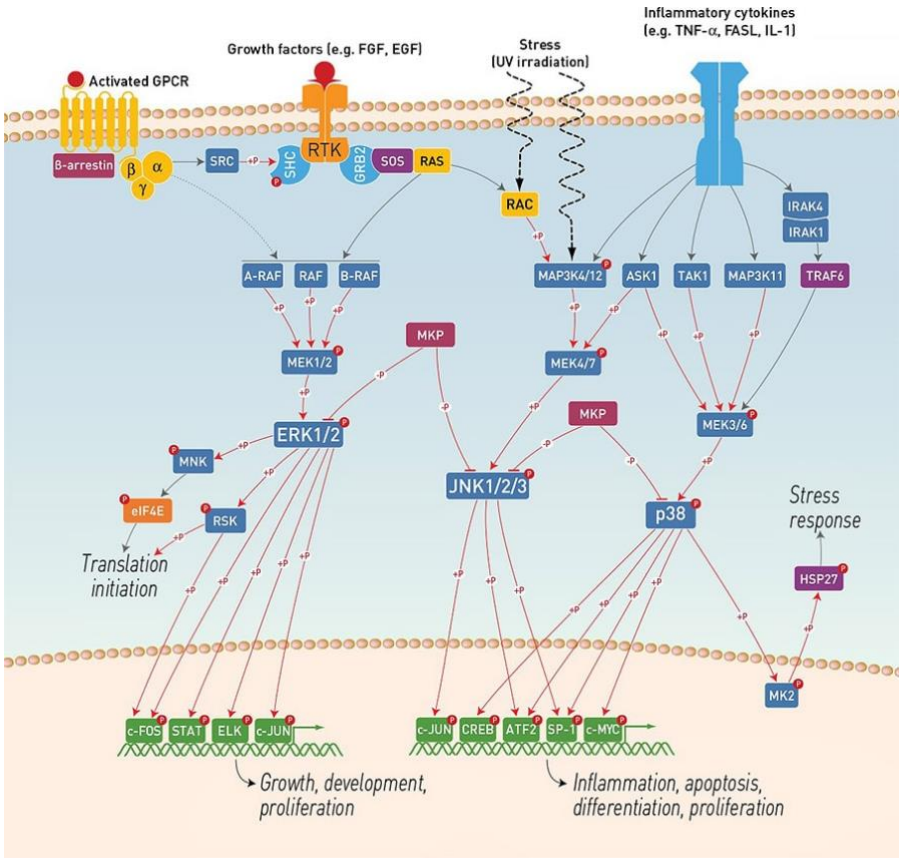

Figure 8. MAPK signal transduction pathway. The major classic MAPK pathway is the Ras-Raf-MEK-ERK1-2 pathway, in which Ras phosphorylates Raf (MKKK), then Raf phosphorylates MEK (MKK) and MEK phosphorylates ERK1-2 (MAPK). Other pathways include p38 and JNK MAPKs in which MKK-4 or MKK-7 phosphorylate JNK, and MKK-3 or MKK-6, which phosphorylate the p38 MAPK. Taken from TermoFisher website.

4.2. Phosphatidylinositol 3-kinase (PI3K)/protein kinase B (PKB, also known as Akt) pathway

Phosphoinositide 3-kinases (PI3Ks), also called phosphatidylinositol 3-kinases, are a family of enzymes involved in cellular functions such as cell growth, differentiation, motility, survival and intracellular trafficking.

The PI3K/PKB-Akt pathway is highly conserved, and its activation is tightly controlled via a multistep process. Activated receptors directly stimulate class 1A PI3Ks. This triggers activation of PI3K and conversion by its catalytic domain of phosphatidylinositol (4,5)-bisphosphate (PIP2) lipids to phosphatidylinositol (3,4,5)-trisphosphate (PIP3). PKB/Akt binds to PIP3 at the plasma membrane, allowing PDK1 to access and phosphorylate Threonin 308 (T308) in the “activation loop,” leading to partial PKB/Akt activation [64]. This PKB/Akt modification is sufficient to further activate other kinases such as mammalian target of rapamycin (mTOR), which activates specific transcription factors (Figure 9). Full activation of Akt would also require phosphorylation at Serine 473 (S473) by a PDK2.

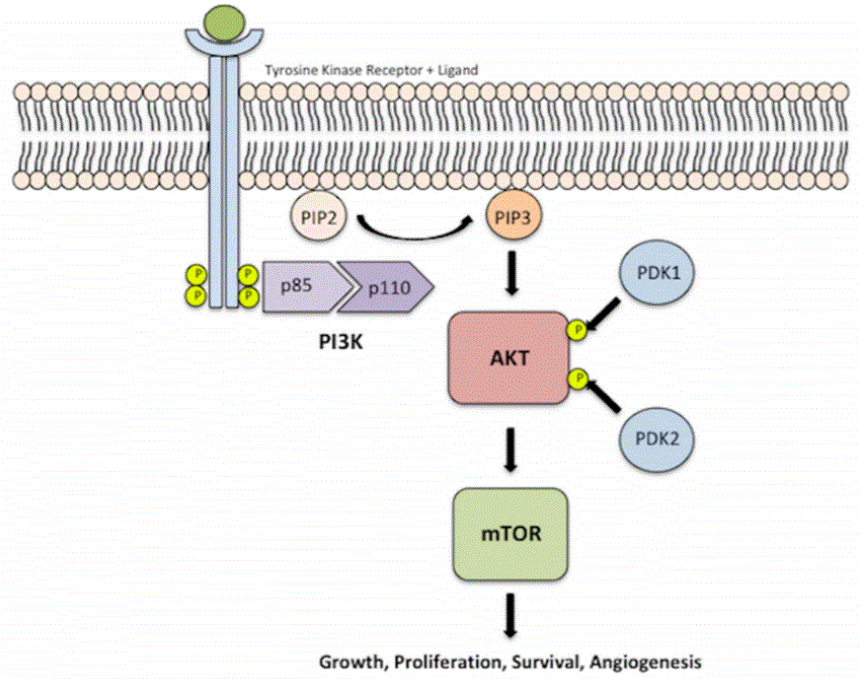

Figure 9. PI3K-Akt-mTOR pathway. Activation of PI3K leads to phosphorylation of the p85 subunit of the PI3K heterodimer, which subsequently activates the catalytic subunit, p110. This phosphorylated heterodimer catalyses the conversion of PIP_2 into PIP_3. PIP_3 mediates the activation of Akt via phosphorylation by PDK-1 at threonine T308 and PDK-2 (mTOR2) at serine residue S473, for maximal Akt activation. Activated Akt then mediates the activation of mTOR, which results in cellular growth, survival, angiogenesis or proliferation. Taken from [65].

Traditional schemes of growth factor, hormone and cytokine receptor signaling networks display PI3K/Akt and Ras/MAPK as two independent parallel pathways. However, there are multiple cross-talk points between these two pathways (Figure 10), whose co-ordinated action determines the cell fate.

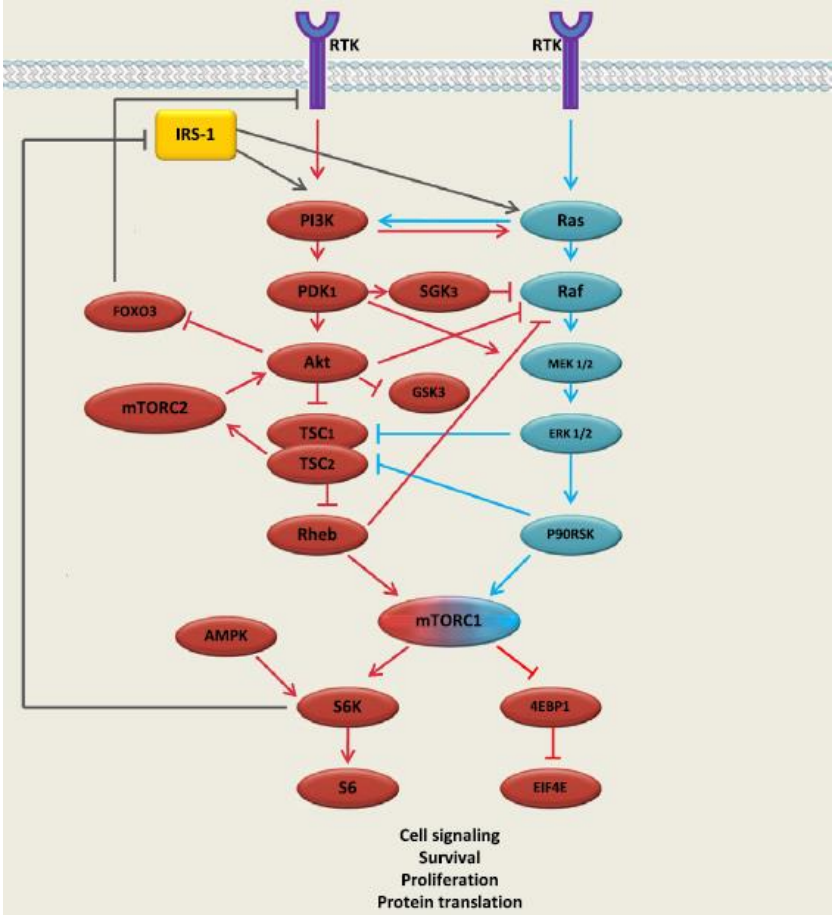

Figure 10. Cross-talk between MAPK and PI3K/Akt pathways. RTK: receptor tyrosine kinase. Image modified from [66]

4.3. JAK/STAT pathway

The janus kinase/signal transducers and activators of transcription (JAK/STAT) pathway is one of a handful of pleiotropic cascades used to transduce a multitude of signals for development and homeostasis in animals, from flies to humans. In mammals, the JAK/STAT pathway is the principal signaling mechanism for a wide array of cytokines and growth factors. JAK activation stimulates cell proliferation, differentiation, cell migration and apoptosis. These cellular events are critical to hematopoiesis, immune development, mammary gland development and lactation, adipogenesis, sexually dimorphic growth and other processes. Predictably, mutations that reduce JAK/STAT pathway activity affect these processes [67]. Conversely, mutations that constitutively activate or fail to regulate JAK signaling properly cause inflammatory disease, erythrocytosis, gigantism and an array of leukemias.

In mammals, the JAK family comprises four members: JAK1, JAK2, JAK 3 and TYK2. JAK activation occurs upon ligand-mediated receptor multimerization because two JAKs are brought into close proximity, allowing trans-phosphorylation. The activated JAKs subsequently phosphorylate additional targets, including both the receptors and the major substrates, STATs. STATs are latent transcription factors that reside in the cytoplasm until activated. The seven mammalian STATs bear a conserved tyrosine residue near the C-terminus that is phosphorylated by JAKs. This phosphotyrosine permits the dimerization of STATs through interaction with a conserved SH2 domain. Phosphorylated STATs enter the nucleus and, once in the nucleus, dimerized STATs bind specific regulatory sequences to activate or repress transcription of target genes (Figure 11). Thus the JAK/STAT cascade provides a direct mechanism to translate an extracellular signal into a transcriptional response.

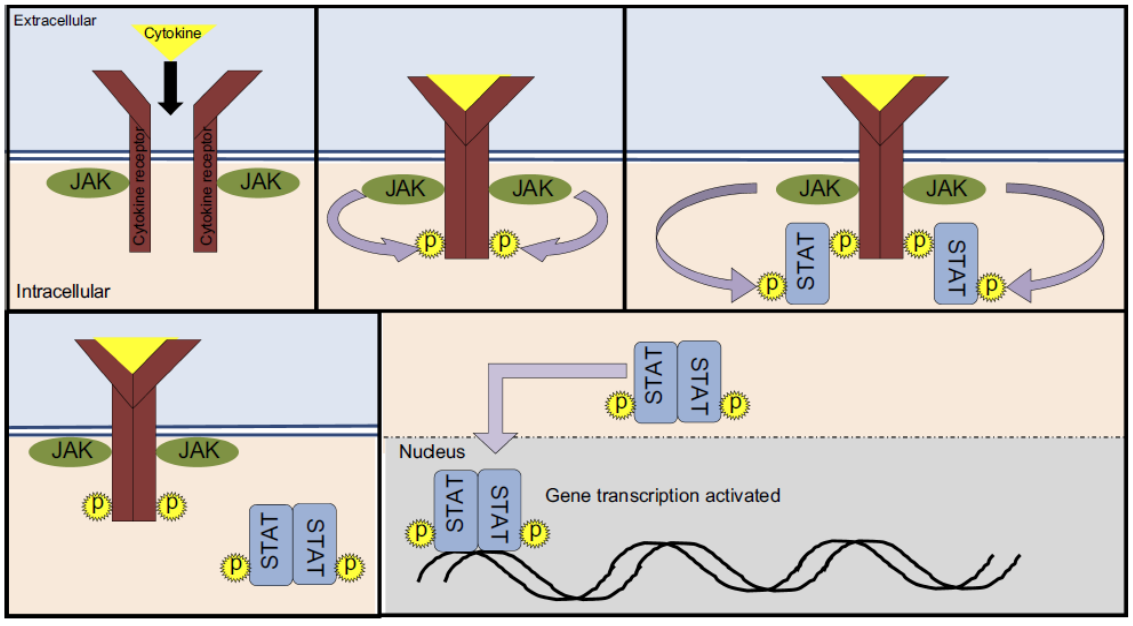

Figure 11. JAK/STAT pathway. Taken from [68].

5. References

1. Hannun YA, Obeid LM. Principles of bioactive lipid signaling: lessons from sphingolipids. Nat Rev Mol Cell Biol. 2008; 9(2): 139-50.
2. Maceyka M, Spiegel S. Sphingolipid metabolites in inflammatory disease. Nature. 2014; 510(7503): 58-67.
3. Hla T, Dannenberg AJ. Sphingolipid signaling in metabolic disorders. Cell Metab. 2012; 16(4): 420-34.
4. Gomez-Larrauri A, Presa N, Dominguez-Herrera A, Ouro A, Trueba M, Gomez-Muñoz A. Role of bioactive sphingolipids in physiology and pathology. Essays Biochem. 2020; 64(3): 579-89.
5. Pastukhov O, Schwalm S, Zangemeister-Wittke U, Fabbro D, Bornancin F, Japtok L, et al. The ceramide kinase inhibitor NVP-231 inhibits breast and lung cancer cell proliferation by inducing M phase arrest and subsequent cell death: NVP-231 induces M phase arrest and cancer cell death. Br J Pharmacol. 2014; 171(24): 5829-44.
6. Hannun YA, Loomis CR, Merrill AH Jr, Bell RM. Sphingosine inhibition of protein kinase C activity and of phorbol dibutyrate binding in vitro and in human platelets. J Biol Chem. 1986; 261(27): 12604-9.
7. Smith ER, Jones PL, Boss JM, Merrill AH Jr. Changing J774A.1 cells to new medium perturbs multiple signaling pathways, including the modulation of protein kinase C by endogenous sphingoid bases. J Biol Chem. 1997; 272(9): 5640-6.
8. Gomez-Muñoz A, Hamza EH, Brindley DN. Effects of sphingosine, albumin and unsaturated fatty acids on the activation and translocation of phosphatidate phosphohydrolases in rat hepatocytes. Biochim biophys acta. 1992; 1127(1): 49-56.
9. Natarajan V, Jayaram HN, Scribner WM, Garcia JG. Activation of endothelial cell phospholipase D by sphingosine and sphingosine-1-phosphate. Am J Respir Cell Mol Biol. 1994; 11(2): 221-9.
10. Keiko Y, Fumio S, Shin-ichi I, Haruo T. Sphingosine activates cellular diacylglycerol kinase in intact Jurkat cells, a human T-cell line. Biochim biophys acta. 1993; 1169(3): 217-24.
11. Spiegel S, Milstien S. Functions of the multifaceted family of sphingosine kinases and some close relatives. J Biol Chem. 2007; 282(4): 2125-9.

12. Blaho VA, Hla T. Regulation of mammalian physiology, development, and disease by the sphingosine 1-phosphate and lysophosphatidic acid receptors. Chem Rev. 2011; 111(10): 6299-320.
13. Gaengel K, Niaudet C, Hagikura K, Laviña B, Muhl L, Hofmann JJ, et al. The sphingosine-1-phosphate receptor S1PR1 restricts sprouting angiogenesis by regulating the interplay between VE-cadherin and VEGFR2. Dev Cell. 2012; 23(3): 587-99.
14. Kupperman E, An S, Osborne N, Waldron S, Stainier DY. A sphingosine-1-phosphate receptor regulates cell migration during vertebrate heart development. Nature. 2000; 406(6792): 192-5.
15. Chae S-S, Paik J-H, Allende ML, Proia RL, Hla T. Regulation of limb development by the sphingosine 1-phosphate receptor S1p1/EDG-1 occurs via the hypoxia/VEGF axis. Dev Biol. 2004; 268(2): 441-7.
16. Mizugishi K, Yamashita T, Olivera A, Miller GF, Spiegel S, Proia RL. Essential role for sphingosine kinases in neural and vascular development. Mol Cell Biol. 2005; 25(24): 11113-21.
17. Watterson K, Sankala H, Milstien S, Spiegel S. Pleiotropic actions of sphingosine-1-phosphate. Prog Lipid Res. 2003; 42(4): 344-57.
18. Waggoner DW, Gómez-Muñoz A, Dewald J, Brindley DN. Phosphatidate phosphohydrolase catalyzes the hydrolysis of ceramide 1-phosphate, lysophosphatidate, and sphingosine 1-phosphate. J Biol Chem. 1996; 271(28): 16506-9.
19. Brindley D. Lipid phosphate phosphatases regulate signal transduction through glycerolipids and sphingolipids. Biochim Biophys Acta Mol Cell Biol Lipids 2002; 1582(1-3): 33-44.
20. Pyne S, Lee SC, Long J, Pyne NJ. Role of sphingosine kinases and lipid phosphate phosphatases in regulating spatial sphingosine 1-phosphate signaling in health and disease. Cell Signal. 2009; 21(1): 14-21.
21. Hannun, Y.A. and L.M. Obeid, The Ceramide-centric universe of lipid-mediated cell regulation: stress encounters of the lipid kind. J Biol Chem. 2002. 277(29): 25847-50.

22. Hannun YA, Obeid LM. Ceramide: an intracellular signal for apoptosis. Trends Biochem Sci. 1995; 20(2): 73-7.
23. Riboni L, Campanella R, Bassi R, Villani R, Gaini SM, Martinelli-Boneschi F, et al. Ceramide levels are inversely associated with malignant progression of human glial tumors. Glia. 2002; 39(2): 105-13.
24. Steinbrecher UP, Gómez-Muñoz A, Duronio V. Acid sphingomyelinase in macrophage apoptosis. Curr Opin Lipidol. 2004; 15(5): 531-7.
25. Turinsky J, O'Sullivan DM, Bayly BP. 1,2-Diacylglycerol and ceramide levels in insulin-resistant tissues of the rat in vivo. J Biol Chem. 1990; 265(28): 16880-5.
26. Mathias S, Dressler KA, Kolesnick RN. Characterization of a ceramide-activated protein kinase: stimulation by tumor necrosis factor alpha. Proc Natl Acad Sci U S A. 1991; 88(22): 10009-13.
27. Basu S, Kolesnick R. Stress signals for apoptosis: ceramide and c-Jun kinase. Oncogene. 1998; 17(25): 3277-85.
28. Cowart LA, Hannun YA. Selective substrate supply in the regulation of yeast de Novo sphingolipid synthesis. J Biol Chem. 2007; 282(16): 12330-40.
29. Hurley JH, Newton AC, Parker PJ, Blumberg PM, Nishizuka Y. Taxonomy and function of C1 protein kinase C homology domains: C1 domains. Protein Sci. 1997; 6(2): 477-80.
30. Bourbon NA, Yun J, Kester M. Ceramide directly activates protein kinase C zeta to regulate a stress-activated protein kinase signaling complex. J Biol Chem. 2000; 275(45): 35617-23.
31. Doornbos RP, Theelen M, van der Hoeven PC, van Blitterswijk WJ, Verkleij AJ, van Bergen en Henegouwen PM. Protein kinase Czeta is a negative regulator of protein kinase B activity. J Biol Chem. 1999; 274(13): 8589-96.
32. Gomez-Muñoz A, Duffy PA, Martin A, O'Brien L, Byun HS, Bittman R, et al. Short-chain ceramide-1-phosphates are novel stimulators of DNA synthesis and cell division: antagonism by cell-permeable ceramides. Mol Pharmacol. 1995; 47(5): 833-9.
33. Gomez-Muñoz A, Frago LM, Alvarez L, Varela-Nieto I. Stimulation of DNA synthesis by natural ceramide 1-phosphate. Biochem J. 1997; 325(2): 435-40.

34. Gangoiti P, Granado MH, Wang SW, Kong JY, Steinbrecher UP, Gómez-Muñoz A. Ceramide 1-phosphate stimulates macrophage proliferation through activation of the PI3-kinase/PKB, JNK and ERK1/2 pathways. Cell Signal. 2008; 20(4): 726-36.
35. Miranda GE, Abrahan CE, Agnolazza DL, Politi LE, Rotstein NP. Ceramide-1-phosphate, a new mediator of development and survival in retina photoreceptors. Invest Ophthalmol Vis Sci. 2011; 52(9): 6580-8.
36. Gangoiti P, Bernacchioni C, Donati C, Cencetti F, Ouro A, Gómez-Muñoz A, et al. Ceramide 1-phosphate stimulates proliferation of C2C12 myoblasts. Biochimie. 2012; 94(3): 597-607.
37. Mitra P, Maceyka M, Payne SG, Lamour N, Milstien S, Chalfant CE, et al. Ceramide kinase regulates growth and survival of A549 human lung adenocarcinoma cells. FEBS Lett. 2007; 581(4): 735-40.
38. Bini F, Frati A, Garcia-Gil M, Battistini C, Granado M, Martinesi M, et al. New signaling pathway involved in the anti-proliferative action of vitamin D_3 and its analogues in human neuroblastoma cells. A role for ceramide kinase. Neuropharmacology. 2012; 63(4): 524-37.
39. Ouro A, Arana L, Riazy M, Zhang P, Gomez-Larrauri A, Steinbrecher U, et al. Vascular endothelial growth factor mediates ceramide 1-phosphate-stimulated macrophage proliferation. Exp Cell Res. 2017; 361(2): 277-83.
40. Abdel Hadi L, Calcaterra F, Brambilla L, Carenza C, Marfia G, Della Bella S, et al. Enhanced phosphorylation of sphingosine and ceramide sustains the exuberant proliferation of endothelial progenitors in Kaposi sarcoma. J Leukoc Biol. 2018; 103(3): 525-33.
41. Gangoiti P, Granado MH, Arana L, Ouro A, Gómez-Muñoz A. Involvement of nitric oxide in the promotion of cell survival by ceramide 1-phosphate. FEBS Lett. 2008; 582(15): 2263-9.
42. Gómez-Muñoz A, Kong JY, Parhar K, Wang SW, Gangoiti P, González M, et al. Ceramide-1-phosphate promotes cell survival through activation of the phosphatidylinositol 3-kinase/protein kinase B pathway. FEBS Lett. 2005; 579(17): 3744-50.

43. Gómez-Muñoz A, Kong JY, Salh B, Steinbrecher UP. Ceramide-1-phosphate blocks apoptosis through inhibition of acid sphingomyelinase in macrophages. J Lipid Res. 2004; 45(1): 99-105.
44. Granado MH, Gangoiti P, Ouro A, Arana L, Gómez-Muñoz A. Ceramide 1-phosphate inhibits serine palmitoyltransferase and blocks apoptosis in alveolar macrophages. Biochim Biophys Acta. 2009; 1791(4): 263-72.
45. Arana L, Ordoñez M, Ouro A, Rivera I-G, Gangoiti P, Trueba M, et al. Ceramide 1-phosphate induces macrophage chemoattractant protein-1 release: involvement in ceramide 1-phosphate-stimulated cell migration. Am J Physiol Endocrinol Metab. 2013; 304(11): E1213-26.
46. Granado MH, Gangoiti P, Ouro A, Arana L, González M, Trueba M, et al. Ceramide 1-phosphate (C1P) promotes cell migration Involvement of a specific C1P receptor. Cell Signal. 2009; 21(3): 405-12.
47. Berwick ML, Dudley BA, Maus K, Chalfant CE. The role of ceramide 1-phosphate in inflammation, cellular proliferation, and wound healing. Adv Exp Med Biol. 2019; 1159: 65–77.
48. Pettus BJ, Bielawska A, Spiegel S, Roddy P, Hannun YA, Chalfant CE. Ceramide kinase mediates cytokine- and calcium ionophore-induced arachidonic acid release. J Biol Chem. 2003; 278(40): 38206-13.
49. Pettus BJ, Bielawska A, Subramanian P, Wijesinghe DS, Maceyka M, Leslie CC, et al. Ceramide 1-phosphate is a direct activator of cytosolic phospholipase A2. J Biol Chem. 2004; 279(12): 11320-6.
50. Lamour NF, Subramanian P, Wijesinghe DS, Stahelin RV, Bonventre JV, Chalfant CE. Ceramide 1-phosphate is required for the translocation of group IVA cytosolic phospholipase A2 and prostaglandin synthesis. J Biol Chem. 2009; 284(39): 26897-907.
51. Sugiura M, Kono K, Liu H, Shimizugawa T, Minekura H, Spiegel S, et al. Ceramide kinase, a novel lipid kinase: Molecular cloning and functional characterization. J Biol Chem. 2002; 277(26): 23294-300.
52. Bajjalieh SM, Martin TF, Floor E. Synaptic vesicle ceramide kinase. A calcium-stimulated lipid kinase that co-purifies with brain synaptic vesicles. J Biol Chem. 1989; 264(24): 14354-60.

53. Dressler KA, Kolesnick RN. Ceramide 1-phosphate, a novel phospholipid in human leukemia (HL-60) cells. Synthesis via ceramide from sphingomyelin. J Biol Chem. 1990; 265(25): 14917-21.
54. Kim T-J, Mitsutake S, Kato M, Igarashi Y. The leucine 10 residue in the pleckstrin homology domain of ceramide kinase is crucial for its catalytic activity. FEBS Lett. 2005; 579(20): 4383-8.
55. Kim T-J, Mitsutake S, Igarashi Y. The interaction between the pleckstrin homology domain of ceramide kinase and phosphatidylinositol 4,5-bisphosphate regulates the plasma membrane targeting and ceramide 1-phosphate levels. Biochem Biophys Res Commun. 2006; 342(2): 611-7.
56. Boath A, Graf C, Lidome E, Ullrich T, Nussbaumer P, Bornancin F. Regulation and traffic of ceramide 1-phosphate produced by ceramide kinase: comparative analysis to glucosylceramide and sphingomyelin: Comparative analysis to glucosylceramide and sphingomyelin. J Biol Chem. 2008; 283(13): 8517-26.
57. Baumruker T, Bornancin F, Billich A. The role of sphingosine and ceramide kinases in inflammatory responses. Immunol Lett. 2005; 96(2): 175-85.
58. Lamour NF, Chalfant CE. Ceramide-1-phosphate: the “missing” link in eicosanoid biosynthesis and inflammation. Mol Interv. 2005; 5(6): 358-67.
59. Lamour NF, Stahelin RV, Wijesinghe DS, Maceyka M, Wang E, Allegood JC, et al. Ceramide kinase uses ceramide provided by ceramide transport protein: localization to organelles of eicosanoid synthesis. J Lipid Res. 2007; 48(6): 1293-304.
60. Hanada K, Kumagai K, Yasuda S, Miura Y, Kawano M, Fukasawa M, et al. Molecular machinery for non-vesicular trafficking of ceramide. Nature. 2003; 426(6968): 803-9.
61. Ouro A, Arana L, Gangoiti P, Rivera I-G, Ordoñez M, Trueba M, et al. Ceramide 1-phosphate stimulates glucose uptake in macrophages. Cell Signal. 2013; 25(4): 786-95.
62. Ray LB, Sturgill TW. Insulin-stimulated microtubule-associated protein kinase is phosphorylated on tyrosine and threonine in vivo. Proc Natl Acad Sci U S A. 1988; 85(11): 3753-7.

63. Plotnikov A, Zehorai E, Procaccia S, Seger R. The MAPK cascades: signaling components, nuclear roles and mechanisms of nuclear translocation. Biochim Biophys Acta. 2011; 1813(9): 1619-33.
64. Alessi DR, James SR, Downes CP, Holmes AB, Gaffney PRJ, Reese CB, et al. Characterization of a 3-phosphoinositide-dependent protein kinase which phosphorylates and activates protein kinase Bα. Curr Biol. 1997; 7(4): 261-9.
65. Adimonye A, Stankiewicz E, Kudahetti S, Trevisan G, Tinwell B, Corbishley C, et al. Analysis of the PI3K-AKT-mTOR pathway in penile cancer: evaluation of a therapeutically targetable pathway. Oncotarget. 2018; 9(22): 16074-86.
66. Saini KS, Loi S, de Azambuja E, Metzger-Filho O, Saini ML, Ignatiadis M, et al. Targeting the PI3K/AKT/mTOR and Raf/MEK/ERK pathways in the treatment of breast cancer. Cancer Treat Rev. 2013; 39(8): 935-46.
67. Igaz P, Tóth S, Falus A. Biological and clinical significance of the JAK-STAT pathway; lessons from knockout mice. Inflamm Res. 2001; 50(9): 435-41.
68. Tran V, Shammas RM, Sauk JS, Padua D. Evaluating tofacitinib citrate in the treatment of moderate-to-severe active ulcerative colitis: design, development and positioning of therapy. Clin Exp Gastroenterol. 2019; 12: 179-91.

Rationale of thesis and Objectives

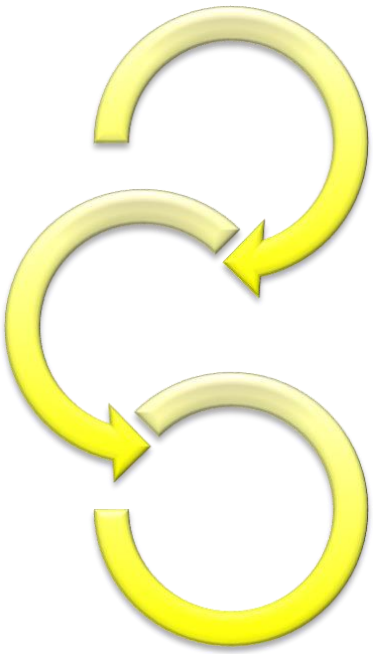

Rationale

Base on previous studies by our group, this thesis was conceived with the idea of shading light on the mechanisms by which ceramide 1-phosphate regulates cell migration in the context of inflammation. To this purpose, we selected two different biological systems: 1) The pre-adipocyte/adipose cell system, which may be implicated in the promotion of inflammation in obesity, and 2) The alveolar macrophage system, which may be associated with the previously observed anti-inflammatory actions of C1P in the lungs. It should be noted that, although in obesity body fat mass increases through the enlargement of existing fat cells, in gross obesity there is also an increase in cell number for which regulation of adipose cell growth / survival will also be studied.

Objectives

Accordingly, the objectives proposed in this thesis were:

1. To study the implication of C1P in survival, proliferation and migration in preadipocytes and to determine the molecular mechanisms involved in these biological actions.

2. To study the implication of C1P in anti-inflammatory processes in alveolar macrophages.

    2.1. To determine the possible effect of C1P in migration of alveolar macrophages and the molecular mechanisms involved in this biological action.

    2.2. To study the possible induction of alveolar macrophage migration by SiO_2 and the effect of the C1P in this action.

Materials and Methods

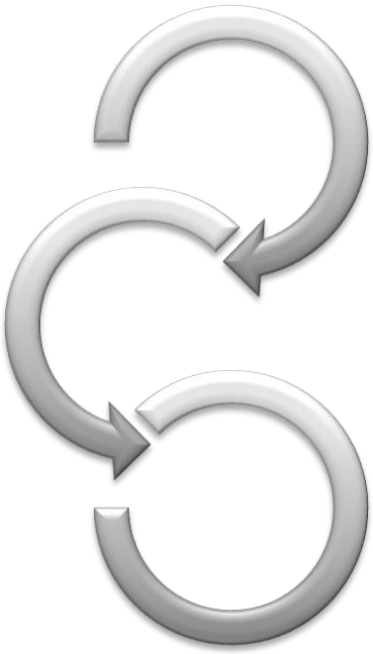

Materials and Methods

1. Materials

1.1. Reagents

Supplier	Reactives
Abcepta	*CERK Ab (#AP7088b)
Avanti Polar Lipids	*C16 Ceramide 1-phosphate
BioRad	*BCA protein assay kit *Electrophoresis buffer *Nitrocellulose membranes *Protein markers *Transfer buffer
Calbiochem-Novabiochem Corporation	*3-(4,5-dimethylthiazole-2-yl)-5-(3-carboxymethoxyphenyl)-2-(4-sulfophenyl)-2H-tetrazolium (MTS) *Phenazine methosulfate (PMS)
Cayman Chemical	*NBD-Ceramide
Cell Signaling Technology	*Akt Ab (#9272) *Phospho-Akt Ab (#9271) *Rabbit HRP Ab (#7074) *STAT3 Ab (#12640) *Phospho-STAT3 Ab (#9145) *Paxillin Ab (#2542) *Phospho-Paxillin Ab (#2541) *ERK1-2 Ab (#9102) *Phospho-ERK1-2 Ab (#9101) *PAK1 Ab (#2602) *Phospho-PAK1 Ab (#2601)
Gibco (Invitrogen)	*Dulbecco´s Modified Eagle´s Medium (DMEM) *Fetal Bovine Serum (FBS) *Newborn Calf Serum (NCS)
Lonza	*Ham´s F12K Medium

Merck	*Chloroform *Glycerol *Na_3HPO_4 *$Na_4P_2O_7$ *NVP-231 *Silicon dioxide (SiO_2)
Panreac	*Methanol *NaCl *Nonfat dried milk powder *Tris
Peprotech	*Mouse Leptin ELISA Development Kit
Santa Cruz Biotechnology, Inc.	*GAPDH Ab
Sigma-Aldrich	*3-isobutyl-1-methylxanthine (IBMX) *Acrylamide *Adenosine triphosphate (ATP) *Bovine Serum Albumin (BSA) *Bromophenol *Crystal violet *Dexamethasone *Dithiothreitol (DTT) *DMSO *EDTA *Fibronectin *Gentamicin *HEPES *Insulin *KCl *L-glutamine *LY294002 *Mercaptoethanol *Paraformaldehyde *PD98059 *Pertussis Toxin *Protease inhibitor cocktail (PIC) *Rosiglitazone *SDS *Tween-20
Thermofisher Scientific	*0.05% Trypsin-EDTA *Dimethylformamide (DMF) *SuperSignal® West Femto Maximun
Tocris	*AZD1480

*Stattic

1.2. Cell lines

1.2.1. 3T3-L1 cell line

The 3T3-L1 cell line is a mouse fibroblast cell line purchased from American Type Culture Collection (ATCC) (Manassas, VA, USA) and cultured following the manufacturer's indications. Cells were grown in 60.8 cm^2 dishes in DMEM supplemented with 10% heat-inactivated newborn calf serum (NCS), 50 mg/l gentamicin, 200 µM L-glutamine and 4.5 g/l glucose. Cells were incubated in a humidified 5% CO_2 incubator at 37 °C and subcultured every 3-4 days, before the culture reached 70% to 80% confluence.

These cells undergo a pre-adipose to adipose-like phenotype conversion, characterized by rapid proliferation that can be inhibited by contact. Relatively high levels of serum in the medium enhanced fat accumulation.

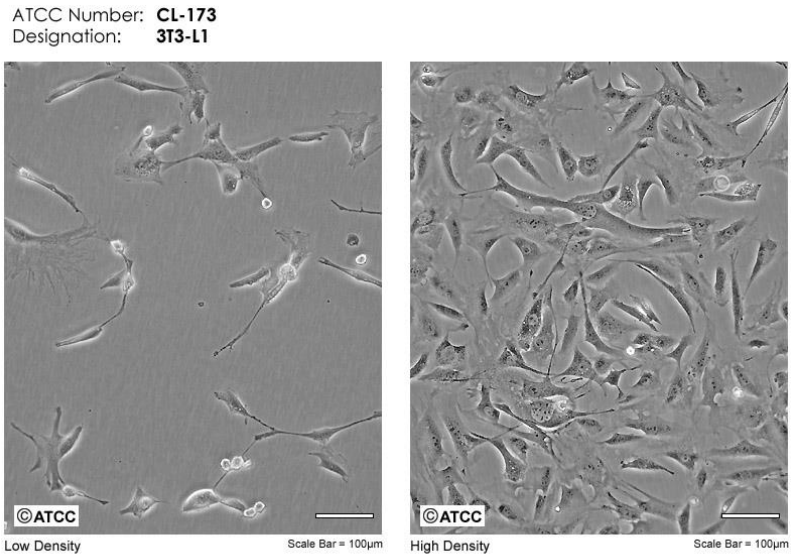

Figure 1. Micrograph of 3T3-L1 cells taken from the ATCC website.

1.2.2. NR8383 cell line

The NR8383 cell line is macrophage (alveolar) cell line derived from rat lung. It was purchased from American Type Culture Collection (ATCC) (Manassas, VA, USA) and cultured following the manufacturer's indications. Cells were grown in 60.8 cm^2 dishes in Ham's F12K supplemented with 15% heat-inactivated fetal bovine serum (FBS), 50 mg/l gentamicin, 200 µM L-glutamine and 1 g/l glucose. Cells were incubated in a humidified 5% CO_2 incubator at 37 °C and subcultured every 3-4 days, before the culture reached 70% to 80% confluence.

The NR8383 cell line provides a homogenous source of highly responsive alveolar macrophages which can be used in vitro to study macrophage related activities.

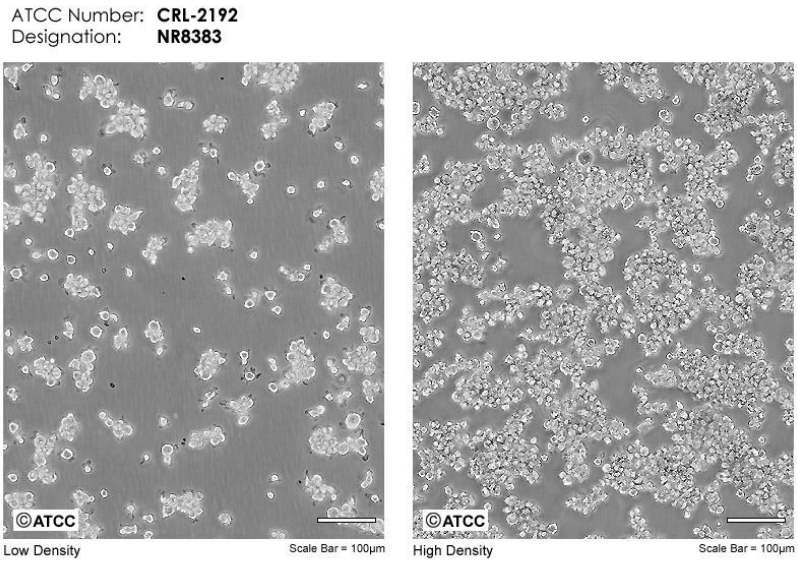

Figure 2. Micrograph of NR8383 cells taken from ATCC website.

2. Methods

2.1. Delivery of C1P to cells in culture

An aqueous dispersion (in the form of liposomes) of C1P was added to cultured cells as previously described [1-3]. Specifically, stock solutions were prepared by sonicating C1P (5 mg) in sterile nanopure water (3 ml) on ice using a probe sonicator until a clear dispersion was obtained. The final concentration of C1P in the stock solution was ≈2.62 Mm in all cases. This procedure is considered preferable to dispersions prepared by adding C1P in organic solvents, because droplet formation in minimized and there are no organic solvent effects on the cells. C1P was then added to the culture in the micromolar range (2 – 40 μM).

2.2. 3T3-L1 preadipocytes differentiation protocol

3T3-L1 cells (20.000-30.000 cells/ cm^2 of the plate) were cultured and grown in DMEM supplemented with 10% newborn calf serum (NCS) until they were about 90-100% confluent. Confluent cells were further incubated for 2 days. Then, confluent cells (day 0) were treated with adipogenic induction medium (DMEM 10% FBS + 0.5 mM IBMX + 1 μg/ml insulin + 0.25 μM dexametasone + 2 μM rosiglitazone) with or without agonists or inhibitors. After 2 days, the medium was removed and cells were further incubated in adipogenesis maintenance medium (DMEM 10% FBS + 1 μg/ml insulin) with or without agonists or inhibitors for another 2 days. Cells were then fed every two days with DMEM supplemented with 10% FBS and 1 μg/ml insulin, with or without agonists or inhibitors. Agonists and/or inhibitors were added every time the medium was changed.

2.3. Determination of CERK activity using NBD-Ceramide as the enzyme substrate in cell homogenates

Each cell type was seeded under different conditions in 6-well plates. After each specific treatment, cells were washed twice with phosphate-buffered saline (PBS) and scrapped in 80 μl of homogenization buffer (20 mM HEPES pH 7.4; 150 mM NaCl; 1 mM DTT + protease inhibitor cocktail (PIC) (1000:1)). Then, the cells were lysed with

three freeze-thaw cycles (in methanol and dry ice) and sonicated. The activity of CERK was measured using a fluorescent assay that was adapted for a microplate reader, according to Don and Rosen [4]. Briefly, cell lysates (50-100 µg total protein in 100 µl of homogenization buffer) were mixed with 2x reaction buffer (100 µl, 40 mM HEPES, 20 mM KCl, 30 mM $MgCl_2$, 20% glycerol, 2 mM DTT, 0.4 mg/ml BSA, 2 mM ATP) containing 20 µM NBD-ceramide. Reactions were allowed to proceed for 20 minutes at 35 °^{o}C in the dark before the lipid extraction was performed. Then, 250 µµl chloroform:methanol (2:1) was added and samples were vortexed and centrifuged at 21,800 g for 30 seconds. Then 100 µl of the upper aqueous phase, containing the NBD-Cer1-P, was transferred to a black 96-well plate and 100 µl of dimethylformamide (DMF) was added before reading the plate. The NBD fluorescence was measured with a Synergy HT (Biotek) plate reader equipped with Gen5 software. NBD fluorescence was quantified using a 495 nm excitation filter and a 520 nm emission filter.

2.4. Quantitative Enzyme-Linked ImmunoSorbent Assays (ELISA)

2.4.1. Determination of leptin concentration in white adipose tissue

White adipose tissue was thawed and homogenized with 1 ml ice-cold homogenization buffer (50 mM HEPES, 137 mM NaCl, 1 mM $MgCl_2$, 1 mM $CaCl_2$, 1% (v/v) NP-40, 10% (v/v) glycerol, 2.5 mM EDTA, 10 mM $Na_4P_2O_7$, 1 µg/ml protease inhibitor cocktail). Then, homogenates were sonicated and centrifuged at 10,000 g for 10 minutes at 4 ºC and the supernatant was then used for the ELISA assay. In order to determine the protein concentration of each sample, a BCA protein assay kit (from Bio-Rad) was used.

Leptin concentration was determined using a “Mouse Standard ELISA Development Kit” (PeproTech) for each cytokine according to the manufacturer’s protocol.

Briefly, a 96-well high reactivity plates were precoated with a specific cytokine antibody for leptin, and incubated overnight. The next day, wells were washed 4 times with wash buffer (0.05% Tween 20 in PBS) and blocked with 1% bovine serum albumin

(BSA) in PBS for 1 hour. Samples were diluted at a 1:3 dilution rate and 100 µµl of each diluted sample was then added in duplicate to the wells. Along with the samples, serial dilutions of a standard solution for the cytokine were also added to the plate. Samples were incubated for 2.5 hours and after incubation, wells were washed again and the biotinylated-detection antibody was added. This antibody binds to the leptin capture antibody complexes. After 2 hour incubation at room temperature and subsequent washes, an Avidin-HRP solution was added to the wells and reactions with biotinylated-detection antibody were allowed to proceed for 30 minutes. After the last wash step, a 2,2'-Azino-bis(3-ethylbenzothiazoline-6-sulfonic acid) diammonium salt (ABTS) solution was added as a substrate. The reaction catalyzed by the enzyme in the presence of the ABTS substrate produces a chromophoric product that enables a colorimetric change (Figure 3). The absorbance was then read at 405 and 650 nm using a PowerWave™ XS (BioTek) microplate reader provided with Gen5 software. To process the data correctly, the absorbance values obtained at 650 nm were subtracted from the values obtained at 405 nm so as to avoid possible interference caused by other possible components in the samples, and the standard solutions were used to perform a calibration curve. Sample concentration values (pg/ml) obtained by the calibration curve were normalized considering the total volume of the supernatants collected and the protein quantity in each sample (pg/mg protein).

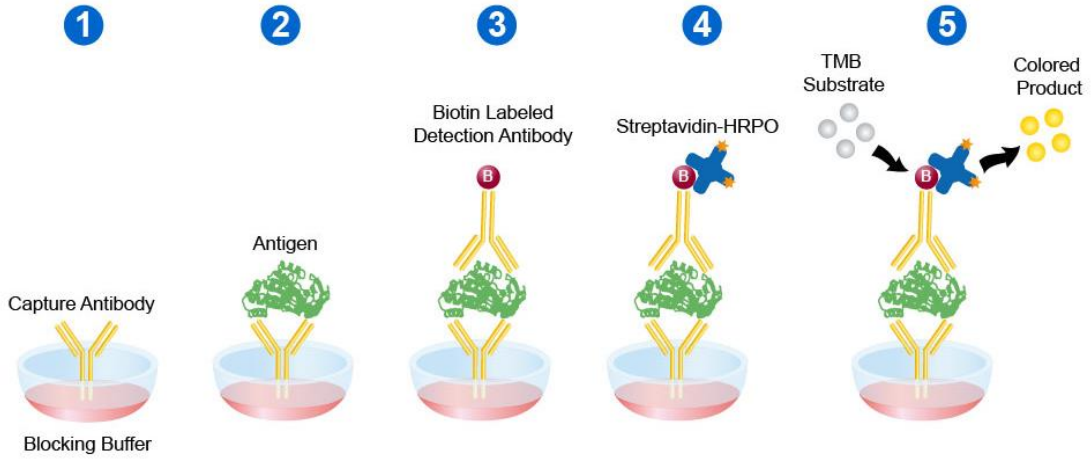

Figure 3. Schematic representation of sandwich ELISA format experiment. Taken from Leinco Technologies website.

2.5. Cell viability assay (MTS-Formazan method)

Cell viability and proliferation were determined using the MTS-formazan colorimetric assay. This assay is based on the rate of reduction of the tetrazolium dye, 3-(4,5 dimethylthiazol-2-yl)-5-(3-carboxymethoxyphenyl)-2-(4-sulfophenyl)-2H-tetrazolium or MTS. MTS in the presence of phenazine methosulfate (PMS) (5% v/v diluted in phosphate-buffered saline (PBS) containing Mg^{2+} and Ca^{2+}), reacts with mitochondrial dehydrogenases producing a formazan product that has a maximum absorbance at 490-500 nm in PBS. Generated formazan is proportional to the number of viable cells in culture for up to 15.000 cells. (Figure 4, taken from P. Gangoiti's thesis, unpublished).

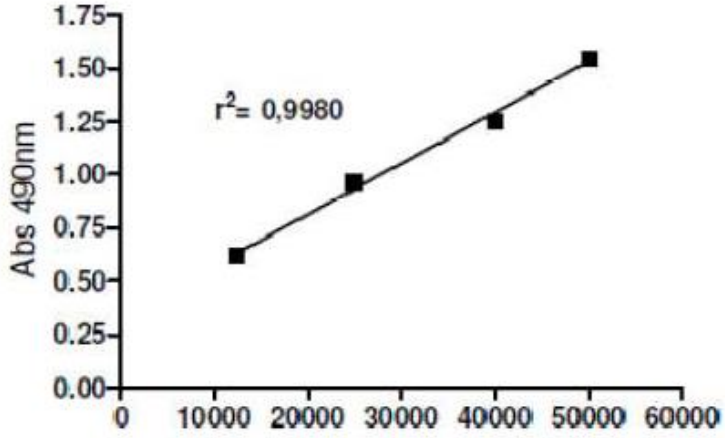

Figure 4. Generated formazan is proportional to the number of viable cells in culture. The indicated cell number was seeded in 96-wells plates in RPMI 1640 supplemented with 10% FBS and 20% L-cell conditioned medium. 20 µl MTS/PMS was added into each well and after 2 hours absorbance was measured at 490nm. The absorbance of the medium (without cells) was subtracted from each absorbance value and results are the mean ± SEM of three independent experiments. R2= 0.998 indicates the linearity between cell number and absorbance values.

- 3T3-L1 cells were seeded at 9 ₓ× 10^3 cells/well in 96-well plates and incubated overnight in DMEM supplemented with 10% NCS. The next day, the medium

was replaced with fresh NCS-free media in the presence or in the absence of agonists and/or inhibitors and cells were incubated for 24 hours.

- NR8383 cells were seeded at 20 $_x\times 10^3$ cells/well in 96-well and incubated for 2 hours in serum-free Ham's F12K. After 2 hours of incubation, agonists and/or inhibitors were added and cells were incubated for 24 hours.

2.6. Crystal violet proliferation assay

Adherent cells, as their name suggests, adhere to cell culture plates. For this reason, the more adherent cells there are, the more cell proliferation there has been. One simple method to detect maintained adherence of cells is the staining of attached cells with crystal violet dye, which binds to proteins and DNA. In the same way, adherent cells detach from cell culture plates during cell death. These characteristics can be used for the indirect quantification of cell death and to determine differences in proliferation upon stimulation with death-inducing or mitogenic agents. Indeed, cells that undergo cell death lose their adherence and are subsequently lost from the population of cells, reducing the amount of crystal violet staining in a culture.

Each cell type was seeded under different conditions in order to obtain the desired confluency:

- 3T3-L1 cells were seeded in 96-well plates at 9×10^3 cells/well and were grown in DMEM containing 10% NCS for 24 hours at 37 ººC to ensure the adhesion of cells to wells.

Then, the proliferation assay was performed using the method described by Feoktistova M. et al, [5]. Briefly, the culture medium was removed and fresh medium (100 µl/well) containing the required agonists or antagonists was added. The cells were then incubated for the desired time and conditions. After that, the medium was removed, the wells were washed twice with PBS and 50 µl/well of 0.5% crystal violet staining solution (20% methanol in distilled water) was added. After 20 minutes of

incubation at room temperature, wells were washed again with PBS and the plate was dried at room temperature for 24 hours. 200 µl of methanol were added to each well and the plate was incubated with its lid on for 20 minutes before the optical density was measured at 570 nm (Figure 5).

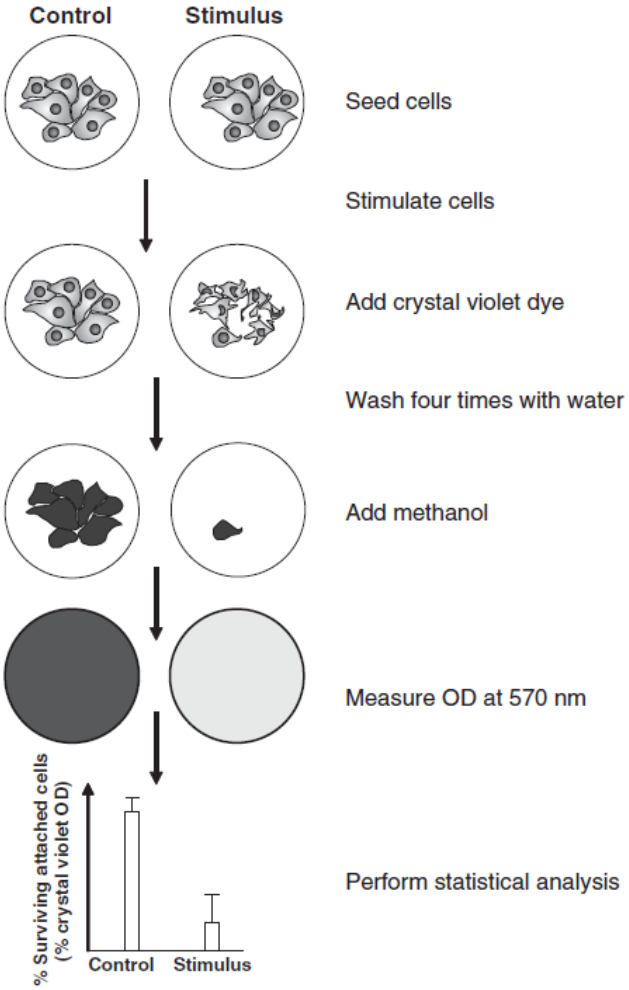

Figure 5. Schematic representation of crystal violet proliferation assay. Taken from [5].

2.7. Determination of cell migration

Cell migration was measured using the Boyden-chamber based cell migration assay, also called transwell migration assay. Twenty four-well chemotaxis chambers (Transwell, Corning Costar) were used for the experiments. Before starting the

migration experiments, the filters of transwell chambers were precoated with 30 µµl of fibronectin (0.2 µg/ µl) to allow cell attachment. Cells were added to the wells in a volume of 100 µl in serum-free medium supplemented with 0.2% fatty-acid free BSA. The number of cells seed depended upon cell type: 5 x 10^4 cells for preadipocytes 3T3-L1 and 10 x 10^4 cells for the alveolar NR8383 macrophages. All cells were added to the upper wells of the 24-well chemotaxis chambers. Agonists diluted in 300 µµl medium supplemented with 0.2% BSA were then added to the lower wells. The cells were incubated in the upper chamber for 2 hours in a cell incubator in order to ensure cell adhesion. When used, inhibitors were added to the upper wells and were pre-incubated for 1 hour prior to agonist addition. Then, inhibitors and agonists were added to the lower wells and next, chambers holding the cells were moved into the lower compartments (Figure 6).

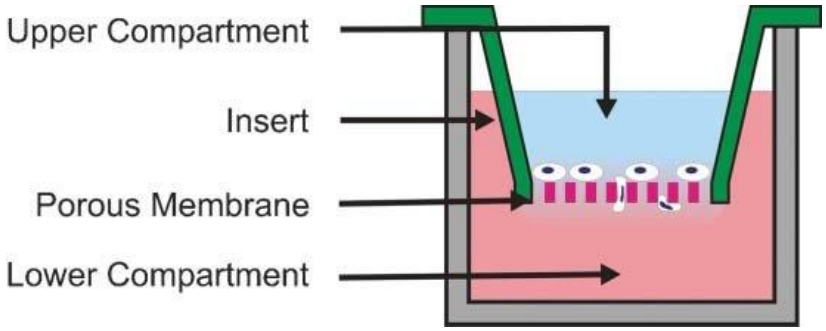

Figure 6. Schematic representation of a Boyden-chamber based cell migration assay. Taken from [6].

After the indicated incubation time, non-migrated cells were removed with a cotton swab, and the filters were fixed with Formaldehyde (5% in PBS) for 20 minutes. Then, formaldehyde was removed and the filters were stained with crystal violet solution (0.1% in PBS) for 20 minutes. After washing the crystal-violet dye with water, the filters were placed on microscopy slides using mineral oil, avoiding bubbles between slides and coverslips. Cell migration was measured by counting the number of migrated cells in a Nikon Elipse 90i microscope equipped with the NIS-Elements 3.0 software. Cells were counted in 8 randomly selected microscopy fields per well, at

100× magnification. The number of migrated cells was normalized by the number of migrated cells in the control chambers.

2.8. Western blotting

Each cell type was seeded under different conditions in order to obtain the desired confluency and protein concentration, using appropriate culture medium for each particular cell type according to the supplier:

- 3T3-L1 cells were incubated in 6-well plates at 1.5 x 10^5 cells/well and were grown in DMEM containing 10% NCS until they were about 90-100% confluent.

- NR8383 cells were incubated in 6-well plates at 1 x 10^6 cells/well and were grown in Ham's F12K containing 15% FBS until they were about 90-100% confluent.

Then, all cell types were incubated with or without agonists for the indicated incubation times in serum-free medium. Cells were then washed with PBS and harvested with ice-cold lysis buffer (50 mM HEPES, 137 mM NaCl, 1 mM $MgCl_2$, 1mM $CaCl_2$, 1% (v/v) NP-40, 10% (v/v) glycerol, 2.5 mM EDTA, 10 mM $Na_4P_2O_7$, 1 µg/ml protease inhibitor cocktail). Samples were lysed by sonication and protein concentration was determined with a BCA protein assay kit (from BioRad). Samples (1-2 µg/µl protein sample) were mixed with 4x loading buffer (125 mM Tris pH 6.8, 50% (v/v) glycerol, 4% SDS, 0.08% (p/v) bromophenol and 50 µµl/ml mercaptoethanol). Samples were then heated at 90ºC for 10 minutes and loaded into polyacrylamide gels (15%, acrylamide) to perform protein separation by SDS-PAGE. Electrophoresis was run at 120 V for 2 hours approximately in electrophoresis buffer (1.92 M glycine, 0.25 M Tris-HCl and 1% SDS). Proteins were then transferred into nitrocellulose membranes. Transference was run at 400 mA for 1 hour and 15 minutes in ice-cold transfer buffer (14.4 g/l glycine, 3 g/l Tris and 20% methanol). Nitrocellulose membranes were blocked for 1 hour with 5% skim milk in Tris-Buffered Saline (TBS) containing 0.01% NaN_3 and 0.1% Tween 20, pH 7.6, so as to avoid unspecific binding of antibodies. The skim milk was then removed and nitrocellulose membranes were incubated overnight with primary antibody diluted in TBS/0.1% Tween (1:1000) at 4 ºC. After three washes

with TBS/0.1% Tween 20, membranes were incubated with Horseradish Peroxidase (HRP)-conjugated secondary antibody at 1:5000 dilution in TBS/0.1% Tween 20 for 1 hour. Bands were visualized by enhanced chemiluminescence and exposed films were analyzed with an ImageLab (BioRad) software in order to quantify the intensity of bands. Results were expressed as arbitrary units and were normalized to total protein bands.

2.9. Preparation of granular nanosized silica (SiO_2)-conditioned medium in NR8383 alveolar macrophages

NR8383 alveolar macrophages were seeded in 6-well plates (2.3 x 10^6 cells/well) and were grown in Ham´s F12K supplemented with 15% FBS. The next day, the medium was replaced with fresh medium without serum. After 2 hours of incubation, vehicle or 50 µg/ml of SiO_2 were added and cells were further incubated for 16 hours. Thereafter, the cells were removed by centrifugation at 400 g for 5 minutes and particles were removed by centrifugation at 15,000 g for 10 minutes at room temperature. The supernatants were immediately used as SiO_2-conditioned medium in further experiments.

2.10. Statistical analyses

Statistical analyses were performed using two-tailed Student`s t-test, with the level of significance set at $p<0.05$.

Symbol	Significance
n.s	p>0.05, not significant
*	p<0.05
**	p<0.01
***	p<0.001

The # symbol was used instead of the * symbol for comparison of values between inhibitor-treated cells versus C1P-treated cells.

3. References

1. Gangoiti P, Granado MH, Wang SW, Kong JY, Steinbrecher UP, Gómez-Muñoz A. Ceramide 1-phosphate stimulates macrophage proliferation through activation of the PI3-kinase/PKB, JNK and ERK1/2 pathways. Cell Signal. 2008; 20(4): 726-36.
2. Gómez-Muñoz A, Kong JY, Parhar K, Wang SW, Gangoiti P, González M, et al. Ceramide-1-phosphate promotes cell survival through activation of the phosphatidylinositol 3-kinase/protein kinase B pathway. FEBS Lett. 2005; 579(17): 3744-50.
3. Gómez-Muñoz A, Kong JY, Salh B, Steinbrecher UP. Ceramide-1-phosphate blocks apoptosis through inhibition of acid sphingomyelinase in macrophages. J Lipid Res. 2004; 45(1): 99-105.
4. Don AS, Rosen H. A fluorescent plate reader assay for ceramide kinase. Anal Biochem. 2008; 375(2): 265-71.
5. Feoktistova M, Geserick P, Leverkus M. Crystal Violet assay for determining viability of cultured cells. Cold Spring Harb Protoc. 2016; 2016(4): 343-46.
6. Keenan TM, Folch A. Biomolecular gradients in cell culture systems. Lab Chip. 2008; 8(1): 34-57.

Chapter 1

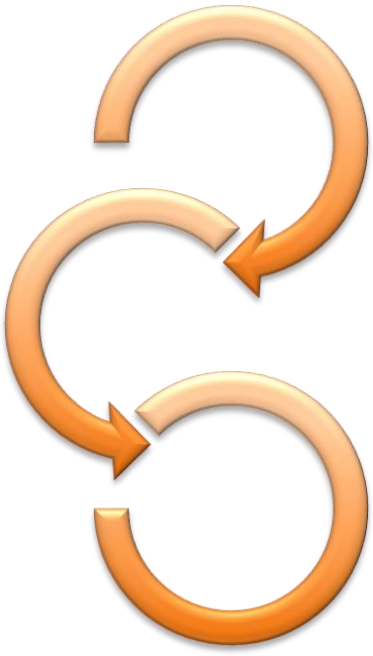

CHAPTER 1:

Implication of C1P in preadipocyte proliferation and migration

1. Introduction

1.1. Adipose tissue

Adipose tissue (AT) accounts for 20 to 28 % of body mass of healthy individuals, a percentage that varies according to gender and energy status, and belongs to the group of connective tissues that confer cohesion to organs or systems [1]. Based on the location, the adipose tissue can be classified as subcutaneous adipose tissue, localized under the skin and which represents the highest proportion, or visceral adipose tissue, which resides in the cavities of the body and surrounds the organs, especially the kidney, the intestines, the gonads, the vasculature and the heart.

The classical role of AT is to insulate, give support to body structures, take up free fatty acids (FFAs) after food intake, store those FFAs (mainly in the form of triacylglycerols) and to release FFAs during the fasting state to ensure sufficient energy status. During the postprandial phase (the phase that occurs after food intake), FFAs are taken up from the blood in AT after hydrolysis of triacylglycerols from triacylglycerol-rich lipoproteins (such as very low-density lipoprotein (VLDL) and chylomicrons) by lipoprotein lipase (LPL) and they are esterified to triacylglycerols and stored in the adipocytes. During the fasting state, nevertheless, mobilization of the adipocyte triacylglycerol occurs by their hydrolysis by hormone sensitive lipase (HSL). Insulin is the main regulator of adipocyte fat content, since it is both a potent inhibitor of HSL and an important activator of LPL [2].

Recently, AT was shown to be not only an energy store or a passive organ of metabolism, but also it has been considered an endocrine organ capable of secreting hormones and cytokines that travel through the bloodstream to reach their target tissues. Among others we can find hormones and cytokines involved in glucose

metabolism (e.g. adiponectin, resistin), lipid metabolism (e.g. cholesteryl ester transfer protein, CETP), inflammation (e.g. TNF-α, IL-6), coagulation (PAI-1), blood pressure (e.g. angiotensinogen, angiotensin II) and feeding behaviour (leptin) [2]. Other adipose tissue functions refer to the regulation of physiological processes such as sexual dimorphism, immunity, reproduction, adipogenesis, angiogenesis, extracellular matrix restructuring, body homeostasis and maintenance of body temperature [3, 4].

The performance of these functions is conferred by the variety of cell types that compose the adipose tissue. Indeed, the AT is characterized by a marked cellular heterogeneity. Among its cellular components, we can find adipocytes, preadipocytes, fibroblasts, endothelial cells and multipotent stem cells, which are able to differentiate into several cell types. Overall, fat tissue is composed of approximately one-third of mature adipocytes, a main cellular component, surrounded by supporting connective tissue that is highly vascularized and innervated. The remaining two-thirds of AT is a combination of small mesenchymal stem cells (MSCs), T regulatory cells, endothelial precursor cells, macrophages and preadipocytes in various stages of development [5].

There are three types of AT according to their functions, coloration, vascularization and structure: white adipose tissue (WAT), brown adipose tissue (BAT) and beige adipose tissue (BEAT).

1.1.1. White adipose tissue (WAT)

WAT is characterized for being a white or yellow tissue with less vascularization and innervation that BAT. White adipocytes have a size that ranges from 20 to 200 μm and contain single and large lipid droplets that appear to comprise the majority of cell volume, while the cytoplasm and nucleus are found at the cell periphery. In those droplets lipids are stored for use when there is energy demand. Of the totality of lipids stored, 90 – 99 % are triacylglycerols.

Although WAT is the main source of energy and its main function is to control energy balance by triacylglycerol storage and mobilization, it also plays a pivotal role as endocrine and paracrine organ. Indeed, WAT mediates numerous physiological and

pathological processes by secreting factors (adipokines and lipokines) that control glucose and lipid metabolism, appetite, immunological responses, inflammatory responses, angiogenesis, blood pressure regulation and reproductive function [6, 7].

1.1.2. Brown adipose tissue (BAT)

The brown coloration of BAT is due to the fact that it is more vascularized and has a high content of mitochondria, which, in turn, have cytochromes, which are responsible for giving colour. Brown adipocytes are typically ellipsoid in shape and range from 15-50 μm in size and contain multilocular lipid droplets. The nucleus of these cells is relatively centralized within the cytoplasm and all other classical organelles are present. The hallmark components of brown adipocytes are their abundant distribution of cristae-rich mitochondria and the largely exclusive expression of the proton transporter uncoupling protein-1 (UCP1).

Unlike WAT, BAT does not have the function of storing energy, but it dissipates energy through thermogenesis. β-adrenergic receptor activation in BAT promotes the stimulation of UCP proteins, which use oxidative phosphorylation proton flow in order to produce heat instead of ATP.

1.1.3. Beige adipose tissue (BEAT)

Recently, adipose cells similar to brown adipocytes, with beige coloration and positive for UCP expression, were shown to be likely to appear in response to certain stimuli such as exercise, exposure to cold or some hormones [8]. They can accumulate in WAT typical deposits and have been called beige or “brite” adipocytes (a combination of the terms brown and white).

Under basal conditions, beige adipocytes express a signature of molecular markers that is similar to that of white adipocytes, but after the mentioned stimuli, they acquire an expression pattern similar to that of brown adipocytes [9].

1.2. Obesity and adipose tissue dysfunction

According to the World Health Organization (WHO), overweight and obesity are defined as the condition where excess or abnormal fat accumulation increases risks to health. Since 1975, the prevalence of obesity has tripled worldwide and is still increasing, currently becoming in one of the biggest health issues that affects all age groups, populations and countries of all income levels [10]. Based on data updated in June 2021 by the WHO, at the end of 2016 more than 1.9 billion adults were overweight. Of these, more than 650 million adults were obese. Overall, 39% of the world's adult population was overweight and about 13% was obese. Furthermore, it is estimated that over 340 million children aged 5-19 were overweight or obese in 2016 [11].

Depending on the degree, duration and the distribution of the excess of adipose tissue, obesity could be associated with various metabolic diseases, such as, hypertension [12], dyslipidemia [13], type II diabetes (T2D) and insulin resistance (IR) [14-16], non-alcoholic fatty liver disease [17, 18], cardiovascular diseases [19-22] and certain forms of cancer [23-25], which increase obesity-associated morbidity and mortality.

From a biochemical perspective, obesity is the result of an imbalance where energy intake exceeds energy expenditure over time. This energy excess leads to fat accumulation, causing an increase in the size of the AT. AT can increase in size in one of two main ways: hypertrophy (increase in size of existing adipocytes) or hyperplasia (formation of new adipocytes through differentiation of resident precursors known as preadipocytes) [26]. Although the number of adipocytes in a given depot is primarily determined early in life and is mostly stable through adulthood [27, 28], during prolonged caloric excess new adipocytes can emerge from differentiation of preadipocytes and can contribute to adipose tissue expansion [29, 30].

The fat accumulation and expansion of AT is associated with local and systemic chronic state of low-grade adipose tissue inflammation. This inflammatory state is

characterized by an increase of immune cell infiltration into obese adipose tissue and increase production and secretion of pro-inflammatory factors (adipokines) into the bloodstream. Alterations in adipokine levels and chronic inflammation in the AT exert profound effects on metabolic pathways, leading to the development of metabolic disorders [31, 32] (Figure 1).

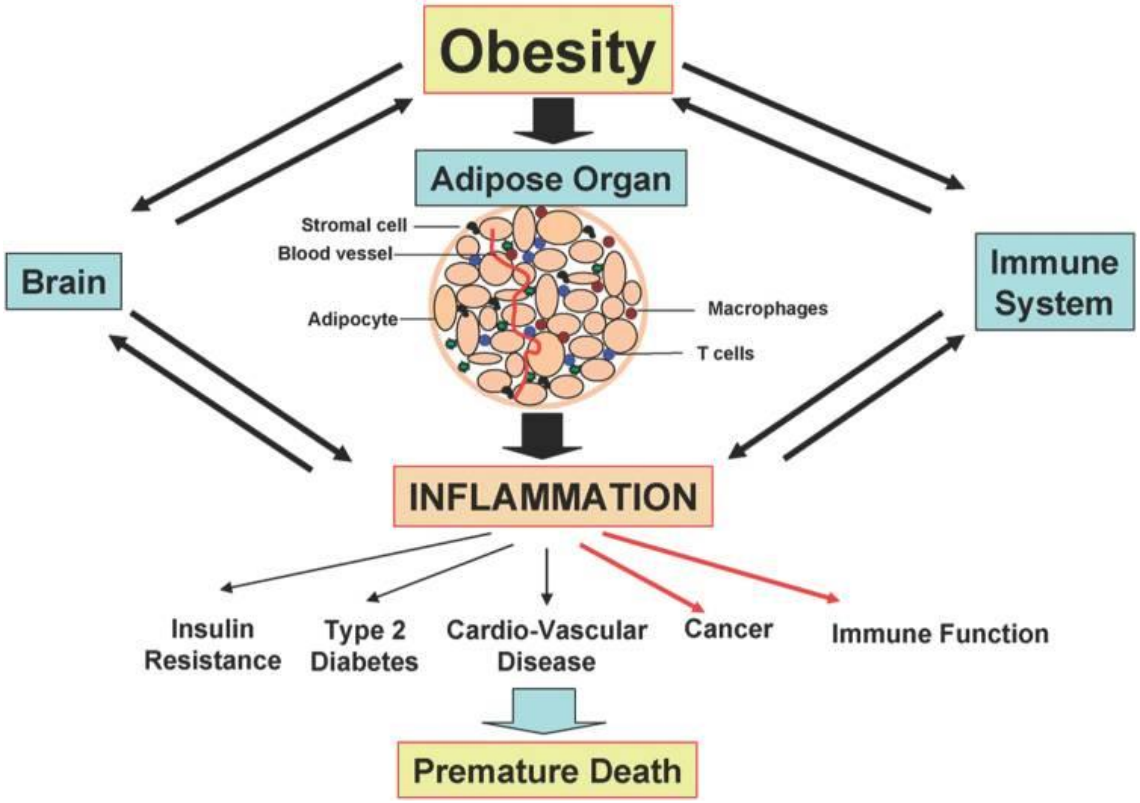

Figure 1. Obesity-associated diseases. Obesity-related inflammation is responsible for secondary disease states of obesity. Taken from [33].

Therefore, understanding the mechanisms that control not only adipogenesis, but also the proliferation of preadipocytes would be an effective approach for developing new strategies for prevention and treatment of obesity-related diseases. Moreover, the study of mechanisms that control the migration of preadipocytes to different fat depots of our body would be also an optimal approach for the mentioned issue.

1.3. Adipogenesis

Adipogenesis is the process by which undifferentiated fibroblast-like preadipocytes are converted to differentiated adipocytes. This process is divided in two different phases: the first phase is named “determination phase”, while the second one is referred to as “terminal differentiation”.

From the transcriptional point of view, the early stage is controlled by members of the CCAAT/enhancer binding proteins (C/EBPs) transcription factors, such as C/EBPβ, which allows the expression of multiple cell-cycle related genes to facilitate mitotic clonal expansion (MCE), a required step for terminal differentiation. C/EBPs are also responsible for the initiation of the second state. However, the late stage of adipocyte differentiation is mainly controlled by peroxisome proliferator-activated receptor gamma transcription factor (PPARγ), which is considered the master regulator of adipogenesis [34] (Figure 2).

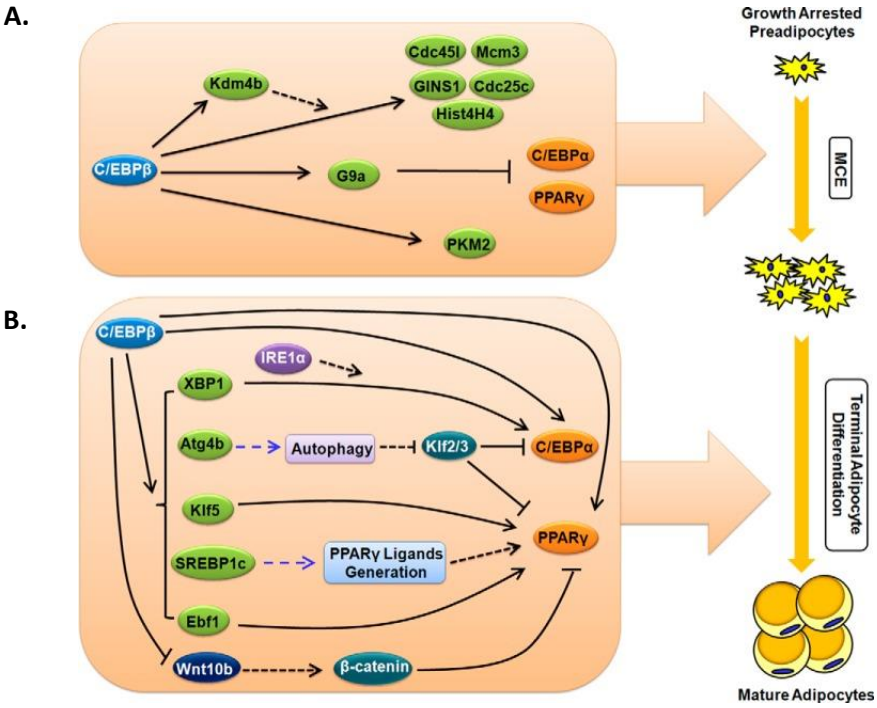

Figure 2. Transcriptional regulation during adipogenesis. A) At the early stage C/EBPs transactivates the expression of multiple cell cycle-related genes to facilitate MCE, a required step for terminal differentiation. B) At the late stage, up-regulation of PPARγ occurs, thereby promoting terminal differentiation. Taken from [35].

One of the most extensively characterized and used cell system for studying adipogenesis is the 3T3-L1 mouse preadipocyte cell line. These cells are derived from Swiss 3T3 mouse embryos and require a glucocorticoid-supplemented differentiation cocktail for induction of adipogenesis [36-38].

1.4. Sphingolipids in obesity

In recent years, the contribution of aberrant production of bioactive lipids to pathophysiological changes associated with obesity has risen to the forefront of lipid research. Indeed, several lines of evidence suggest that sphingolipids or the enzymes involved in their metabolism not only regulate vital cellular functions such as proliferation, apoptosis, autophagy, migration or cell differentiation [39-41], but are also implicated in inflammatory responses [42-45] and in the pathogenesis of a variety of inflammation-associated diseases including atherosclerosis, obesity, diabetes and cancer [46-54].

In particular, ceramides have been associated with insulin resistance and the development of type II diabetes, and sphingosine and sphingosine 1-phosphate levels are altered in the obese state [55, 56]. Another important ceramide metabolite is ceramide 1-phosphate (C1P), which was initially demonstrated to be a relevant regulator of cell proliferation and survival [57-64] and to actively participate in inflammatory responses [44, 65]. However, the mechanisms or signaling pathways by which C1P exerts its biological actions have only been partially described.

Understanding the molecular mechanisms that regulate the proliferation, survival and migration of preadipocytes can be a crucial step for developing novel therapeutic strategies to control obesity and obesity-related pathologies. For this reason, the purpose of this study was to assess whether C1P might be able to regulate those biological processes and to elucidate the mechanisms or signaling pathways by which C1P might exert its biological actions.

2. Results

2.1. Adipogenic induction medium (AIM) induces 3T3-L1 cell differentiation

3T3-L1 cells have the capacity to differentiate from a fibroblast phenotype to mature adipocytes and are widely used for studying adipogenesis and the biochemistry of adipocytes. In the present study, we first examined whether adipogenic induction medium (AIM), which is a culture medium consisting of DMEM supplemented with 10% NCS and an adipogenic cocktail composed of 0.5 mM IBMX, 1 µg/ml insulin, 0.25 µM dexamethasone and 2 µM rosiglitazone, could induce 3T3-L1 cell differentiation.

Induction of 3T3-L1 cell differentiation triggers deep phenotypical changes of preadipocytes that become spherical and filled with lipid droplets. To confirm that phenotypical change, 3T3-L1 cells were treated with AIM and then time-lapse micrographs of 3T3-L1 cells were taken after AIM treatment. Figure 3 shows that indeed, AIM induces 3T3-L1 cell differentiation.

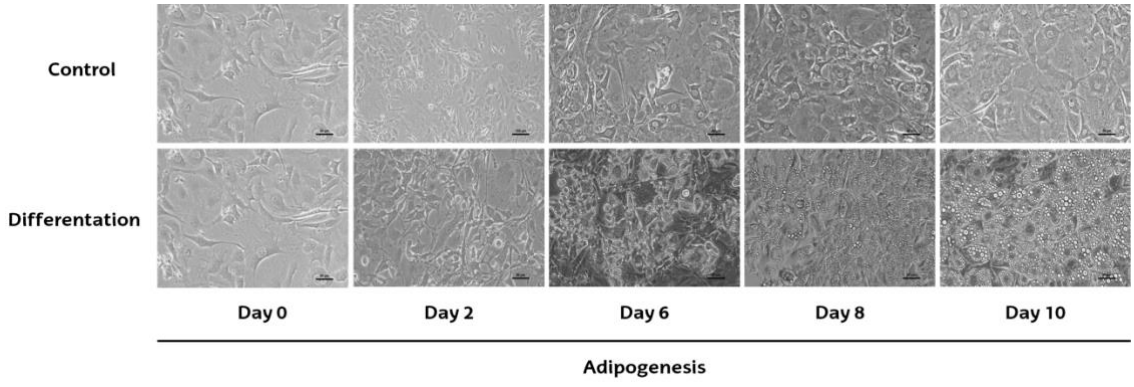

Figure 3. Adipogenic induction medium (AIM) promotes 3T3-L1 cell differentiation. 3T3-L1 cells were seeded in 6-well plates (2 x 10^5 cells/well) and they were grown in DMEM containing 10% NCS until they were about 90-100% confluent. Cells were further incubated for 2 days before inducing cell differentiation. After two days, cells were subjected to adipogenic induction media (AIM) in order to induce cell differentiation, as described in *Materials and Methods*. At the indicated time points, cells were visualized with a Nikon Eclipse TS100 microscope at 200x magnification.

In addition to fat droplets, leptin secretion was also tested. Leptin is a hormone highly secreted by adipocytes in the obese state and its role is to regulate fat storage, so it is an appropriate adipogenic biomarker to confirm whether AIM induces 3T3-L1 cell differentiation. It was observed that 10 days after induction of differentiation, when most of cells are already differentiated, leptin secretion was significantly increased (Figure 4).

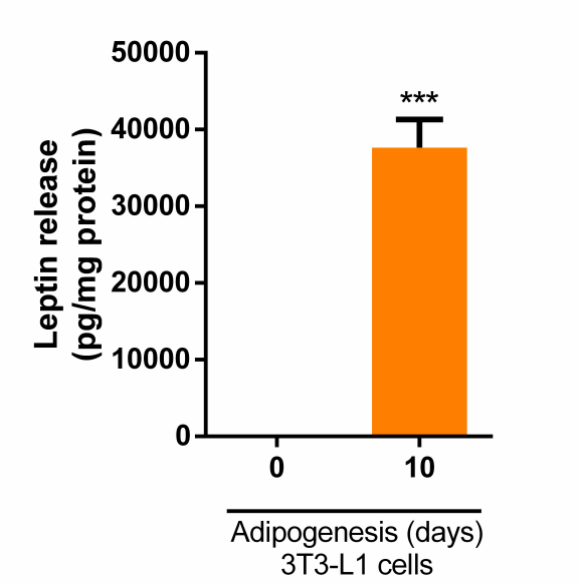

Figure 4. Adipogenic induction medium (AIM) induces leptin release in 3T3-L1 cells. 3T3-L1 cells were seeded in 6-well plates (2 x 10^5 cells/well) and they were grown in DMEM containing 10% NCS until they were about 90-100% confluent. Confluent cells were further incubated for 2 days before inducing cell differentiation. After two days, cells were subjected to adipogenic induction media (AIM) in order to induce cell differentiation, as described in *Materials and Methods*. Then, culture medium was collected at indicated time points, centrifuged and the cells were harvested in lysis buffer in order to measure protein concentration. The leptin concentration in supernatant was measured using an ELISA kit, as indicated in *Materials and Methods*. Results are normalized to the protein concentration and are the mean ± SEM of 5 independent experiments performed in duplicate (***$p<0.001$).

2.2. CERK expression and activity are increased in differentiated 3T3-L1 adipocytes

Sphingolipid metabolism has been previously described to be implicated in the pathogenesis of a variety of diseases including obesity, diabetes, and cardiovascular

diseases [46-53]. Due to the importance of this group of lipids in obesity-associated diseases and taking into consideration that the ceramide content is decreased in differentiated 3T3-L1 adipocytes [66], we hypothesized that ceramide kinase (CERK), the enzyme that converts ceramide to C1P, might be implicated in this process. To address this question, 3T3-L1 cell differentiation was induced with AIM and CERK expression and activity were measured. As shown in Figure 5, CERK expression gradually increased in 3T3-L1 adipocyte differentiated cells.

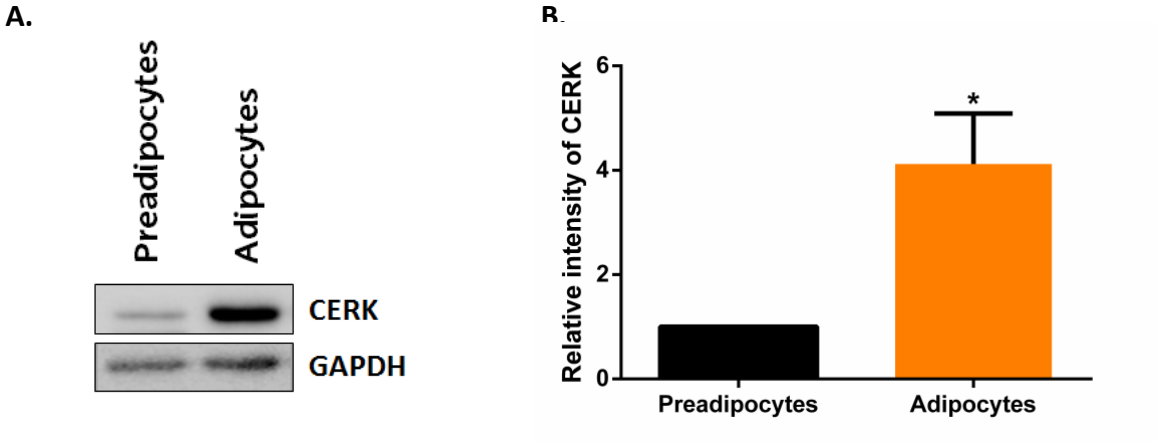

Figure 5. CERK expression increases in differentiated 3T3-L1 adipocytes. 3T3-L1 cells were seeded in 6-well plates (2 x 10^5 cells/well) and grown in DMEM containing 10% NCS (GM) until they were about 90-100% confluent. Cells were then further incubated for 2 days before inducing cell differentiation. After two days, cells were cultured in either GM or AIM. GM-treated cells were maintained in DMEM 10% NCS whereas AIM-treated cells were induced to differentiate until day 10, as described in *Materials and Methods*. A) On day 10 after induction of differentiation, cells were harvested and processed for Western blot analysis. CERK expression was detected by Western blotting using a specific antibody to CERK and equal loading of protein was assessed with an antibody against GAPDH. B) Results of the scanning densitometry of exposed film. Data are expressed as arbitrary units of intensity and are the mean ± SEM of 4 independent experiments (*$p<0.05$).

The parallel increase of CERK during adipogenesis was also tested with a direct enzyme assay. We observed that CERK activity was higher in differentiated adipocytes, whereas preadipocytes showed less enzyme activity (Figure 6).

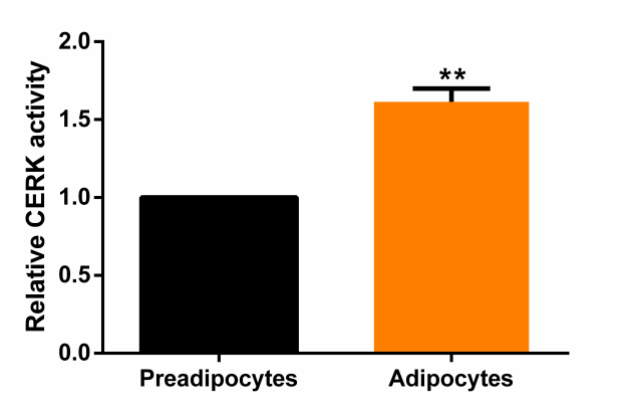

Figure 6. CERK activity is increased in differentiated 3T3-L1 adipocytes. 3T3-L1 cells were seeded in 6-well plates (2 x 10^5 cells/well) and they were grown in DMEM containing 10% NCS (GM) until they were about 90-100% confluent. Confluent cells were further incubated for 2 days before inducing cell differentiation. After two days, cells were cultured in either GM or AIM. GM-treated cells were maintained in DMEM 10% NCS whereas AIM-treated cells were induced to differentiation until day 10, as described in *Materials and Methods*. On day 10 after induction of differentiation, cells were harvested and CERK activity assay was performed as described in *Materials and Methods*. Data are expressed as the mean ± SEM of 3 independent experiments (**p<0.01).

The implication of CERK in adipogenesis was tested using specific CERK siRNA to silence the gene encoding this kinase. Figure 7A shows that the content of TAG was substantially reduced in CERK siRNA-treated adipocytes when compared to control cells, or cells that were transfected with negative (Neg) siRNA. Knockdown of CERK by siRNA treatment was confirmed by immunoblotting (Figure 7B). In addition, the secretion of leptin, which is a central regulator of energy balance and late marker of adipogenesis, was also significantly reduced (Figure 7C).

A. **B.**

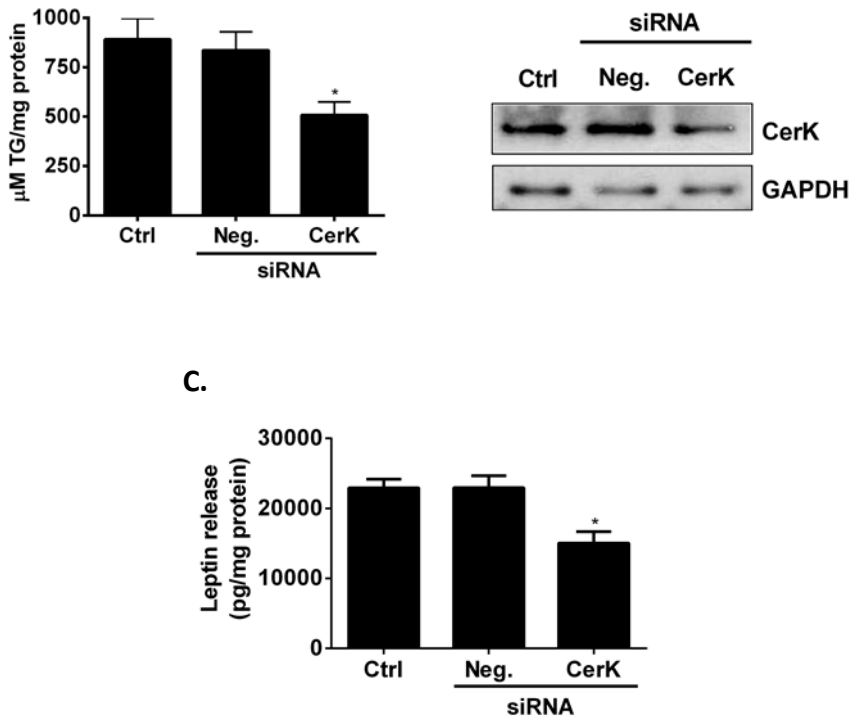

Figure 7. CerK downregulation leads to depletion of TG content and inhibition of leptin secretion in 3T3-L1 cells. 3T3-L1 preadipocytes were seeded in 100 mm diameter dishes at 5 x 10^5 cells/plate and incubated for 48 h. They were then electroporated in the absence of siRNA (ctrl) or in the presence of negative (scrambled) siRNA (Neg siRNA) or CerK siRNA, and were then differentiated up to day 4. A) Triacylglycerol (TG) content of cells was measured at day 4 after differentiation. B) CerK knockdown using specific siRNA was confirmed by immunoblotting. Equal loading of protein was assessed with an antibody against GAPDH. C) Leptin concentration in supernatants was measured at day 4 after differentiation using an ELISA kit. Figure taken from [37].

2.3. Ceramide 1-phosphate (C1P) protects 3T3-L1 preadipocytes from cell death by inducing phosphorylation of STAT3 and late (second) phosphorylation of ERK1-2 and Akt

Our group previously described that C1P is an important regulator of cell survival in macrophages [62, 63, 67, 68]. Due to the importance of the maintenance of the number of preadipocytes in obesity and obesity-associated diseases, we sought to investigate whether C1P might also protect 3T3-L1 preadipocytes against cell death. In order to answer this question, 3T3-L1 cell death was induced by depriving the preadipocytes of NCS and then C1P at different concentrations was added. Figure 8

shows that C1P protects 3T3-L1 preadipocytes against cell death in a dose-dependent manner after 24 h of incubation.

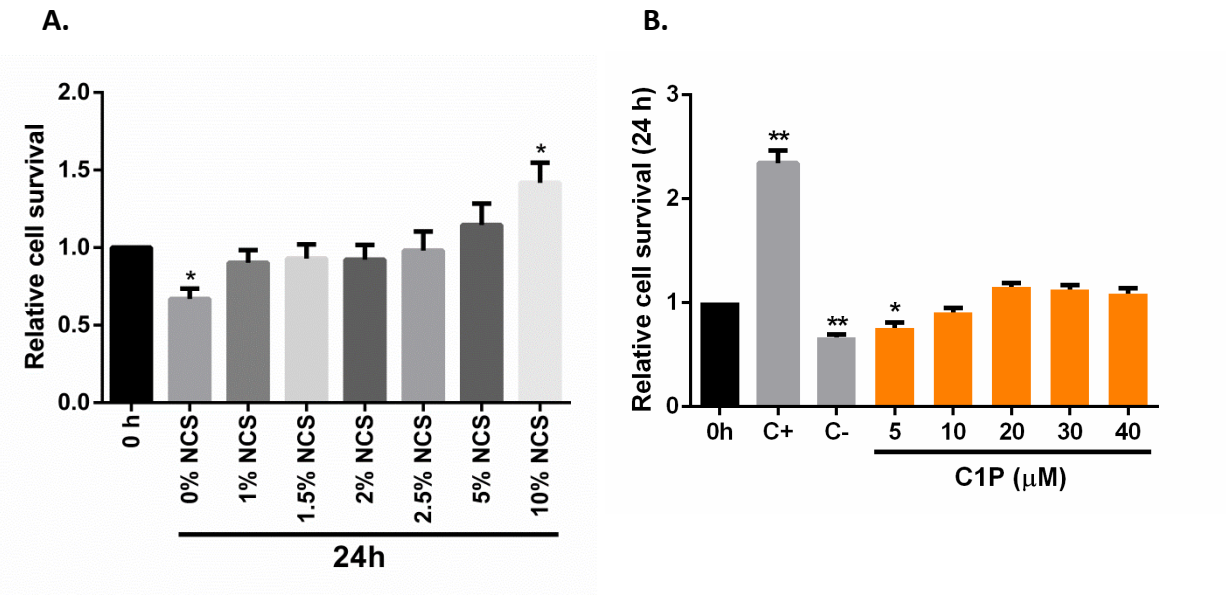

Figure 8. C1P protects 3T3-L1 preadipocytes against cell death. 3T3-L1 cells were seeded in 96-well plates (9 x 10^4 cells/well) and incubated overnight in DMEM supplemented with 10% NCS. A) The next day, the cells were washed and the medium was replaced with different concentrations of NCS. After 24 hours of incubation crystal violet proliferation assay was performed as described in *Materials and Methods*. Data are expressed as the mean ± SEM of 4 independent experiments (*p<0.05). B) The next day, the cells were washed and the medium was replaced with different concentrations of C1P in serum-free medium (C+: DMEM with 10% NCS and C-: DMEM with no (0%) NCS). Cells were incubated for 24 hours and crystal violet proliferation assay was performed as described in *Materials and Methods*. Data are expressed as the mean ± SEM of 4 independent experiments (*p<0.05; **p<0.01).

To investigate into the mechanisms by which C1P regulates cell survival, we tested to see whether C1P could phosphorylate ERK1-2, Akt and STAT3, which are key proteins involved in signal transduction processes. To this end, 3T3-L1 cells were incubated with C1P (20 μM) and the level of phosphorylation of these proteins was determined at different time points. Figure 9 shows that C1P stimulated the phosphorylation of ERK1-2, Akt and STAT3 in the preadipocytes. Interestingly, a

bimodal phosphorylation pattern of ERK1-2 and Akt was observed. In particular, rapid phosphorylation of the ERK1-2 and Akt kinases was observed as early as 5 min to come down to almost normal levels by 60 min. Interestingly, and contrary to STAT3, a second (although less intense) phosphorylation phase for ERK1-2 and Akt was observed after 8-24 h of C1P addition to the cells (Figure 9A-D).

A.

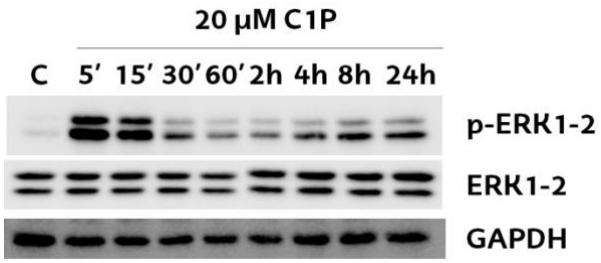

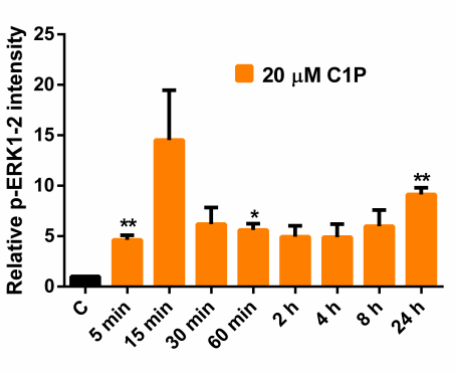

C.

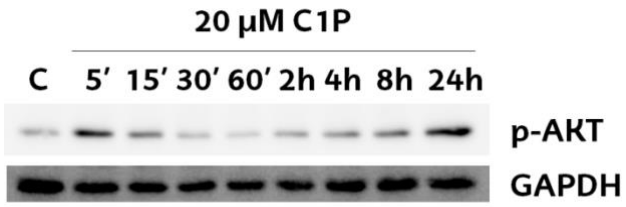

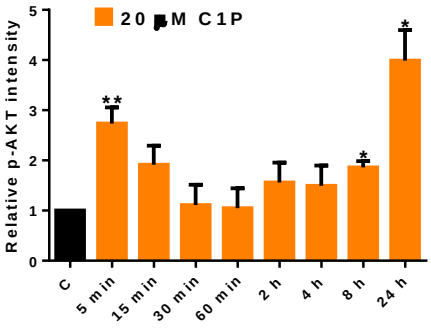

E.

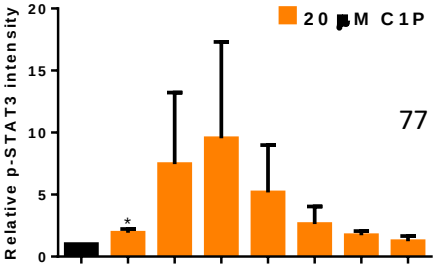

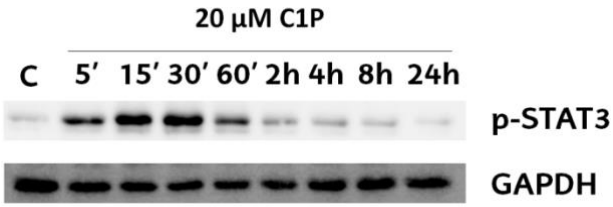

Figure 9. C1P induces ERK1-2, Akt and STAT3 phosphorylation in 3T3-L1 preadipocytes. 3T3-L1 cells were seeded in 6-well plates (2 x 10^5 cells/well) and grown in DMEM supplemented with 10% NCS. The next day, the cells were washed and the medium was replaced with medium without serum. After 2 hours of incubation, 20 µM of C1P was added and cells were harvested at the indicated time points. The presence of p-ERK1-2 (A), p-Akt (C) and p-STAT3 (E) were detected by Western blotting using specific antibodies, as described in *Materials and Methods*. Equal loading of protein was monitored using a specific antibody to GAPDH. B), D) and F) Results of scanning densitometry of exposed films. Data are expressed as arbitrary units of intensity of the bands and are the mean ± SEM of 6-7 independent experiments (*p<0.05; **p< 0.01).

Firstly, we tested to see whether the JAK/STAT pathway was involved in C1P-induced cell protection. Figure 10 shows, that both the JAK2 inhibitor, AZD1480, and Stattic, a STAT3 inhibitor, abolished the protection of cell death induced by C1P, suggesting that the JAK2/STAT3 pathway is involved in this process.

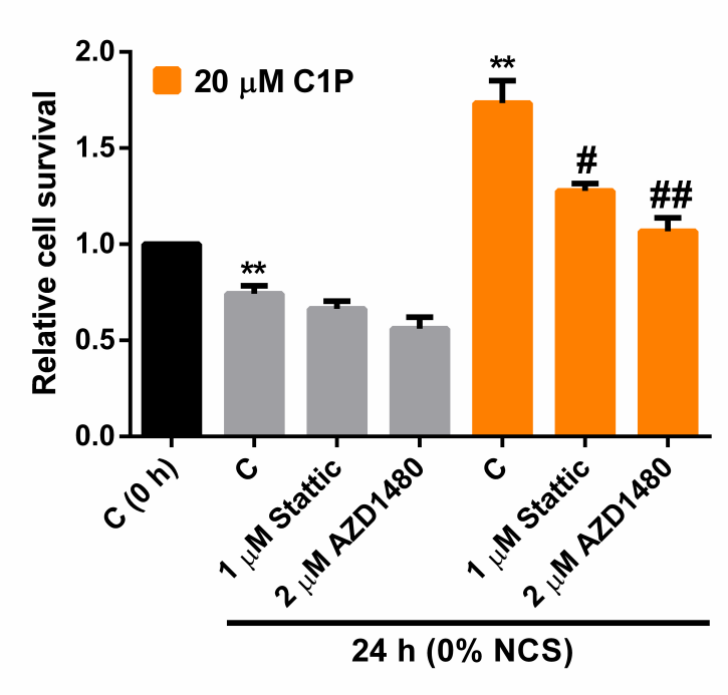

Figure 10. Inhibitors of the JAK2/STAT3 pathway (AZD1480 and Stattic) abolish the protection of cell death induced by C1P in 3T3-L1 preadipocytes. 3T3-L1 cells were seeded in 96-well plates (9 x 10^4 cells/well) and incubated overnight in DMEM supplemented with 10% NCS. The next day (0 h), the cells were washed and the medium was replaced by medium without serum for 2 hours. Then inhibitors were added and, after 1 hour of preincubation, 20 μM C1P was added as indicated. Cells were incubated for 24 hours and crystal violet proliferation assay was performed as described in *Materials and Methods*. Data are expressed as the mean ± SEM of 4 independent experiments (**p<0.01; $^{\#}$p<0.05; $^{\#\#}$p<0.01).

Secondly, we demonstrated that inhibiting the second (late) phosphorylation phase (not the early one) of ERK1-2 and Akt (with the selective inhibitors PD98059 and LY294002, respectively) partially reduced the protection of cell death that was induced by C1P (Figure 11A). It should be noted that in order to specifically inhibit the second (late) phosphorylation of ERK1-2 and Akt, the inhibitors of these kinases were added to the cells 30 min after C1P stimulation, when the first (rapid) phosphorylation of the kinases had already taken place. In this concern, it should be borne in mind that cell signaling processes are triggered immediately after activation (phosphorylation) of mediator effectors, so addition of the inhibitors at a time when the first phosphorylation process had already ended may not compromise any subsequent signaling cascade elicited by the rapid phosphorylation of these kinases.

On another hand, our group previously established that C1P-promoted cell survival is a receptor-independent process whereas stimulation of cell migration by C1P requires prior interaction of exogenous C1P with a specific Gi protein-coupled (pertussis toxin, Ptx-sensitive) receptor in which rapid phosphorylation of ERK1-2 and Akt plays a crucial role [45] (see below). Figure 11B shows that long preincubation (4 hours) of the cells with Ptx did not inhibit the cell death protection induced by C1P, suggesting that the first phosphorylation of ERK1-2 and Akt is not implicated in this process (the second ERK1-2 and Akt phosphorylation phase is most likely achieved after C1P has entered the cells in a receptor independent manner, a process that is rather slow when taking into consideration the low permeability of cell membranes to phospholipids, including C1P).

A.

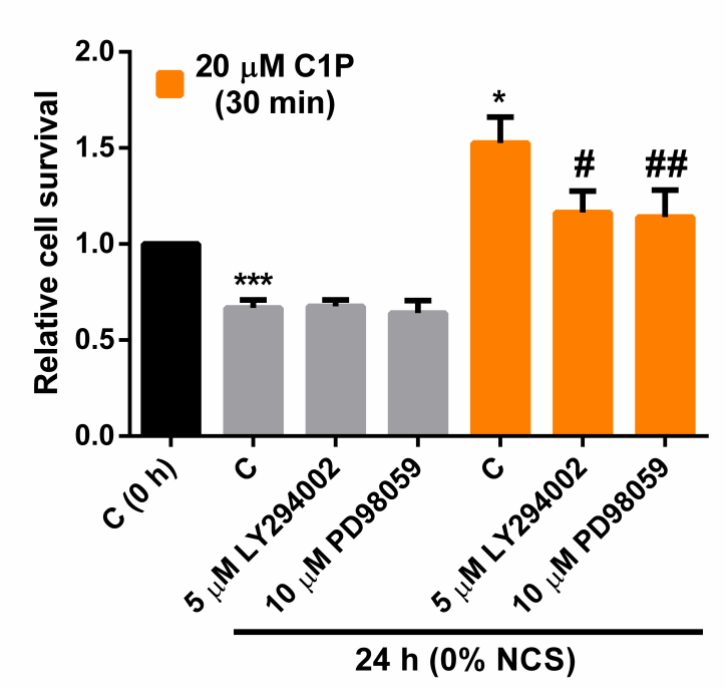

B.

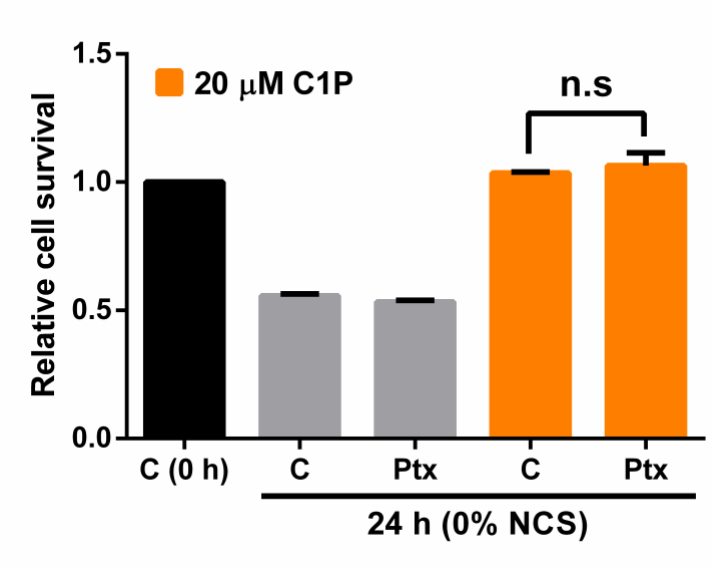

Figure 11. Inhibition of the second (late) phosphorylation of ERK1-2 and Akt reduces the protection of cell death induced by C1P. Lack of effect of pertussis toxin. 3T3-L1 cells were seeded in 96-well plates (9 x 10^4 cells/well) and incubated overnight in DMEM supplemented with 10% NCS. The next day (0 h), the cells were washed and the medium was replaced with medium without serum for 2 hours. A) Inhibitors were added 30 minutes after C1P (20 μM) addition. Cells were incubated for 24 hours and crystal violet proliferation assay was performed as described in *Materials and Methods*. Data are expressed as the mean ± SEM of 6 independent experiments (*p<0.05; ***p<0.001; $^{\#}$p<0.05; $^{\#\#}$p<0.01). B) Cells were preincubated with 0.1 μg/ml Ptx for 4 hours prior to C1P (20 μM) addition. Cells were incubated for 24 hours and crystal violet proliferation assay was performed as described in *Materials and Methods*. Data are expressed as the mean ± SEM of 2 independent experiments.

2.4. Ceramide 1-phosphate (C1P) stimulates 3T3-L1 cell proliferation by inducing the phosphorylation of STAT3 and the second phosphorylation of ERK1-2 and Akt

Ceramide 1-phosphate was first shown to stimulate cell growth in fibroblasts and macrophages [61, 69]. Later studies, described C1P as a potent stimulator of cell growth in primary bone marrow-derived macrophages (BMDM) [57], C2C12 myoblasts [58], and different types of cancer cells such as A549 human lung adenocarcinoma [70]. In this study, we tested to see whether C1P was able to stimulate the proliferation of 3T3-L1 preadipocytes. In order to achieve this question, we carried out a crystal violet proliferation assay in 3T3-L1 cells incubated with 2.5% NCS, a serum concentration that prevents the cells from entering apoptosis but that is not sufficient to stimulate proliferation (Figure 8A). Figure 12 shows that C1P promotes cell

proliferation in a dose-dependent manner, with optimal concentration being attained at 20 µM C1P.

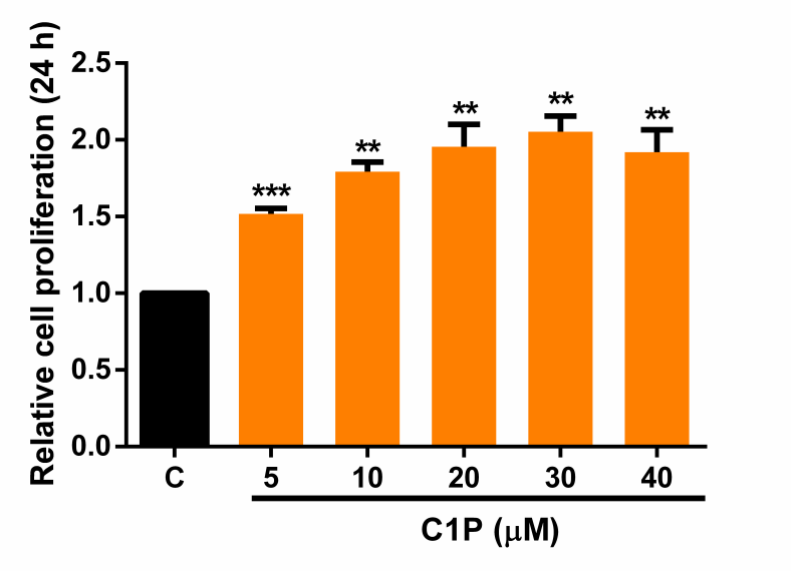

Figure 12. C1P induces cell proliferation in 3T3-L1 preadipocytes. . 3T3-L1 cells were seeded in 96-well plates (9 x 10^4 cells/well) and incubated overnight in DMEM supplemented with 10% NCS. The next day, the cells were washed and the medium was replaced with 2.5% NCS. After 2 hours of incubation C1P was added. Cells were incubated for 24 hours and crystal violet proliferation assay was performed as described in *Materials and Methods*. Data are expressed as the mean ± SEM of 4 independent experiments (*p<0.05; **p<0.01; ***p<0.001).

To investigate into the mechanisms by which C1P regulates adipocyte proliferation, we tested to see the possible implication of ERK1-2, Akt and STAT3 in this process. Figure 13 shows that the JAK2 inhibitor AZD1480 and the STAT3 inhibitor Stattic significantly reduced C1P-stimulated 3T3-L1 cell proliferation, suggesting that the JAK2/STAT3 pathway is implicated in this process.

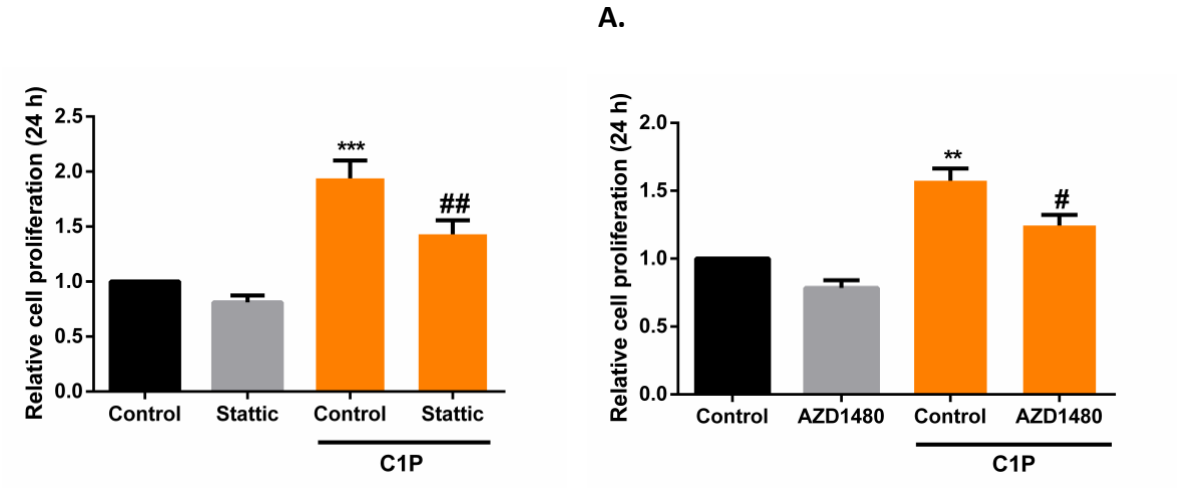

Figure 13. Stattic and AZD1480 inhibit cell proliferation induced by C1P in 3T3-L1 preadipocytes. 3T3-L1 cells were seeded in 96-well plates (9 x 10^4 cells/well) and incubated overnight in DMEM supplemented with 10% NCS. The next day, the cells were washed and the medium was replaced with fresh medium supplemented with 2.5% NCS for 2 hours. Then inhibitors were added and, after 1 hour of preincubation, 20 µM C1P was added to indicated wells. Cells were incubated for 24 hours and crystal violet proliferation assay was performed as described in *Materials and Methods*. Data are expressed as the mean ± SEM of 4-8 independent experiments (**p<0.01; ***p<0.001; $^{\#}$p<0.05; $^{\#\#}$p<0.01).

Concerning the MAPK/ERK1-2 and PI3K/Akt pathways, we demonstrated that also inhibition of the second (late) phosphorylation of ERK1-2 and Akt (with PD98059 and LY294002, respectively) partially blocked C1P-stimulated 3T3-L1 cell proliferation, suggesting that these pathways are also implicated in the mitogenic effect of C1P in these cells. Moreover, toxin pertussis did not inhibit the cell proliferation induced by C1P, suggesting that the first phosphorylation of ERK1-2 and Akt, which is receptor-mediated [71] is not implicated in C1P-stimulated cell proliferation (Figure 14).

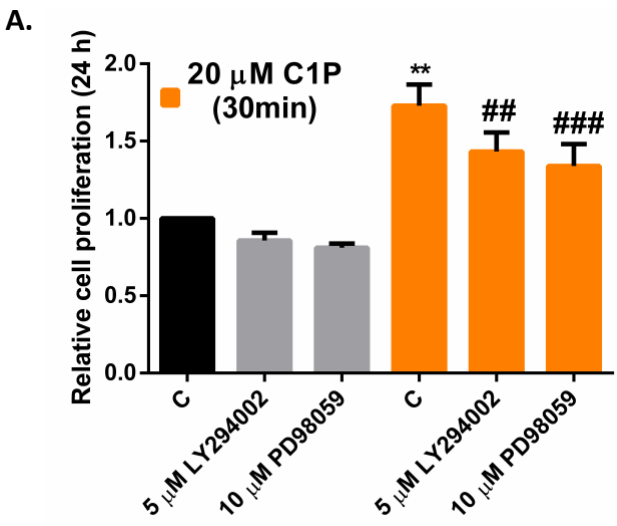

B.

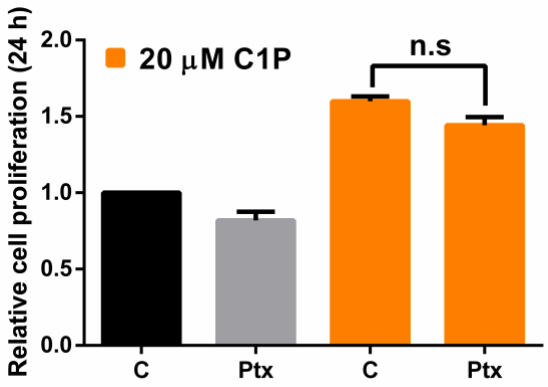

Figure 14. Implication of ERK1-2 and Akt in the stimulation of 3T3-L1 cell proliferation by C1P. 3T3-L1 cells were seeded in 96-well plates (9 x 10^4 cells/well) and incubated overnight in DMEM supplemented with 10% NCS. The next day, the cells were washed and the medium was replaced with fresh medium with 2.5% NCS for 2 hours. A) First, 20 µM C1P was added to the cells, and 30 minutes later, the inhibitors were added. The cells were then incubated for 24 hours and crystal violet proliferation assay was performed as described in *Materials and Methods*. Data are expressed as the mean ± SEM of 6 independent experiments (**p<0.01; $^{\#\#}$p<0.01; $^{\#\#\#}$p<0.001). B) Cells were preincubated with 0.1 µg/ml Ptx for 4 hours prior to addition of 20 µM C1P. The cells were then incubated for 24 hours and crystal violet proliferation assay was performed as described in *Materials and Methods*. Data are expressed as the mean ± SEM of 2 independent experiments.

2.5. 3T3-L1 preadipocytes migrate spontaneously. Implication of CERK

Cell migration is a central process in the development and maintenance of multicellular organisms. Tissue formation during embryonic development, wound healing and immune responses all require the orchestrated movement of cells in particular directions to specific locations.

Concerning adipocytes, it should be noted that preadipocyte migration is essential in the process differentiation to mature adipocytes. The process of adipose tissue organogenesis is characterized by the formation of a vascularized primitive fat organ, followed by migration of preadipocytes into defined fat cell clusters [72], but the molecules regulating this process are unknown. Due to the biological importance of this process in the organism, we first, tested to see whether 3T3-L1 preadipocytes have the ability to move spontaneously. Figure 15A shows that 3T3-L1 preadipocytes migrate spontaneously after 24 h of culture in the absence of any chemoattractant.

Our group previously demonstrated that CERK is implicated in spontaneous cell migration of PANC-1 and MIA PaCa-2 human pancreatic cancer cells [73], so we hypothesized that this kinase might also be implicated in the spontaneous migration of preadipocytes. To address this question, we used a selective inhibitor of CERK, NVP-231 and, as shown in Figure 15B, CERK is not implicated in this process.

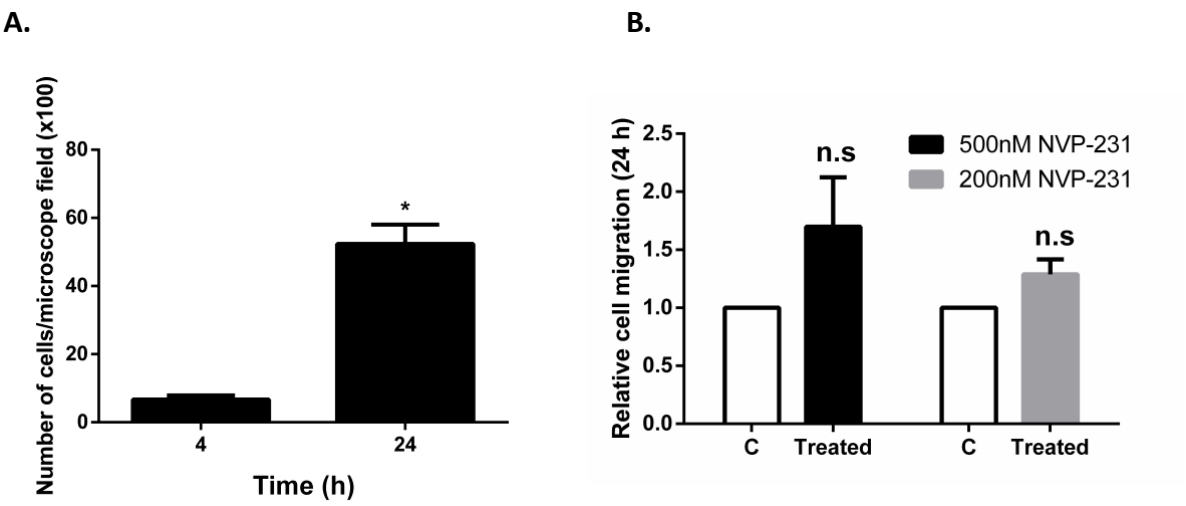

Figure 15. CERK is not implicated in the spontaneous migration of 3T3-L1 preadipocytes. Preadipocyte migration was measured using a Boyden chamber-based cell migration assay. Cells (5 x 10^4 cells/well) were seeded in the upper wells of 24-well chambers coated with fibronectin. A) After 2 hours of incubation, chambers holding the cells were moved into the lower compartments. Cells were further incubated for the indicated times and cell migration was measured as described in *Materials and Methods*. Results are expressed as the number of migrated cells/microscope field (x100) and are the mean ± SEM of 3 independent experiments performed in duplicate (*p<0.05). B) After 1 hour of incubation, cells were preincubated with NVP-231 or vehicle for 1 hour. Cells were further incubated for 24 hours and cell migration was measured as described in *Materials and Methods*. Results are expressed as the number of migrated cells relative to the number of cells migrated in the control chamber and are the mean ± SEM of 3 independent experiments performed in duplicate.

2.6. Ceramide 1-phosphate (C1P) enhances cell migration in 3T3-L1 preadipocytes

Our group previously established that C1P induces migration of different cell types, such as mouse (RAW264.7 and J774.A1) and human (THP-1) monocytes/macrophages or human pancreatic cancer cells (PANC-1 and MIA PaCa-2) [71, 73, 74], or human prostate cancer PC-3 cells [54]. To test whether C1P enhances migration of 3T3-L1 preadipocytes, we carried out the Boyden chamber-based migration assays using different concentrations of C1P. We observed that C1P enhanced 3T3-L1 cell migration in a dose-dependent manner, with optimal effect being attained at 20 µM C1P (Figure 16A-B). In addition, we performed time-course experiments to determine the optimal time point at which C1P exerts this effect. As shown in Figure 16C-D, maximal cell migration occurred after 24 hours of incubation with C1P.

A.

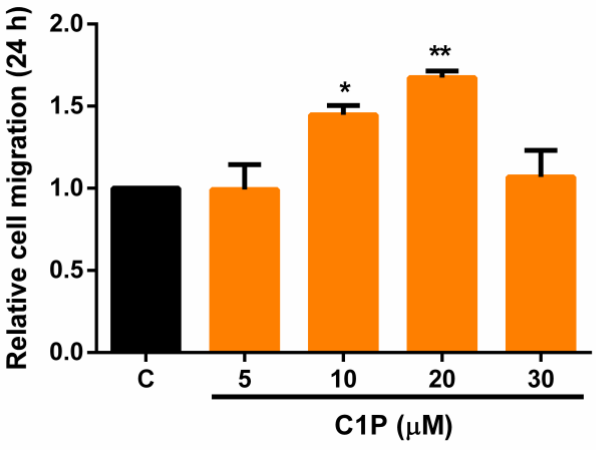

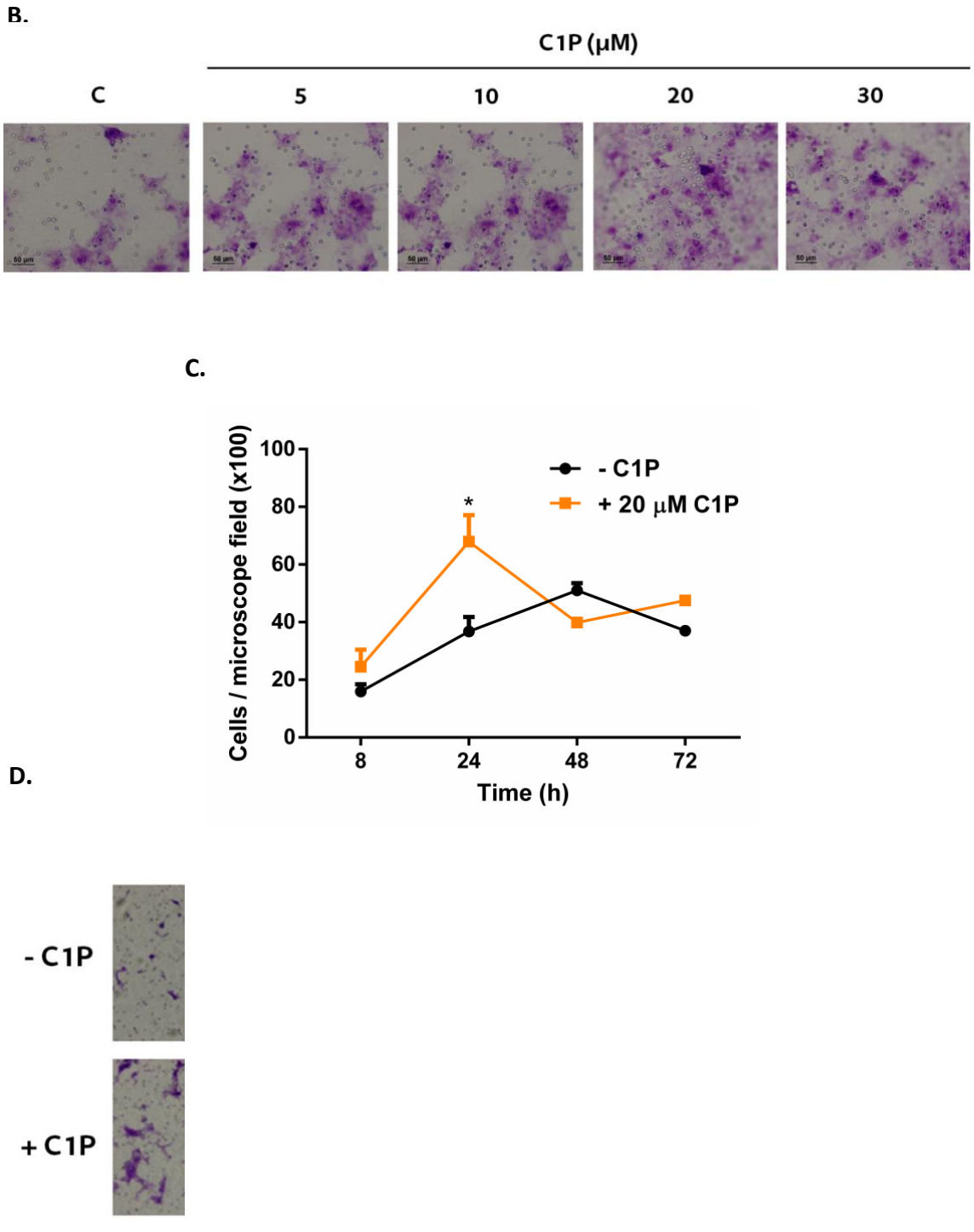

Figure 16. C1P enhances cell migration in 3T3-L1 preadipocytes. Preadipocyte migration was measured using a Boyden chamber-based cell migration assay. Cells (5 x 10^4 cells/well) were seeded in the upper wells of 24-well chambers coated with

fibronectin. After 2 hours of incubation, chambers holding the cells were moved into the lower compartments which were filled with different concentrations of C1P. Cells were further incubated for indicated times and cell migration was measured as described in *Materials and Methods*. A) Results are expressed as the number of migrated cells relative to the number of cells migrated in the control chamber and are the mean ± SEM of 3 independent experiments performed in duplicate (*p<0.05; ** p<0.01). C) Results are expressed as the number of migrated cells/microscope field (x100) and are the mean ± SEM of 3 independent experiments performed in duplicate (*p<0.05). B) and D) Microscopic images of 3T3-L1 migrated cells in chambers with 8 µm pore size.

2.7. PI3K and ERK1-2 kinases are implicated in C1P-enhanced cell migration in 3T3-L1 preadipocytes

Two of the best characterized pathways linked to cell motility functions are the Phosphoinositide 3-kinase (PI3K)/Protein kinase B (PKB/Akt) and the Mitogen activated protein kinase (MAPK)/Extracellular signal-regulated kinase (ERK1-2) pathways [42, 71, 73, 75]. To test if these pathways were involved in C1P-enhanced cell migration, we performed Boyden chamber-based migration assays using potent pharmaceutical specific inhibitors of PI3K and MAPK, LY294002 and PD98059 respectively.

First, we confirmed that LY294002 and PD98059 inhibited the phosphorylation of PKB/Akt and ERK1-2, respectively, elicited by C1P (Figure 17).

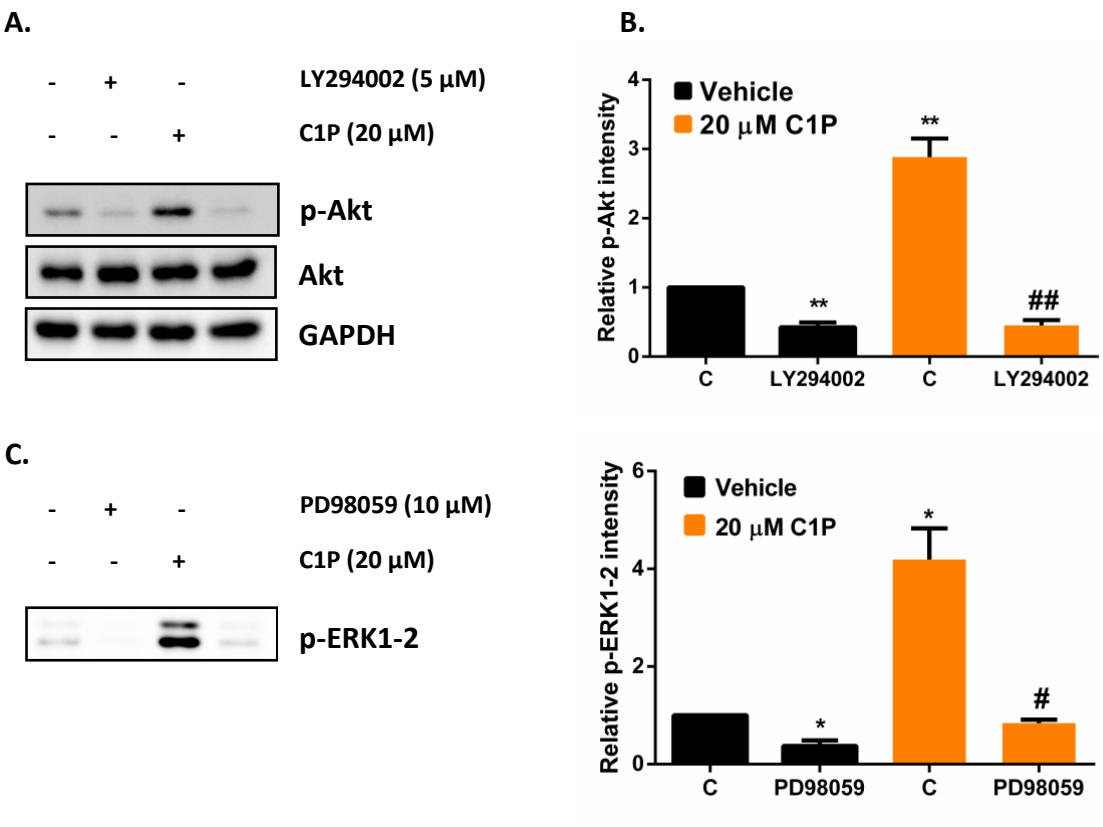

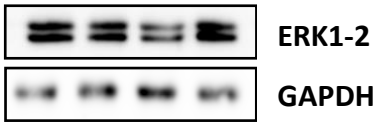

Figure 17. LY294002 and PD98059 inhibit C1P-induced Akt and ERK1-2 phosphorylation, respectively, in 3T3-L1 preadipocytes. 3T3-L1 cells were seeded in 6-well plates (2 x 10^5 cells/well) and they were grown in DMEM supplemented with 10% NCS. The next day, the cells were washed and the medium was replaced with fresh medium without serum. A) After 2 hours of incubation, cells were preincubated with either vehicle or 5 µM LY294002 for 1 hour prior to 20 µM of C1P addition. After 5 minutes of incubation with 20 µM of C1P, cells were harvested and the presence of p-Akt protein was detected by Western blotting, as described in *Materials and Methods*, using specific antibody to p-Akt. Equal loading of protein was monitored using a specific antibody to total Akt and GAPDH. B) Results of scanning densitometry of exposed film. Data are expressed as arbitrary units of intensity of the p-Akt protein and are the mean ± SEM of 4 independent experiments (**p< 0.01; $^{\#\#}$p< 0.01). C) After 2 hours of incubation, cells were preincubated with either vehicle or 10 µM PD98059 for 1 hour prior to 20 µM of C1P addition. After 5 minutes of incubation with 20 µM of C1P, cells were harvested and the presence of p-ERK1-2 protein was detected by Western blotting, as described in *Materials and Methods*, using specific antibody to p-ERK1-2. Equal loading of protein was monitored using a specific antibody to ERK1-2 and GAPDH. D) Results of scanning densitometry of exposed film. Data are expressed as arbitrary units of intensity of the p-ERK1-2 protein and are the mean ± SEM of 3 independent experiments (*p<0.05; $^{\#}$p<0.05).

Then, we observed that inhibiting the activity of PI3K and ERK1-2 in 3T3-L1 preadipocytes completely blocked C1P-enhanced cell migration (Figure 18). These results suggest that both PI3K and ERK1-2 are implicated in the regulation of C1P-stimulated preadipocyte migration.

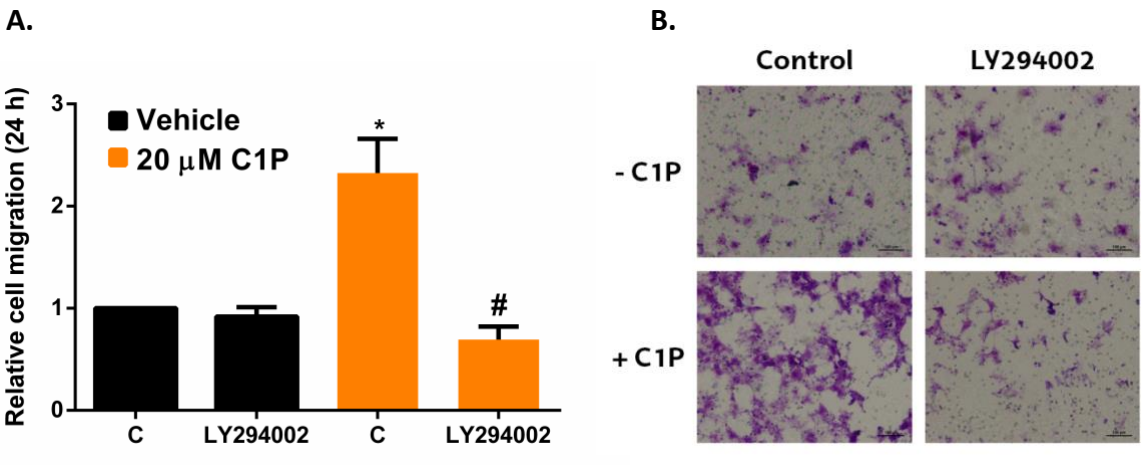

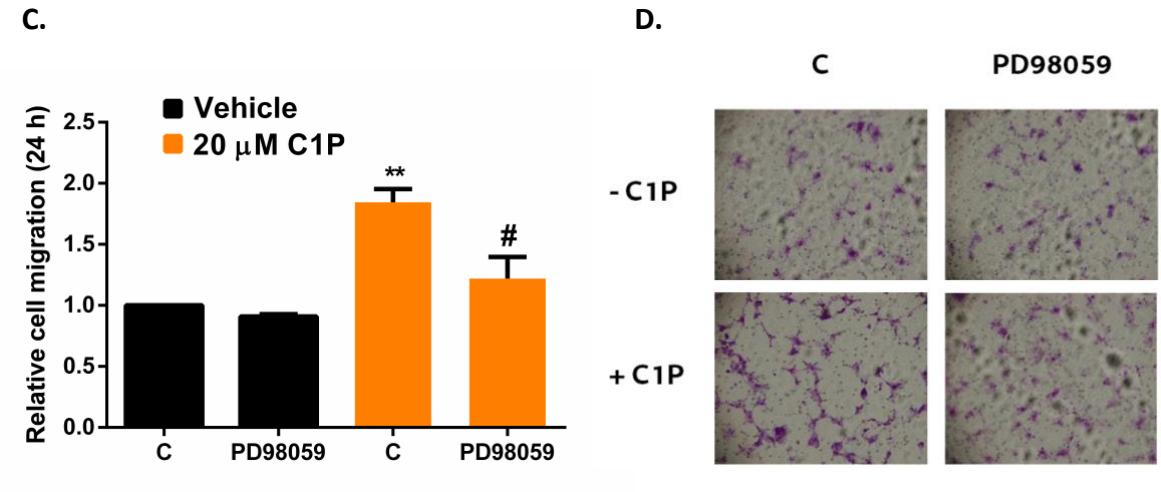

Figure 18. LY294002 and PD98059 block C1P-enhanced migration in 3T3-L1 preadipocytes. Migration was measured using a Boyden chamber-based cell migration assay. Cells (5 x 10^4 cells/well) were seeded in the upper wells of 24-well chambers coated with fibronectin, and incubated for 2 hours. Later, cells were preincubated with vehicle or with 5 μM of LY294002 (A) or 10 μM of PD98059 (C). After 1 hour of incubation, either vehicle, inhibitors or 20 μM of C1P were added to the lower wells and cells were moved into the lower compartments. Cells were further incubated for 24 hours and cell migration was measured as described in *Materials and Methods*. Results are expressed as the number of migrated cells relative to the number of cells migrated in the control chamber and are the mean ± SEM of 5 independent experiments performed in duplicate (*p<0.05; **p<0.01; $^{\#}$p<0.05). B) and D) Microscopic images of 3T3-L1 migrated cells in chambers with 8 μm pore size.

2.8. Implication of the JAK2/STAT3 pathway in C1P-enhanced cell migration in 3T3-L1 preadipocytes

The signal transducer and activator of transcription (STAT) protein family includes intracellular latent transcription factors that facilitate the cellular signaling initiated by stimuli from growth factors or cytokines. Signal transducer and activator of transcription 3 (STAT3) is the most prominent of all the STATs and is involved in many cellular processes, such as cell growth and proliferation, differentiation, migration, and cell death through apoptosis [76-78]. It has been established that STAT3 is phosphorylated and activated by janus kinase 2 (JAK2) [79]. Using specific inhibitors of JAK2 and STAT3, AZD1480 and Stattic respectively, we first confirmed that both of

these inhibitors blocked the STAT3 phosphorylation induced by C1P in these cells (Figure 19). In a second set of studies, we have demonstrated that these two inhibitors almost completely blocked C1P-stimulated cell migration in the preadipocytes suggesting that the JAK2/STAT3 pathway is involved in the regulation of this process (Figure 20).

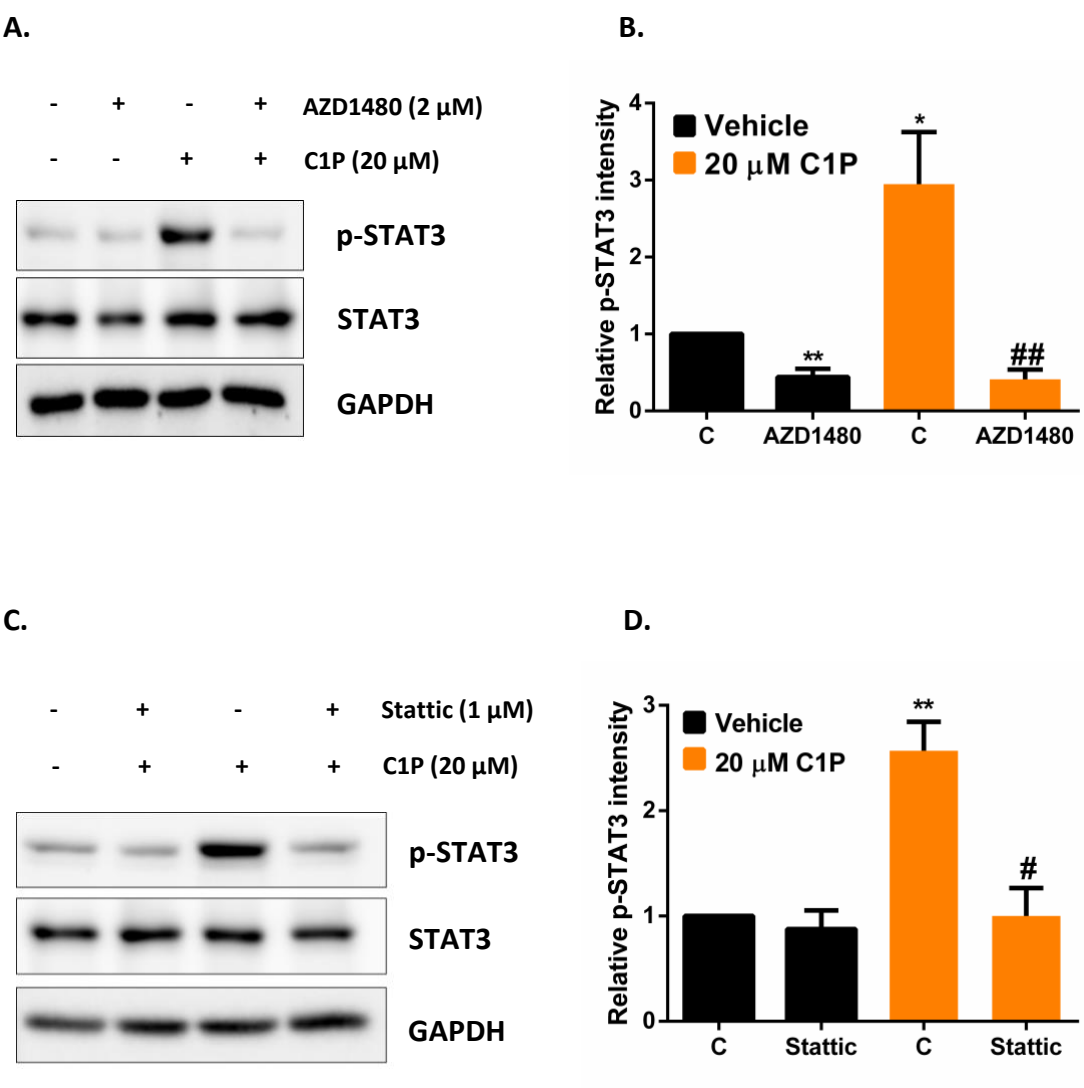

Figure 19. AZD1480 and Stattic inhibit C1P-induced STAT3 phosphorylation in 3T3-L1 preadipocytes. 3T3-L1 cells were seeded in 6-well plates (2 x 10^5 cells/well) and they were grown in DMEM supplemented with 10% NCS. The next day, the cells were washed and the medium was replaced with fresh medium without serum. A) After 2 hours of incubation, cells were preincubated with either vehicle or 2 µM AZD1480 for 1 hour prior to 20 µM of C1P addition. After 5 minutes of incubation with 20 µM of C1P, cells were harvested and the presence of p-STAT3 protein was detected by Western blotting, using a specific antibody to p-STAT3, as described in *Materials and Methods*. Equal loading of protein was monitored using a specific antibody to total STAT3 and GAPDH. B) Results of scanning densitometry of the exposed film. Data are expressed as arbitrary units of intensity of the p-STAT3 protein and are the mean ± SEM of 6 independent experiments (*p<0.05; **p< 0.01; $^{\#\#}$p< 0.01). C) After 2 hours of incubation, cells were preincubated with either vehicle or 1 µM Stattic for 1 hour prior to 20 µM of C1P addition. After 5 minutes of incubation with 20 µM of C1P, cells were harvested and the presence of p-STAT3 protein was detected by Western blotting, using a specific antibody to p-STAT3, as described in *Materials and Methods*. Equal loading of protein was monitored using a specific antibody to STAT3 and GAPDH. D) Results of scanning densitometry of the exposed film. Data are expressed as arbitrary units of intensity of the p-STAT3 protein and are the mean ± SEM of 4 independent experiments (*p<0.05; $^{\#}$p<0.05).

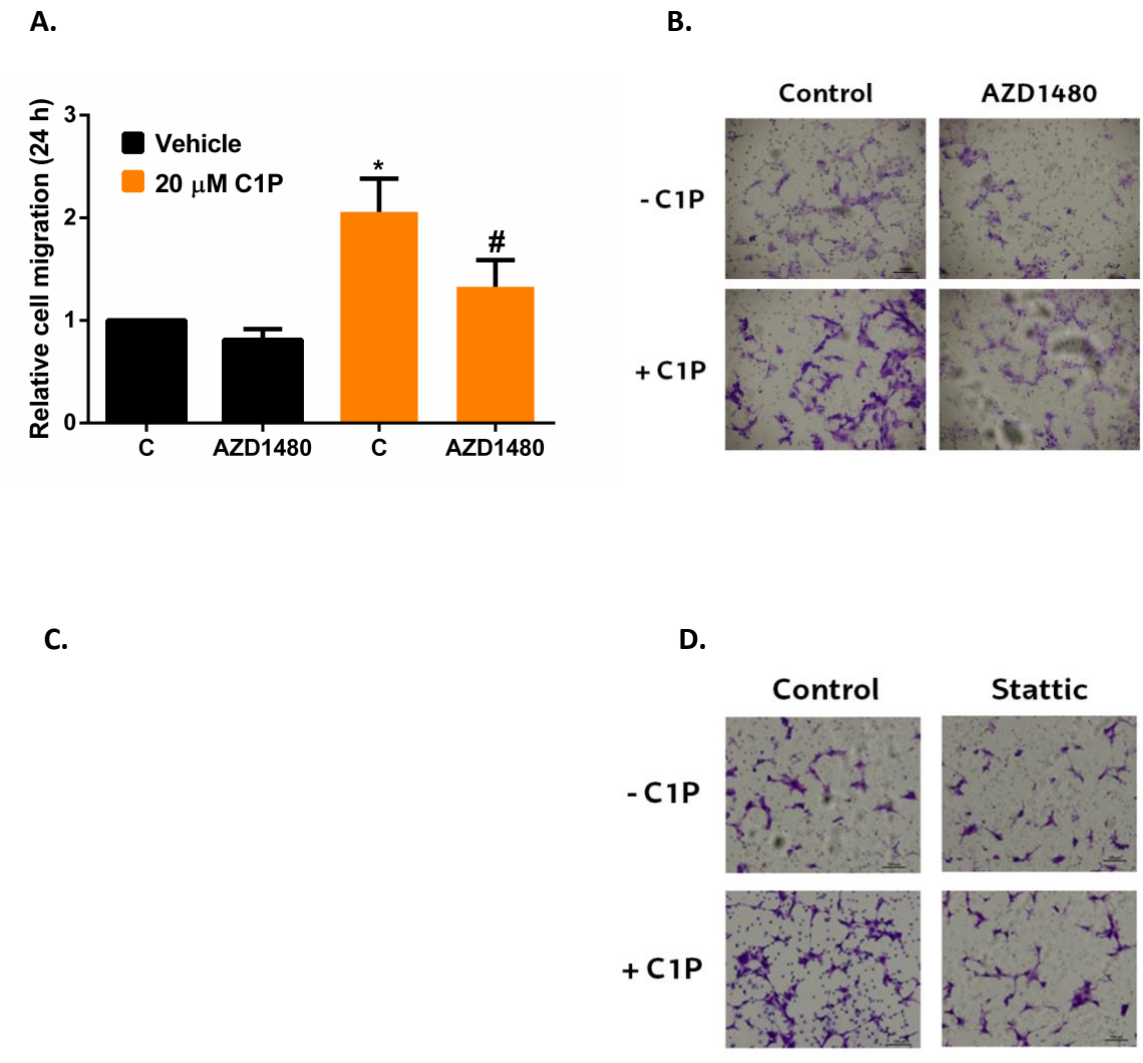

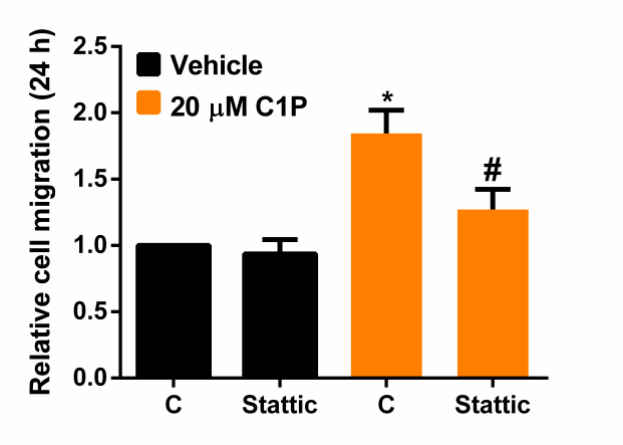

Figure 20. AZD1480 and Stattic block C1P-enhanced migration in 3T3-L1 preadipocytes. Cell migration was measured using a Boyden chamber-based cell migration assay. Cells (5 x 10^4 cells/well) were seeded in the upper wells of 24-well chambers coated with fibronectin, and incubated for 2 hours. Then, cells were preincubated with vehicle or with 2 µM of AZD1480 (A) or 1 µM of Stattic (C). After 1 hour of incubation, either vehicle, inhibitors and/or 20 µM of C1P were added to the lower wells and the cells were immersed in the wells. Cells were further incubated for 24 hours and cell migration was measured as described in *Materials and Methods*. Results are expressed as the number of migrated cells relative to the number of cells migrated in the control chamber and are the mean ± SEM of 3-6 independent experiments performed in duplicate (*$p<0.05$; $^{\#}p<0.05$). B) and D) Microscopic images of 3T3-L1 migrated cells in chambers with 8 µm pore size.

2.9. Pertussis toxin (Ptx) inhibits C1P-enhanced cell migration in 3T3-L1 preadipocytes through inhibition of the PI3K/Akt and MEK/ERK1-2 pathways

To evaluate whether C1P induced the enhancement of cell migration through prior interaction with its putative receptor, the preadipocytes were pre-treated with Ptx. We found that Ptx at a concentration as low as 0.1 µg/ml not only blocked C1P-induced cell migration completely, but it also reduced the spontaneous migration of the preadipocytes (Figure 21).

A.

B.

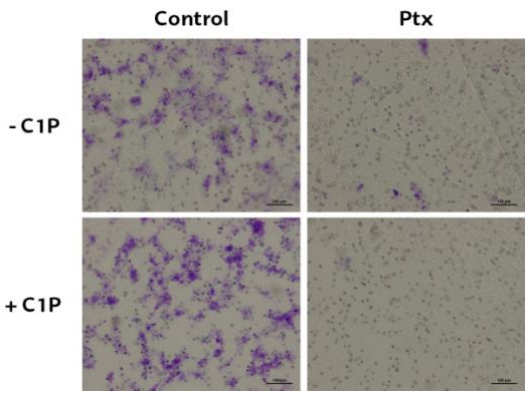

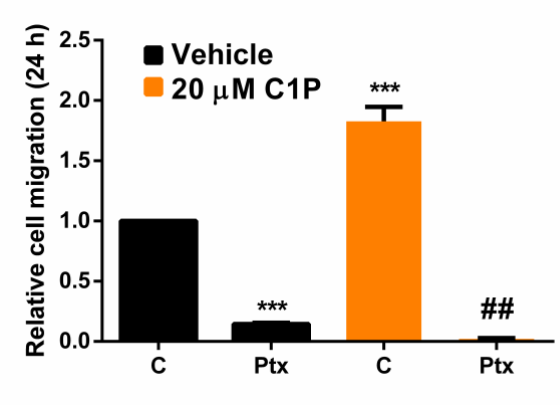

Figure 21. Pertussis toxin (Ptx) inhibits both spontaneous and C1P-enhanced cell migration in 3T3-L1 preadipocytes. Cell migration was measured using a Boyden chamber-based cell migration assay. Cells (5 x 10^4 cells/well) were seeded in the upper wells of 24-well chambers coated with fibronectin, and incubated for 2 hours. Then, cells were preincubated for 4 hours with vehicle or with 0.1 μg/ml of Ptx. After this preincubation, either vehicle, Ptx or 20 μM of C1P were added to the lower wells and cells were immersed in the wells. Cells were further incubated for 24 hours and cell migration was measured as described in *Materials and Methods*. A) Results are expressed as the number of migrated cells relative to the number of cells migrated in the control chamber and are the mean ± SEM of 4 independent experiments performed in duplicate (***$p<0.001$; $^{\#\#}p<0.01$). B) Microscopic images of 3T3-L1 migrated cells in chambers with 8 μm pore size.

In addition to the latter findings, we observed that C1P-induced Akt and ERK1-2 phosphorylation was also inhibited when treated with Ptx (Figure 22), suggesting that PI3K/Akt and MEK/ERK1-2 pathways are stimulated when C1P interacts with its Ptx-sensitive GPCR. However, C1P-induced STAT3 phosphorylation was not inhibited when treated with Ptx, thereby indicating that this pathway does not dependent upon GPCR activation.

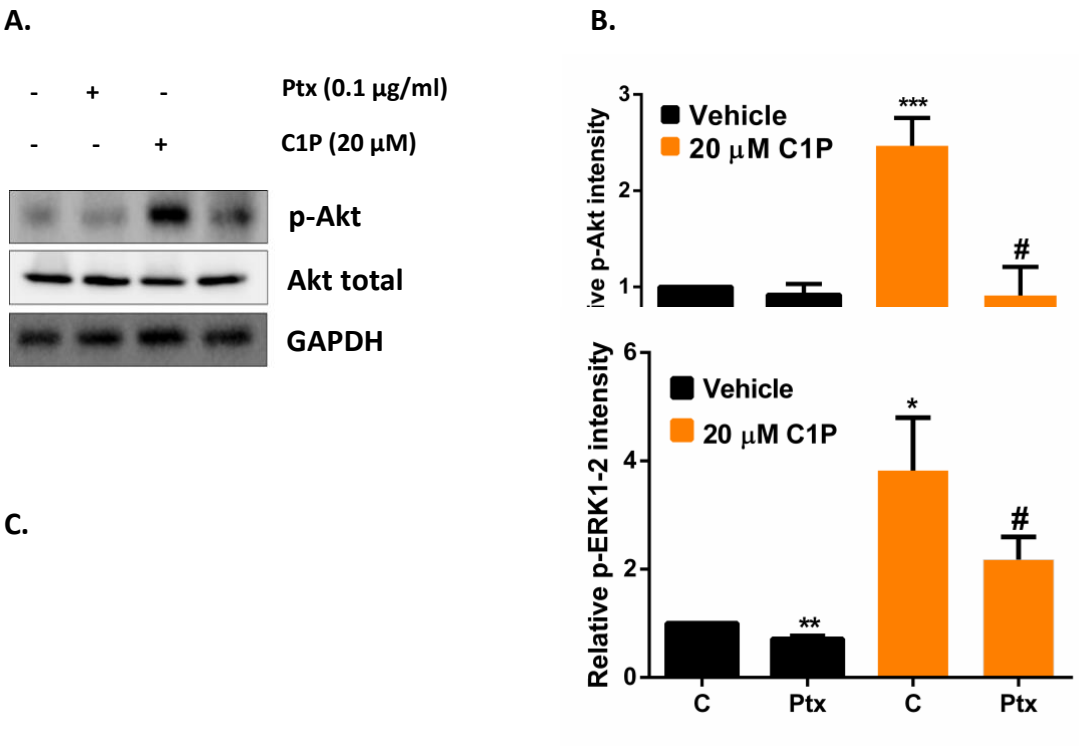

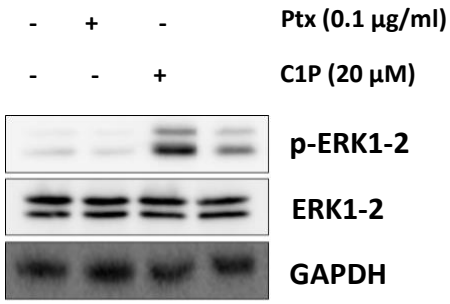

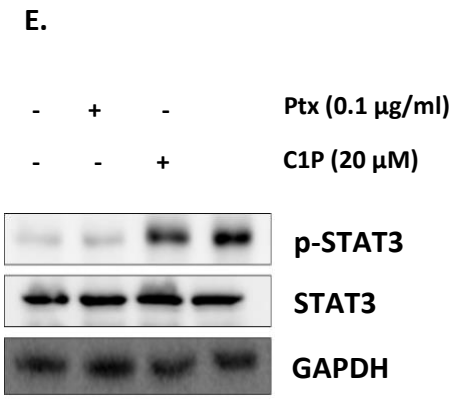

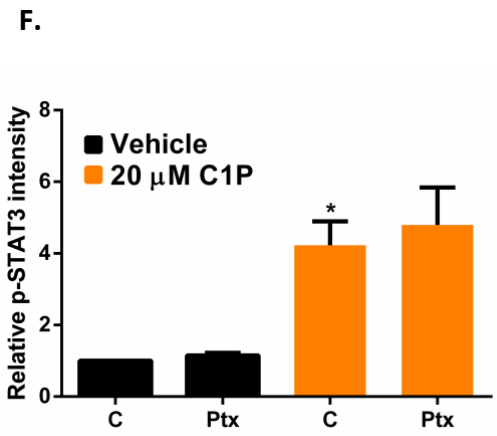

Figure 22. Pertussis toxin (Ptx) inhibits C1P-induced Akt and ERK1-2 phosphorylation in 3T3-L1 preadipocytes, but it does not affect STAT3 phosphorylation. 3T3-L1 cells were seeded in 6-well plates (2 x 10^5 cells/well) and they were grown in DMEM supplemented with 10% NCS. The next day, the cells were washed and the medium was replaced with medium without serum. After 2 hours of incubation, cells were preincubated with either vehicle or 0.1 µg/ml of Ptx for 4 hours prior to addition of 20 µM C1P. 5 minutes later the cells were harvested and the presence of p-Akt (A), p-ERK1-2 (C) and p-STAT3 (E) proteins were detected by Western blotting, using specific antibodies to p-Akt, p-ERK1-2 and p-STAT3 respectively, as described in *Materials and Methods*. Equal loading of protein was monitored using a specific antibody to total Akt, ERK1-2, STAT3 or GAPDH. B) D) and F) Results of scanning densitometry of the exposed films. Data are expressed as arbitrary units of intensity of the p-Akt, p-ERK1-2 and p-STAT3 proteins and are the mean ± SEM of 3-11 independent experiments (*p<0.05; **p<0.01; ***p<0.001; $^{\#}$p<0.05).

2.10. Lack of toxicity of the inhibitors used on 3T3-L1 preadipocytes

All commonly used chemical inhibitors in cell signaling studies may be toxic for cells at certain concentrations or incubation times. To test if any of the inhibitors used in this work were toxic for the 3T3-L1 preadipocytes at the times and concentrations that were used we performed cell viability assays. We observed that none of these pharmacological inhibitors caused any significant decrease in cell viability of the preadipocytes (Figure 23).

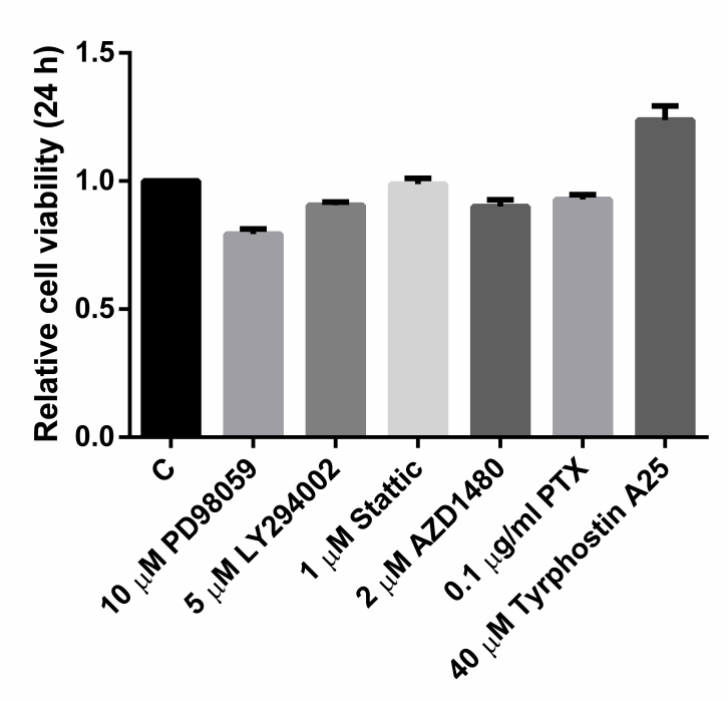

Figure 23. Cell viability after treatment with the chemical inhibitors used in experiments. 3T3-L1 cells were seeded in 96-well plates (9 x 10^3 cells/well) and incubated overnight in DMEM supplemented with 10% NCS. The next day, the cells were washed and the medium was replaced with fresh medium without serum. Chemical inhibitors were added to the cells at the indicated concentrations. Cell viability was measured after 24 hours of incubation, using the MTS-formazan assay, as indicated in *Materials and Methods*. Results are the mean ± SEM of 3-7 independent experiments performed in triplicate.

3. Discussion

In this chapter of the thesis, we have explored the effects of the bioactive sphingolipid ceramide 1-phosphate (C1P) on the survival, proliferation and migration of 3T3-L1 preadipocytes, actions that are closely related to different illnesses including obesity. The 3T3-L1 cell line has the capacity to differentiate from a fibroblast phenotype to mature adipocyte one, as confirmed using an adipogenic induction medium composed of IBMX, dexamethasone, rosiglitazone and insulin. In particular, this biological system has been widely used for studying adipogenesis and adipogenesis-associated diseases like obesity.

Obesity can be defined as the condition where excess or abnormal fat (adipose tissue) accumulation compromises health. Depending on the degree, duration and the distribution of excess of the adipose tissue, obesity could be associated with various metabolic diseases, including hypertension [12], dyslipidemia [13], type II diabetes (T2D), insulin resistance [IR) [14-16], non-alcoholic fatty liver disease [17, 18], cardiovascular diseases [19-22] or certain forms of cancer [23-25], which increase obesity-associated morbidity and mortality.

From a biochemical perspective, obesity is the result of an imbalance where energy intake exceeds energy expenditure over time. This energy excess leads to fat accumulation, causing an increase in the size of adipose tissue. In the adulthood, the body fat mass builds up by increasing the adipocyte size (enlarging existing adipocytes,

a process named hypertrophy) and/or by increasing the number of adipocytes (a process named hyperplasia) from their precursor cells, the preadipocytes [80]. The process in fat tissues in which an elongated preadipocyte differentiates to a round lipid-filled mature adipocyte is called adipogenesis. It has been reported that some cytokines, such as plasminogen activator inhibitor-1 (in human preadipocytes) [72] and macrophage inflammatory protein-related protein-2 (in 3T3-L1 preadipocytes) [81], act as chemotactic agents, potentially contributing to the increased tissue mass during adipogenesis. Thus, not only preadipocyte survival and proliferation, but also enhancement of preadipocyte migration to different fat depots may be one of the factors that induce hyperplasia. More recently, accumulating evidence suggests that overweight or obese people are more prone to develop severe disease and fatal outcome from Severe Acute Respiratory Syndrome coronavirus 2 (SARS-CoV-2), which causes the COVID-19 disease [82]. Obesity is a low grade inflammatory state in which proinflammatory cytokines, including interleukin (IL)-6 or tumor necrosis factor-alpha (TNF□) are increased in the circulation. These and other proinflammatory cytokines are produced by macrophages that infiltrate the obese adipose tissue. STAT3 is also a critical determinant for obese models and is a subject of intense investigation towards drug development to treat obesity-associated illnesses. On another hand, it should be noted that angiotensin-converting enzyme 2 (ACE2), which is the receptor of the spike protein (S) of SARS-CoV-2 and a major, if not the only path for virus entry into cells, is highly expressed in the adipocytes of obese patients and mice [83, 84] a fact that may contribute to exacerbation of the disease.

In this thesis, we have investigated into the mechanisms by which C1P regulates adipogenesis. We have demonstrated that C1P induces the phosphorylation of ERK1-2, Akt, and STAT3 in 3T3-L1 preadipocytes, which are key proteins that are involved in many signal transduction processes, and are implicated in obesity-associated metabolic disorders. Noteworthy, our group first found that C1P phosphorylates ERK1-2 and Akt in macrophages [62, 85, 86]. In the present study, we have observed for the first time a bimodal phosphorylation pattern of ERK1-2 and Akt, in which a rapid phosphorylation (5 minutes) is followed by a second, although less intense, phosphorylation of ERK1-2 and Akt after 8-24 h of C1P administration to the cells. We

found that the rapid (first) phosphorylation of ERK1-2 and Akt is inhibited by pertussis toxin (Ptx), which suggests that exogenous C1P interacts with a specific Gi protein-coupled (Ptx-sensitive) receptor to induce rapid phosphorylation of these kinases. However, C1P also caused phosphorylation of STAT3, but this effect did not follow any bimodal pattern and was not inhibited by Ptx, suggesting that the JAK2/STAT3 pathway is independent of GPCR activation. In fact, it has been reported that the JAK/STAT3 pathway is associated with tyrosine kinase activation [87].

Regarding the second ERK1-2 and Akt phosphorylation phase, which occurs after 8-24 h of C1P addition, it is most likely that this is achieved in a receptor independent manner after C1P has entered the cells, a process that is rather slow when taking into consideration the low permeability of cell membranes to phospholipids. Also of importance is the fact that the rapid phosphorylation of STAT3 is not inhibited by Ptx, suggesting another possible (non Ptx-sensitive) mechanism of action of C1P, such as for instance a possible interaction with tyrosine kinase receptors. Nonetheless, it should be emphasized that with the available data this hypothesis is merely speculative and so, it should be judged with caution. Further work is obviously necessary to associate STAT phosphorylation (activation) by C1P with possible tyrosine kinase receptor interactions.

In this thesis, we have demonstrated that C1P stimulates cell survival and proliferation of 3T3-L1 preadipocytes. In particular, we have observed that preadipocyte cell death induced by incubation of the cells with serum-free medium was reversed by C1P and that the bioactive sphingolipid induced preadipocyte proliferation under quiescence conditions. Furthermore, we have shown that these effects were regulated by JAK2/STAT3, MEK/ERK1-2 and PI3K/Akt pathways. The implication of MEK/ERK1-2 and PI3K/Akt in survival and cell proliferation induced by C1P has been also described in BMDM [60, 62] and rat vascular smooth muscle cells [86]. Moreover, we have demonstrated that in the case of MEK/ERK1-2 and PI3K/Akt signaling cascades, survival and cell proliferation was stimulated by a second (late) phosphorylation phase induced by C1P and not by the rapid phosphorylation of these kinases, which takes place within minutes, suggesting that stimulation of cell survival and proliferation is elicited by intracellular C1P in a receptor independent manner. Of

interest, studies carried out in collaboration with Bittman and co-workers using photosensitive cell permeable C1P analogs (caged-C1P) also suggested that cell survival and proliferation are processes regulated by intracellularly generated C1P [88].

Another relevant finding in this thesis is that C1P regulates the migration of 3T3-L1 preadipocytes. First, we observed that 3T3-L1 preadipocytes migration can occur spontaneously, a process that may be essential for preadipocytes to differentiate into mature adipocytes. Indeed, preadipocytes migrate into defined fat cell clusters before undergoing differentiation [72]. In this thesis we have demonstrated that C1P enhances cell migration in 3T3-L1 preadipocytes, which is in agreement with previous work by our group using different cell types such as RAW264.7, J774.A1 and human THP-1macrophages [68, 74] or human pancreatic cancer cells PANC-1 and MIA PaCa-2 [71, 73]. The stimulation of cell migration by C1P has been confirmed by Ratajczak and co-workers, showing that the bioactive sphingolipid regulates migration and invasion of a variety of cancer cells, including human leukemia, rhabdomyosarcoma and lung cancer cells, as well as hematopoietic stem/progenitor cells (HSPC), multipotent stromal cells and human umbilical vein endothelial cells [89, 90]. In this thesis we found that C1P-enhanced 3T3-L1 preadipocyte migration is regulated by the JAK2/STAT3, MEK/ERK1-2 and PI3K/Akt signaling pathways, as inhibition of these pathways led to blockade of this process. Furthermore, we observed that C1P-stimulated preadipocyte migration was inhibited when the cells were preincubated with Ptx suggesting the intervention of a Gi protein putative receptor in the regulation of this process, Indeed, Ptx partially inhibited the first (rapid) phosphorylation of ERK1-2 and Akt. It should also be noted that Ptx did not inhibit the phosphorylation of STAT3, suggesting the JAK/STAT3 pathway is independent of Gi protein receptor activation and that other (non Ptx-sensitive) type of receptor might be implicated in C1P-stimulated preadipocyte migration.

Taken together, the results presented in this chapter demonstrate that the bioactive sphingolipid C1P is implicated in preadipocyte survival, proliferation and migration. We have shown that these effects are regulated by the JAK2/STAT3, MEK/ERK1-2 and PI3K/Akt signaling cascades. These findings add up important knowledge for understanding the molecular mechanisms that regulate biological

processes in preadipocytes, and may be crucial for developing novel therapeutic strategies to control obesity and obesity-related pathologies. The scheme shown below emphasizes the signaling pathways involved in C1P-stimulated survival, proliferation and migration in preadipocytes.

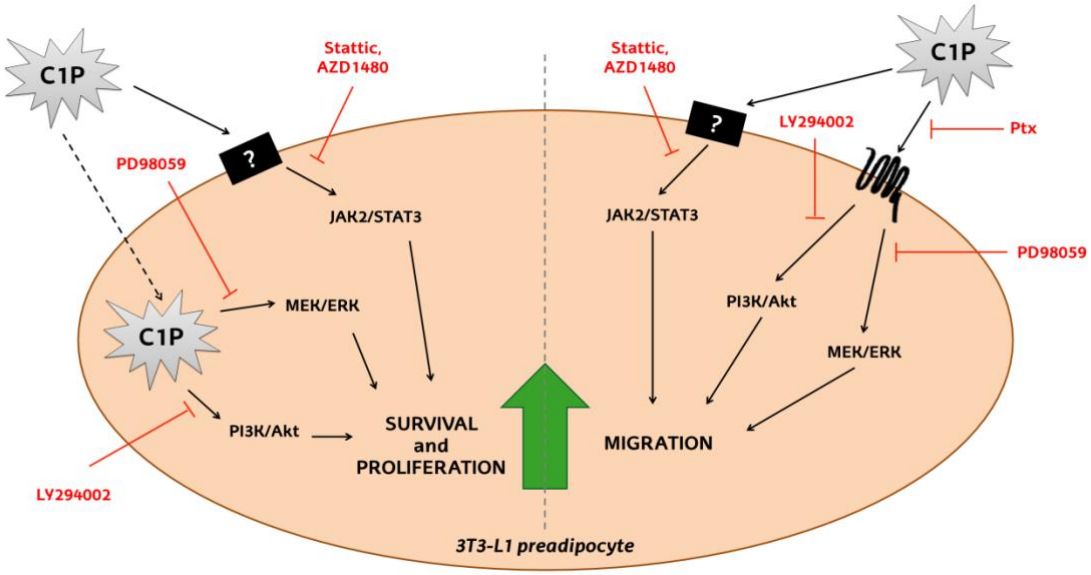

Figure 24. Working model for the implication of C1P in cell survival, proliferation and migration in 3T3-L1 preadipocytes.

4. References

1. Frigolet ME, Gutiérrez-Aguilar R. The colors of adipose tissue. Gac Med Mex. 2020; 156(2): 142-9.
2. Hajer GR, van Haeften TW, Visseren FLJ. Adipose tissue dysfunction in obesity, diabetes, and vascular diseases. Eur Heart J. 2008; 29(24): 2959-71.
3. Bays HE, González-Campoy JM, Bray GA, Kitabchi AE, Bergman DA, Schorr AB, et al. Pathogenic potential of adipose tissue and metabolic consequences of adipocyte hypertrophy and increased visceral adiposity. Expert Rev Cardiovasc Ther. 2008; 6(3): 343-68.
4. Tozzi M, Novak I. Purinergic receptors in adipose tissue as potential targets in metabolic disorders. Front Pharmacol. 2017; 8.
5. Curat CA, Miranville A, Sengenès C, Diehl M, Tonus C, Busse R, et al. From blood monocytes to adipose tissue-resident macrophages: induction of diapedesis by human mature adipocytes. Diabetes. 2004; 53(5): 1285-92.
6. Wozniak SE, Gee LL, Wachtel MS, Frezza EE. Adipose tissue: the new endocrine organ? A review article. Dig Dis Sci. 2009; 54(9): 1847-56.
7. Lefterova MI, Lazar MA. New developments in adipogenesis. Trends Endocrinol Metab. 2009; 20(3): 107-14.
8. Harms M, Seale P. Brown and beige fat: development, function and therapeutic potential. Nat Med. 2013; 19(10): 1252-63.
9. Ishibashi J, Seale P. Medicine. Beige can be slimming. Science. 2010; 328(5982): 1113-4.
10. Schetz M, De Jong A, Deane AM, Druml W, Hemelaar P, Pelosi P, et al. Obesity in the critically ill: a narrative review. Intensive Care Med. 2019; 45(6): 757-69.
11. https://www.who.int/es/news-room/fact-sheets/detail/obesity-and-overweight (Reviewed September 2021).
12. Dorresteijn JAN, Visseren FLJ, Spiering W. Mechanisms linking obesity to hypertension: Obesity-related hypertension. Obes Rev. 2012; 13(1): 17-26.
13. Franssen R, Monajemi H, Stroes ESG, Kastelein JJP. Obesity and dyslipidemia. Med Clin North Am. 2011; 95(5): 893-902.
14. Kahn SE, Hull RL, Utzschneider KM. Mechanisms linking obesity to insulin resistance and type 2 diabetes. Nature. 2006; 444(7121): 840-6.

15. McCarthy MI. Genomics, type 2 diabetes, and obesity. N Engl J Med. 2010; 363(24): 2339-50.
16. Drong AW, Lindgren CM, McCarthy MI. The genetic and epigenetic basis of type 2 diabetes and obesity. Clin Pharmacol Ther. 2012; 92(6): 707-15.
17. Masuoka HC, Chalasani N. Nonalcoholic fatty liver disease: an emerging threat to obese and diabetic individuals: Nonalcoholic fatty liver disease. Ann N Y Acad Sci. 2013; 1281(1): 106-22.
18. Speliotes EK. Genetics of common obesity and nonalcoholic fatty liver disease. Gastroenterology. 2009; 136(5): 1492-5.
19. Rocha VZ, Libby P. Obesity, inflammation, and atherosclerosis. Nat Rev Cardiol. 2009; 6(6): 399-409.
20. Hansson GK, Libby P. The immune response in atherosclerosis: a double-edged sword. Nat Rev Immunol. 2006; 6(7): 508-19.
21. Tzotzas T, Evangelou P, Kiortsis DN. Obesity, weight loss and conditional cardiovascular risk factors: Conditional cardiovascular risk factors and obesity. Obes Rev. 2011; 12(5): e282-9.
22. Apovian CM, Gokce N. Obesity and cardiovascular disease. Circulation. 2012; 125(9): 1178-82.
23. Khandekar MJ, Cohen P, Spiegelman BM. Molecular mechanisms of cancer development in obesity. Nat Rev Cancer. 2011; 11(12): 886-95.
24. Basen-Engquist K, Chang M. Obesity and cancer risk: recent review and evidence. Curr Oncol Rep. 2011; 13(1): 71-6.
25. Hursting SD, Dunlap SM. Obesity, metabolic dysregulation, and cancer: a growing concern and an inflammatory (and microenvironmental) issue: Obesity, metabolic syndrome, and cancer. Ann N Y Acad Sci. 2012; 1271(1): 82-7.
26. Ghaben AL, Scherer PE. Adipogenesis and metabolic health. Nat Rev Mol Cell Biol. 2019; 20(4): 242-58.
27. Spalding KL, Arner E, Westermark PO, Bernard S, Buchholz BA, Bergmann O, et al. Dynamics of fat cell turnover in humans. Obstet Gynecol Surv. 2008; 63(9): 577-8.
28. Hirsch J, Han PW. Cellularity of rat adipose tissue: effects of growth, starvation, and obesity. J Lipid Res. 1969; 10(1): 77-82.

29. Wang QA, Tao C, Gupta RK, Scherer PE. Tracking adipogenesis during white adipose tissue development, expansion and regeneration. Nat Med. 2013; 19(10): 1338-44.
30. Vishvanath L, MacPherson KA, Hepler C, Wang QA, Shao M, Spurgin SB, et al. Pdgfr β + mural preadipocytes contribute to adipocyte hyperplasia induced by high-fat-diet feeding and prolonged cold exposure in adult mice. Cell Metab. 2016; 23(2): 350-9.
31. Mancuso P. The role of adipokines in chronic inflammation. ImmunoTargets Ther. 2016; 47.
32. Guilherme A, Virbasius JV, Puri V, Czech MP. Adipocyte dysfunctions linking obesity to insulin resistance and type 2 diabetes. Nat Rev Mol Cell Biol. 2008; 9(5): 367-77.
33. Dixit VD. Adipose-immune interactions during obesity and caloric restriction: reciprocal mechanisms regulating immunity and health span. J Leukoc Biol. 2008; 84(4): 882-92.
34. Sarjeant K, Stephens JM. Adipogenesis. Cold Spring Harb Perspect Biol. 2012; 4(9): a008417.
35. Guo L, Li X, Tang Q-Q. Transcriptional regulation of adipocyte differentiation: a central role for CCAAT/enhancer-binding protein (C/EBP) β. J Biol Chem. 2015; 290(2): 755-61.
36. Spiegelman BM, Ginty CA. Fibronectin modulation of cell shape and lipogenic gene expression in 3T3-adipocytes. Cell. 1983; 35(3 Pt 2): 657-66.
37. Ordoñez M, Presa N, Trueba M, Gomez-Muñoz A. Implication of Ceramide Kinase in Adipogenesis. Mediators Inflamm. 2017; 2017: 1-7.
38. Zebisch K, Voigt V, Wabitsch M, Brandsch M. Protocol for effective differentiation of 3T3-L1 cells to adipocytes. Anal Biochem. 2012; 425(1): 88-90.
39. Hannun YA, Obeid LM. Principles of bioactive lipid signaling: lessons from sphingolipids. Nat Rev Mol Cell Biol. 2008; 9(2): 139-50.
40. Presa N, Gomez-Larrauri A, Rivera I-G, Ordoñez M, Trueba M, Gomez-Muñoz A. Regulation of cell migration and inflammation by ceramide 1-phosphate. Biochim Biophys Acta. 2016; 1861(5): 402-9.

41. Spiegel S, Merrill AH Jr. Sphingolipid metabolism and cell growth regulation. FASEB J. 1996; 10(12): 1388-97.
42. Chalfant CE, Spiegel S. Sphingosine 1-phosphate and ceramide 1-phosphate: expanding roles in cell signaling. J Cell Sci. 2005; 118(Pt 20): 4605-12.
43. Pettus BJ, Bielawska A, Spiegel S, Roddy P, Hannun YA, Chalfant CE. Ceramide kinase mediates cytokine- and calcium ionophore-induced arachidonic acid release. J Biol Chem. 2003; 278(40): 38206-13.
44. Pettus BJ, Bielawska A, Subramanian P, Wijesinghe DS, Maceyka M, Leslie CC, et al. Ceramide 1-phosphate is a direct activator of cytosolic phospholipase A2. J Biol Chem. 2004; 279(12): 11320-6.
45. Gomez-Muñoz A, Presa N, Gomez-Larrauri A, Rivera I-G, Trueba M, Ordoñez M. Control of inflammatory responses by ceramide, sphingosine 1-phosphate and ceramide 1-phosphate. Prog Lipid Res. 2016; 61: 51-62.
46. Chatterjee S. Sphingolipids in atherosclerosis and vascular biology. Arterioscler Thromb Vasc Biol. 1998; 18(10): 1523-33.
47. Shimabukuro M, Zhou YT, Levi M, Unger RH. Fatty acid-induced beta cell apoptosis: a link between obesity and diabetes. Proc Natl Acad Sci U S A. 1998; 95(5): 2498-502.
48. Augé N, Nègre-Salvayre A, Salvayre R, Levade T. Sphingomyelin metabolites in vascular cell signaling and atherogenesis. Prog Lipid Res. 2000; 39(3): 207-29.
49. Unger RH, Orci L. Diseases of liporegulation: new perspective on obesity and related disorders. FASEB J. 2001; 15(2): 312-21.
50. Hojjati MR, Li Z, Zhou H, Tang S, Huan C, Ooi E, et al. Effect of myriocin on plasma sphingolipid metabolism and atherosclerosis in apoE-deficient mice. J Biol Chem. 2005; 280(11): 10284-9.
51. Summers SA, Nelson DH. A role for sphingolipids in producing the common features of type 2 diabetes, metabolic syndrome X, and Cushing's syndrome. Diabetes. 2005; 54(3): 591-602.
52. Summers SA. Ceramides in insulin resistance and lipotoxicity. Prog Lipid Res. 2006; 45(1): 42-72.

53. Holland WL, Brozinick JT, Wang L-P, Hawkins ED, Sargent KM, Liu Y, et al. Inhibition of ceramide synthesis ameliorates glucocorticoid-, saturated-fat-, and obesity-induced insulin resistance. Cell Metab. 2007; 5(3): 167-79.
54. Camacho L, Zabala-Letona A, Cortazar AR, Astobiza I, Dominguez-Herrera A, Ercilla A, et al. Identification of androgen receptor metabolic correlome reveals the repression of ceramide kinase by androgens. Cancers. 2021; 13(17): 4307.
55. Larsen PJ, Tennagels N. On ceramides, other sphingolipids and impaired glucose homeostasis. Mol Metab. 2014; 3(3): 252-60.
56. Moon M-H, Jeong J-K, Park S-Y. Activation of S1P2 receptor, a possible mechanism of inhibition of adipogenic differentiation by sphingosine 1--phosphate. Mol Med Rep. 2015; 11(2): 1031-6.
57. Gangoiti P, Arana L, Ouro A, Granado MH, Trueba M, Gómez-Muñoz A. Activation of mTOR and RhoA is a major mechanism by which Ceramide 1-phosphate stimulates macrophage proliferation. Cell Signal. 2011; 23(1): 27-34.
58. Gangoiti P, Bernacchioni C, Donati C, Cencetti F, Ouro A, Gómez-Muñoz A, et al. Ceramide 1-phosphate stimulates proliferation of C2C12 myoblasts. Biochimie. 2012; 94(3): 597-607.
59. Gangoiti P, Granado MH, Arana L, Ouro A, Gomez-Muñoz A. Activation of protein kinase C-alpha is essential for stimulation of cell proliferation by ceramide 1-phosphate. FEBS Lett. 2010; 584(3): 517-24.
60. Gangoiti P, Granado MH, Wang SW, Kong JY, Steinbrecher UP, Gómez-Muñoz A. Ceramide 1-phosphate stimulates macrophage proliferation through activation of the PI3-kinase/PKB, JNK and ERK1/2 pathways. Cell Signal. 2008; 20(4): 726-36.
61. Gomez-Muñoz A, Duffy PA, Martin A, O'Brien L, Byun HS, Bittman R, et al. Short-chain ceramide-1-phosphates are novel stimulators of DNA synthesis and cell division: antagonism by cell-permeable ceramides. Mol Pharmacol. 1995; 47(5): 833-9.
62. Gómez-Muñoz A, Kong JY, Parhar K, Wang SW, Gangoiti P, González M, et al. Ceramide-1-phosphate promotes cell survival through activation of the phosphatidylinositol 3-kinase/protein kinase B pathway. FEBS Lett. 2005; 579(17): 3744-50.

63. Gómez-Muñoz A, Kong JY, Salh B, Steinbrecher UP. Ceramide-1-phosphate blocks apoptosis through inhibition of acid sphingomyelinase in macrophages. J Lipid Res. 2004; 45(1): 99-105.
64. Ouro A, Arana L, Riazy M, Zhang P, Gomez-Larrauri A, Steinbrecher U, et al. Vascular endothelial growth factor mediates ceramide 1-phosphate-stimulated macrophage proliferation. Exp Cell Res. 2017; 361(2): 277-83.
65. Baudiß K, Ayata CK, Lazar Z, Cicko S, Beckert J, Meyer A, et al. Ceramide-1-phosphate inhibits cigarette smoke-induced airway inflammation. Eur Respir J. 2015; 45(6): 1669-80.
66. Choi K-M, Lee Y-S, Choi M-H, Sin D-M, Lee S, Ji S-Y, et al. Inverse relationship between adipocyte differentiation and ceramide level in 3T3-L1 cells. Biol Pharm Bull. 2011; 34(6): 912-6.
67. Gangoiti P, Granado MH, Arana L, Ouro A, Gómez-Muñoz A. Involvement of nitric oxide in the promotion of cell survival by ceramide 1-phosphate. FEBS Lett. 2008; 582(15): 2263-9.
68. Granado MH, Gangoiti P, Ouro A, Arana L, Gómez-Muñoz A. Ceramide 1-phosphate inhibits serine palmitoyltransferase and blocks apoptosis in alveolar macrophages. Biochim Biophys Acta. 2009; 1791(4): 263-72.
69. Gomez-Muñoz A, Frago LM, Alvarez L, Varela-Nieto I. Stimulation of DNA synthesis by natural ceramide 1-phosphate. Biochem J. 1997; 325(2): 435-40.
70. Mitra P, Maceyka M, Payne SG, Lamour N, Milstien S, Chalfant CE, et al. Ceramide kinase regulates growth and survival of A549 human lung adenocarcinoma cells. FEBS Lett. 2007; 581(4): 735-40.
71. Granado MH, Gangoiti P, Ouro A, Arana L, González M, Trueba M, et al. Ceramide 1-phosphate (C1P) promotes cell migration Involvement of a specific C1P receptor. Cell Signal. 2009; 21(3): 405-12.
72. Crandall DL, Busler DE, McHendry-Rinde B, Groeling TM, Kral JG. Autocrine regulation of human preadipocyte migration by plasminogen activator inhibitor-1. J Clin Endocrinol Metab. 2000; 85(7): 2609-14.
73. Rivera I-G, Ordoñez M, Presa N, Gangoiti P, Gomez-Larrauri A, Trueba M, et al. Ceramide 1-phosphate regulates cell migration and invasion of human pancreatic cancer cells. Biochem Pharmacol. 2016; 102: 107-19.

74. Arana L, Ordoñez M, Ouro A, Rivera I-G, Gangoiti P, Trueba M, et al. Ceramide 1-phosphate induces macrophage chemoattractant protein-1 release: involvement in ceramide 1-phosphate-stimulated cell migration. Am J Physiol Endocrinol Metab. 2013; 304(11): E1213-26.
75. Gomez-Muñoz A, Gangoiti P, Arana L, Ouro A, Rivera I-G, Ordoñez M, et al. New insights on the role of ceramide 1-phosphate in inflammation. Biochim Biophys Acta. 2013; 1831(6): 1060-6.
76. Bowman T, Garcia R, Turkson J, Jove R. STATs in oncogenesis. Oncogene. 2000; 19(21): 2474-88.
77. Bromberg J. Stat proteins and oncogenesis. J Clin Invest. 2002; 109(9): 1139-42.
78. Levy DE, Lee C-K. What does Stat3 do? J Clin Invest. 2002; 109(9): 1143-8.
79. Nicolas CS, Peineau S, Amici M, Csaba Z, Fafouri A, Javalet C, et al. The JAK/STAT pathway is involved in synaptic plasticity. Neuron. 2012; 73(2): 374-90.
80. Omatsu-Kanbe M, Inoue K, Fujii Y, Yamamoto T, Isono T, Fujita N, et al. Effect of ATP on preadipocyte migration and adipocyte differentiation by activating P2Y receptors in 3T3-L1 cells. Biochem J. 2006; 393(Pt 1): 171-80.
81. Kim C-S, Kawada T, Yoo H, Kwon B-S, Yu R. Macrophage inflammatory protein-related protein-2, a novel CC chemokine, can regulate preadipocyte migration and adipocyte differentiation. FEBS Lett. 2003; 548(1-3): 125-30.
82. Caci G, Albini A, Malerba M, Noonan DM, Pochetti P, Polosa R. COVID-19 and obesity: Dangerous liaisons. J Clin Med. 2020; 9(8): 2511.
83. Patel VB, Basu R, Oudit GY. ACE2/Ang 1-7 axis: A critical regulator of epicardial adipose tissue inflammation and cardiac dysfunction in obesity. Adipocyte. 2016; 5(3): 306-11.
84. Engeli S, Schling P, Gorzelniak K, Boschmann M, Janke J, Ailhaud G, et al. The adipose-tissue renin–angiotensin–aldosterone system: role in the metabolic syndrome? Int J Biochem Cell Biol. 2003; 35(6): 807-25.
85. Gomez-Muñoz A, Gangoiti P, Rivera I-G, Presa N, Gomez-Larrauri A, Ordoñez M. Caged ceramide 1-phosphate (C1P) analogs: Novel tools for studying C1P biology. Chem Phys Lipids. 2016; 194: 79-84.
86. Kim T-J, Kang Y-J, Lim Y, Lee H-W, Bae K, Lee Y-S, et al. Ceramide 1-phosphate induces neointimal formation via cell proliferation and cell cycle progression

upstream of ERK1/2 in vascular smooth muscle cells. Exp Cell Res. 2011; 317(14): 2041-51.

87. Igaz P, Tóth S, Falus A. Biological and clinical significance of the JAK-STAT pathway; lessons from knockout mice. Inflamm Res. 2001; 50(9): 435-41.
88. Lankalapalli RS, Ouro A, Arana L, Gómez-Muñoz A, Bittman R. Caged ceramide 1-phosphate analogues: synthesis and properties. J Org Chem. 2009; 74(22): 8844-7.
89. Kim C, Schneider G, Abdel-Latif A, Mierzejewska K, Sunkara M, Borkowska S, et al. Ceramide-1-phosphate regulates migration of multipotent stromal cells and endothelial progenitor cells--implications for tissue regeneration. Stem Cells. 2013; 31(3): 500-10.
90. Abdelbaset-Ismail A, Cymer M, Borkowska-Rzeszotek S, Brzeźniakiewicz-Janus K, Rameshwar P, Kakar SS, et al. Bioactive phospholipids enhance migration and adhesion of human leukemic cells by inhibiting heme oxygenase 1 (HO-1) and inducible nitric oxygenase synthase (iNOS) in a p38 MAPK-dependent manner. Stem Cell Rev. 2019; 15(1): 139-54.

Chapter 2

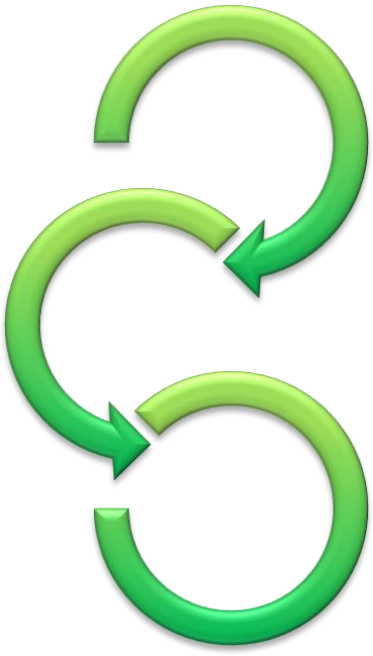

CHAPTER 2:

Implication of C1P in the regulation of alveolar macrophage migration

1. Introduction

1.1. Alveolar macrophages

Macrophages and macrophage-like cells are present in all mammalian organs. In the lung, there are two distinct macrophage populations: alveolar macrophages and interstitial macrophages. Alveolar macrophages are in close contact with type I and II epithelial cells of alveoli [1], whereas interstitial macrophages reside in the parenchyma between the microvascular endothelium and alveolar epithelium [2].

Alveolar macrophages derive from yoke sac procurers of fetal monocytes and populate the alveoli shortly after birth, persisting over the lifespan via self-renewing embryo-derive populations independently of bone marrow contribution [3, 4]. However, due to inflammatory events, bone marrow-derived monocytes are also recruited to the lung and differentiated into alveolar macrophages [5]. This differentiation is mediated in part by granulocyte-macrophage colony-stimulating factor (GM-CSF) [6].

Regarding the functional phenotype of alveolar macrophages, it is modulated by the unique microenvironment of the lung and they are critical for tissue homeostasis, host defense, clearance of surfactant and cell debris, pathogen recognition, initiation and resolution of lung inflammation and repair of damaged tissue [7]. Alveolar macrophages are the first line of defense against pollutants and pathogenic microbes that initiate an innate immune response in the lung and two phenotypes of them have been identified: classically activated macrophages (M1 macrophages) and alternatively activated macrophages (M2 macrophages). While M1 macrophages respond to microbial factors and Th1 pro-inflammatory cytokines to exhibit glycolytic metabolism

that is associated with inflammatory cytokine release, enhanced bacterial killing and the recruitment of immune cells into the lung parenchyma and alveolus, the M2 macrophages are induced by exposure to the Th2 cytokines to exhibit oxidative metabolism that is associated with anti-inflammatory cytokine release, phagocytosis of apoptotic cells and collagen deposition that contribute to the resolution of inflammation and repair of damaged tissues [8, 9].

Alveolar macrophages have high plasticity, so in response to the different mediators released in the microenvironment they are phenotypically and functionally modified to adopt pro-inflammatory, pro-fibrotic, anti-inflammatory, anti-fibrotic, pro-asthmatic, pro-resolving or tissue regenerating properties [10, 11]. Indeed, the polarization states of alveolar macrophages are not mutually exclusive and can exhibit elements of both M1 and M2 macrophages simultaneously depending on environmental signals [12].

Therefore, understanding the function and regulatory mechanisms of alveolar macrophages could lead to novel therapies for pulmonary diseases. In this line, NR8383 cell line, an alveolar macrophage cell line originally derived by broncho-alevolar lavage procedure of an adult male Sprague-Dawley rat, provides a homogenous source of highly responsive alveolar macrophages which can be used in vitro to study macrophage related activities. Indeed, this cell line was shown to exhibit many characteristics and functions of freshly isolated rat alveolar macrophages [13, 14].

1.2. Chronic obstructive pulmonary disease (COPD) and Silicosis

Chronic obstructive pulmonary disease (COPD) is a chronic respiratory disorder that progresses slowly and is characterized by an obstructive ventilator pattern caused by chronic inflammation of the airways and lung parenchyma. This chronic inflammation is normally triggered by the inhalation of noxious gases, such as cigarette smoke, or particles [15, 16] and is characterized by the accumulation of macrophages

and neutrophils in the lungs [17]. Typically, there are two major clinical features of COPD: chronic bronchitis and emphysema (Figure 1). On the one hand, chronic bronchitis results from chronic inflammation of small and medium-size airways and leads to airflow limitation, dyspnea, chronic cough and sputum production. Emphysema, on the other hand, is the result of inflammatory processes that destroy elastic tissue in the terminal airspaces (air sacs or alveoli) and lung parenchyma, causing the loss of lung elastic recoil, airflow limitation, dyspnea and hypoxemia.

Regarding noxious particles, one of the most common is silica (SiO_2), which could cause silicosis. Indeed, silicosis is caused by inhaling crystalline silica dust, and it could be pathologically characterized by diffuse pulmonary interstitial inflammation and fibrosis. Crystalline silica dust is widely distributed naturally and workers engaged in construction, building or refurbishments are the largest occupational group exposing to it [18].

In 1995, the World Health Organization (WHO) and the International Labour Organization set the goal to eliminate silicosis worldwide by 2030, but the silicosis population is still expanding. A study conducted in 2015 demonstrated that the prevalence of silicosis in South African gold miners kept a relatively high level between 1984 and 2009 [19], and in India, an estimated 11.5 million workers are still exposing to silica dust [20]. Moreover, in 2016, the Global Burden of Disease Study estimated 10.400 deaths per year [21]. Therefore, silicosis is still a severe global health problem and unfortunately, there is no effective treatment for it.

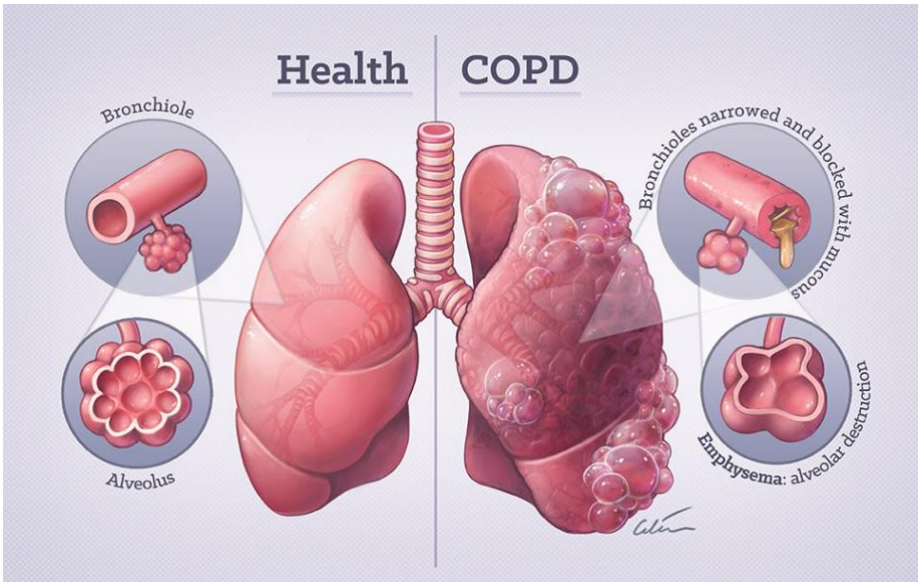

Figure 1. Schematic representation of the two major clinical features of COPD: chronic bronchitis and emphysema. Taken from Medical Research Institute of New Zealand website.

1.3. Macrophage migration: regulation and relationship to disease

Cell migration is an essential physiological process that is critical for embryogenesis, organogenesis, would healing or cell differentiation, but it is also relevant in the regulation of immune responses leading to inflammation. Uncontrolled inflammation, however, is detrimental for cells and can lead to disease. Tissue infiltration of macrophages could exacerbate pathological processes, such as chronic inflammation, neurodegenerative disorders, cancer development or obesity [14, 22-24]. Also, production of abnormal chemotactic signals may induce the migration of cells to inappropriate sites in the organism, thereby altering tissue homeostasis. Thus, cell migration plays a critical role in chronic inflammatory diseases [25].

Cell migration is a complex process that requires strict coordination of the following steps: cell polarization, protrusion and cell adhesion. These processes are regulated by complex signaling networks initiated by integrins and other receptors, but the molecular mechanisms involved in that regulation are not completely understood. Thus, understanding the mechanisms that support cell migration is essential for the development of new strategies for treating inflammatory diseases.

Interestingly, some of the pathways involved in the regulation of cell migration have been shown to be modulated by bioactive sphingolipids. In particular, our group demonstrated that C1P can induce cell migration in different cell types, including mouse and human monocytes or human pancreatic cancer cells [26-28], an action that requires interaction of C1P with a pertussis toxin (Ptx)-sensitive receptor [26-28]. Understanding the molecular mechanisms that regulate alveolar macrophage migration in physiological and inflammatory states may be important for developing new therapies for pulmonary inflammatory diseases. For this reason, in this chapter we sought to determine the implication of C1P in the regulation of cell migration under physiological or silica-induced inflammatory states in NR8383 alveolar macrophages.

2. Results

2.1. NR8383 alveolar macrophages migrate spontaneously independently of glucose concentration

Alveolar macrophages are the first line of defense against pollutants and pathogenic microbes in the lung, so they are built to respond rapidly to migratory stimuli. Hence, we first tested to evaluate whether NR8383 alveolar macrophages were able to migrate spontaneously. Using a Boyden chamber-based migration assay at different time points we observed that macrophages underwent spontaneous migration over time reaching maximal values after 24 hours on incubation (Figure 2).

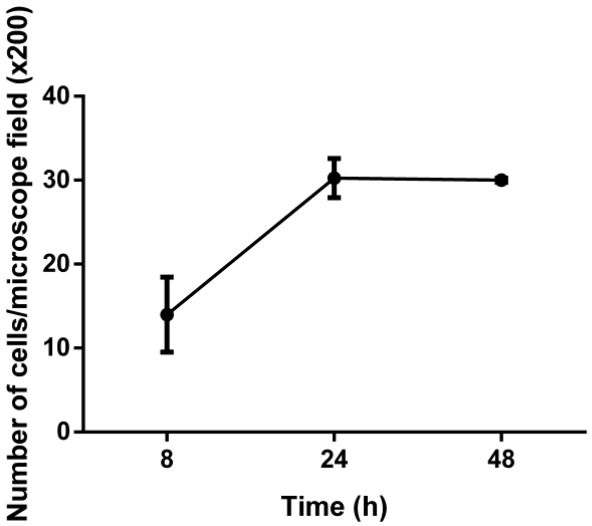

Figure 2. NR8383 macrophages migrate spontaneously. Macrophage migration was measured using a Boyden chamber-based cell migration assay. Cells (10^5 cells/well) were seeded in the upper wells of 24-well chambers coated with fibronectin. After 2 hours of incubation, chambers holding the cells were immersed in the lower compartments. Cells were further incubated for indicated times and cell migration was measured as described in *Materials and Methods*. Results are expressed as the number of migrated cells/microscope field (x200) and are the mean ± SEM of 3 independent experiments performed in duplicate.

It is known that the concentration of glucose is a key factor for migration of different cell types, including mouse RAW264.7 macrophages [29]. Hence, we sought to evaluate whether glucose might affect migration of the alveolar macrophages. Figure 3 shows that contrary to RAW264.7 macrophages, glucose did not affect migration of alveolar NR8383 cells.

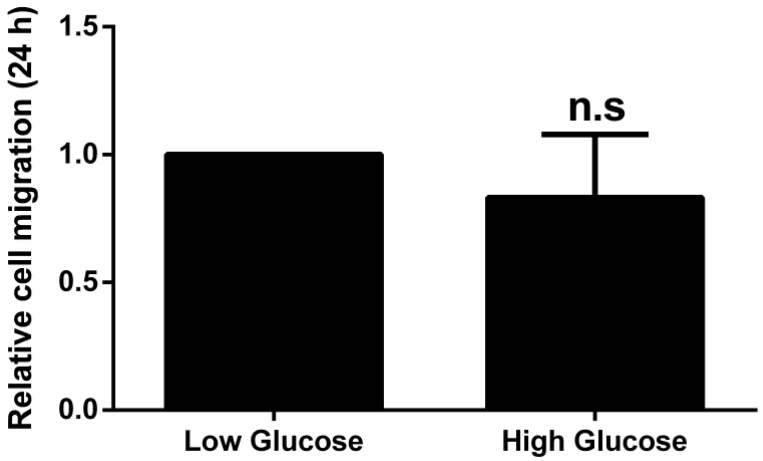

Figure 3. Glucose concentration does not affect the spontaneous migration of NR8383 macrophages. Macrophage migration was measured using a Boyden chamber-based cell migration assay. Cells (10^5 cells/well) were seeded in the upper wells of 24-well chambers coated with fibronectin. After 2 hours of incubation, chambers holding the cells were immersed in the lower compartments containing medium with low (1.8 g/L) or high (4.5 g/L) of glucose. The cells were further incubated for 24 hours and cell migration was measured as described in *Materials and Methods*. Results are expressed as the number of migrated cells relative to the number of cells migrated in the control chamber and are the mean ± SEM of 2 independent experiments performed in duplicate (n.s. $p>0.05$).

2.2. C1P inhibits cell migration in NR3838 macrophages

Our group previously established that C1P induces migration of different cell types, including mouse (RAW264.7 and J774.A1) and human (THP-1) monocytes/macrophages or human pancreatic cancer cells (PANC-1 and MIA PaCa-2) [26-28]. Moreover, in chapter 1 of this thesis we showed that C1P also enhances the migration of 3T3-L1 preadipocytes. To test the effect of C1P in NR8383 alveolar macrophages, we carried out the Boyden chamber-based migration assay with different concentrations of C1P. Surprisingly, we observed that C1P inhibited cell migration, with maximal inhibition attained at 10 µM C1P (Figure 4A-B). The inhibitory effect of C1P on alveolar macrophage migration remained stable for at least 48 hours (Figure 4C-D).

A.

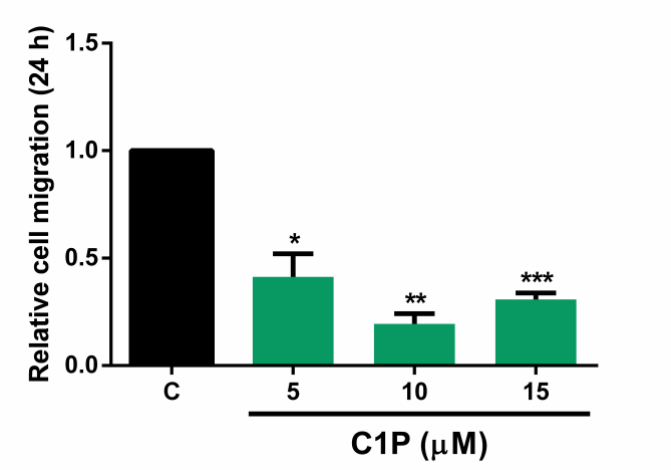
Relative cell migration (24 h)
1.5
1.0
0.5
0.0
*
**
***
C
5
10
15
C1P (μM)

B.

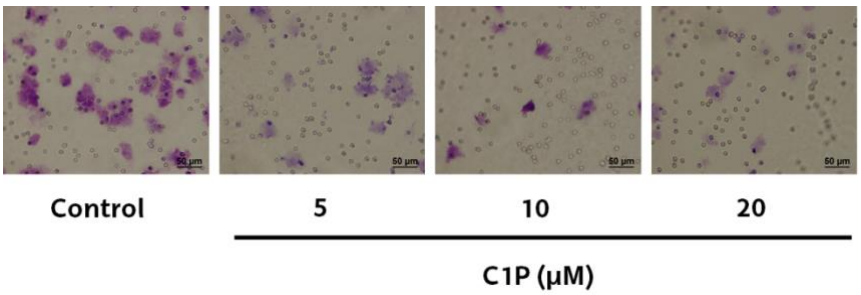
Control
5
10
20
C1P (μM)

C.

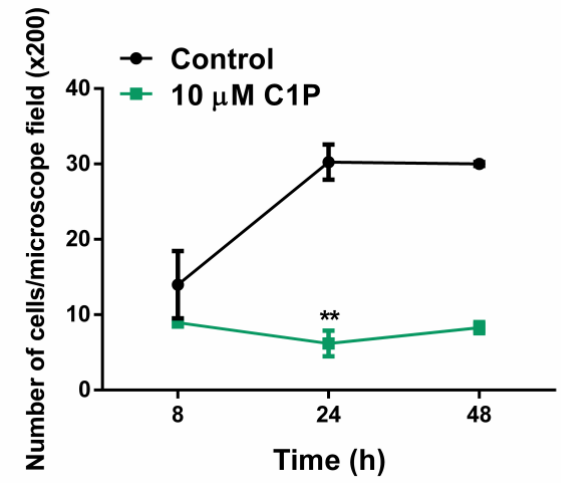
Number of cells/microscope field (x200)
Control
10 μM C1P
40
30
20
10
0
**
8
24
48
Time (h)

D.

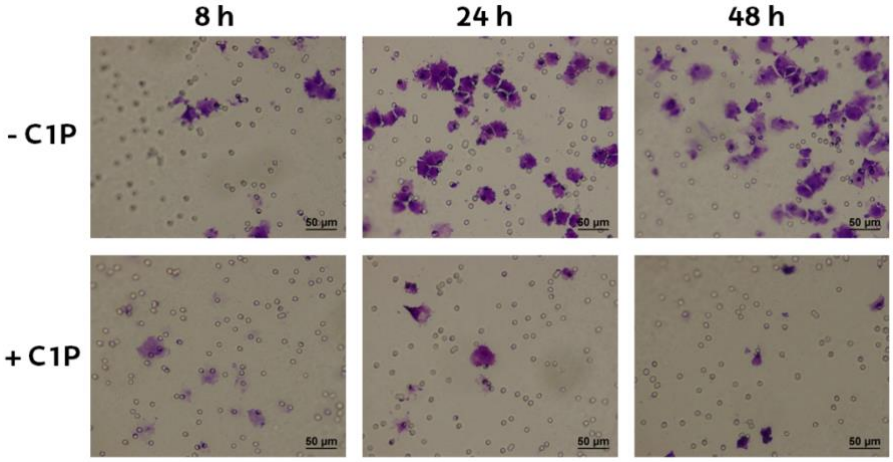

Figure 4. C1P inhibits cell migration in NR8383 macrophages. Macrophage migration was measured using a Boyden chamber-based cell migration assay. Cells (10^5 cells/well) were seeded in the upper wells of 24-well chambers coated with fibronectin. A) After 2 hours of incubation, cells were preincubated with vehicle or different concentrations of C1P for 1 hour. Chambers holding the cells were immersed in the lower compartments containing different concentrations of C1P. Cells were further incubated for 24 hours and cell migration was measured as described in *Materials and Methods*. Results are expressed as the number of migrated cells relative to the number of cells migrated in the control chamber and are the mean ± SEM of 4 independent experiments performed in duplicate (*p<0.05; **p<0.01; ***p<0.001). C) After 2 hours of incubation, cells were preincubated with vehicle or 10 µM C1P for 1 hour. Chambers holding the cells were immersed in the lower compartments which were filled with vehicle or 10 µM of C1P. Cells were further incubated for indicated times and cell migration was measured as described in *Materials and Methods*. Results are expressed as the number of migrated cells/microscope field (x200) and are the mean ± SEM of 3 independent experiments performed in duplicate (**p<0.01). B) and D) NR8383 migrated cells in chambers with 8 µm pore size.

2.3. C1P inhibits Akt, ERK1-2, Paxillin and PAK1 phosphorylation in NR8383 macrophages

Some of the best characterized pathways linked to cell migration are Phosphoinositide 3-kinase (PI3K)/Protein kinase B (PKB/Akt) and Mitogen activated protein kinase kinase (MEK)/Extracellular signal-regulated kinase (ERK1-2) (MAPK), with PAK1 often being upstream of these pathways, which are al activated by specific phosphorylations [26, 27, 30-33]. An important protein involved in the regulation of cell chemotaxis is Paxillin, which can be upstream or downstream of ERK1-2 and Akt [34, 35]. Paxillin is a multifunctional and multidomain focal adhesion adapter protein which serves an important scaffolding role at focal adhesions by recruiting structural

and signaling molecules involved in cell migration, when phosphorylated on specific Tyr and Ser residues [32]. To test if these pathways were targeted by C1P, we incubated NR8383 cells with 10 µM C1P and measured the level of phosphorylation at different times. In agreement with the inhibition of cell migration, we observed that C1P caused dephosphorylation of PKB/AKT, ERK1-2, Paxillin and PAK1 (Figure 5).

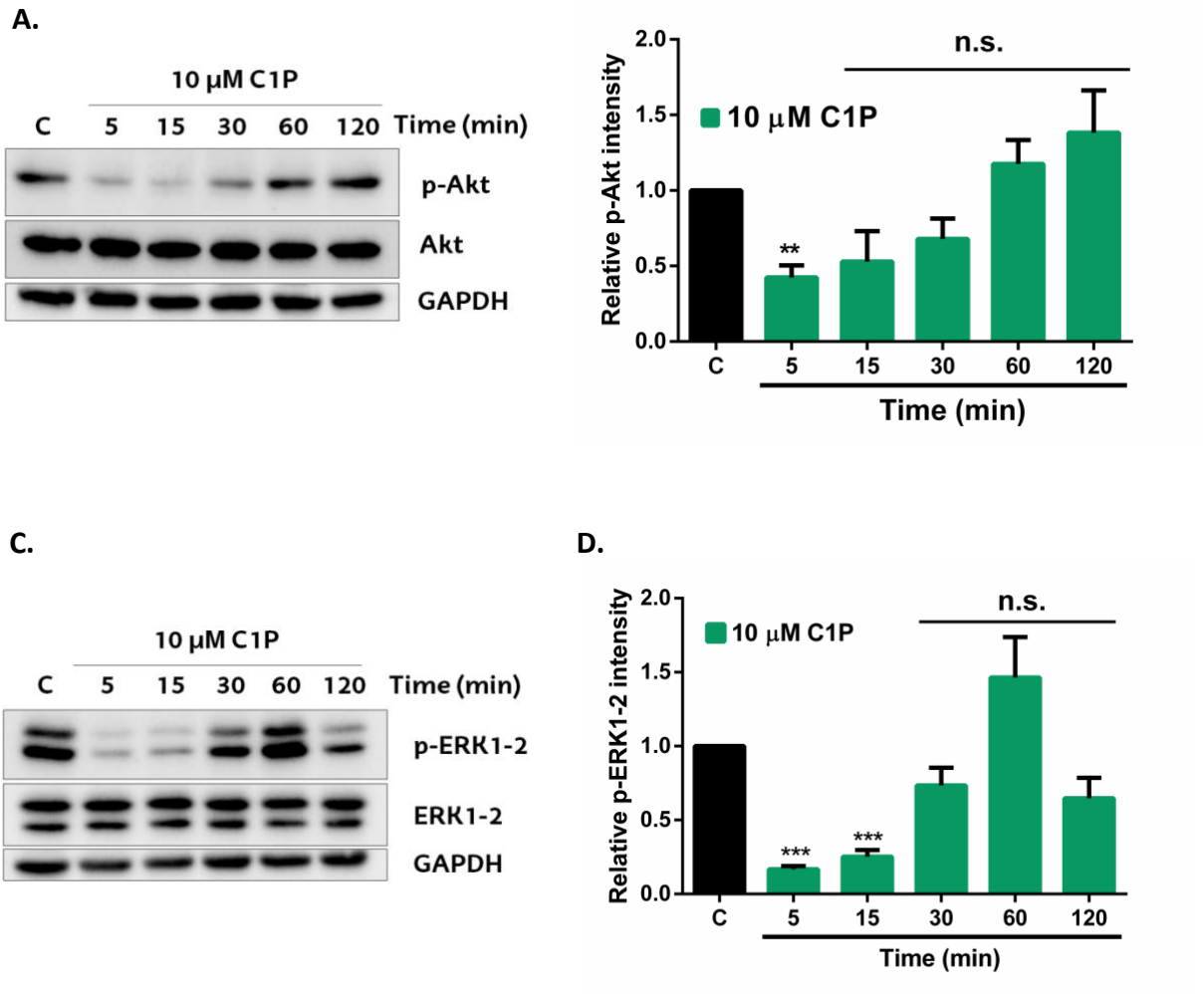

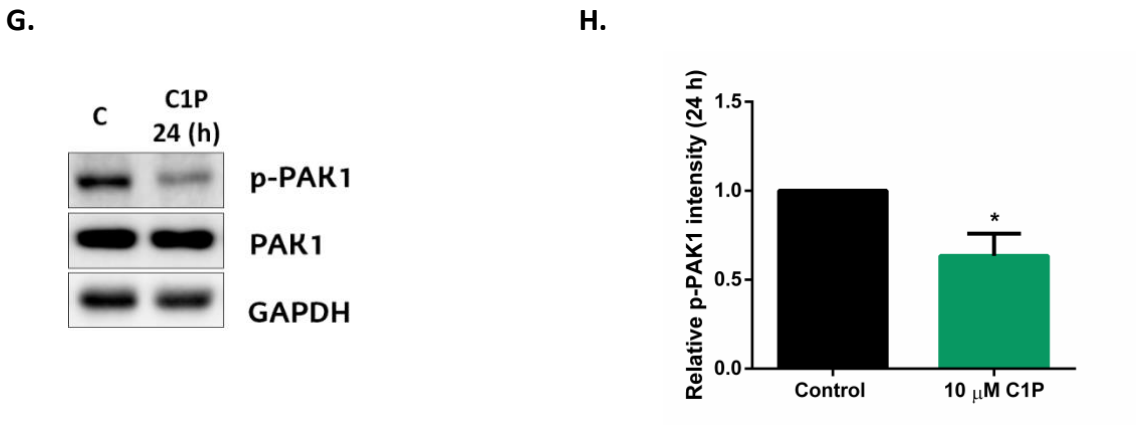

Figure 5. C1P inhibits Akt, ERK1-2, Paxillin and PAK1 phosphorylation in NR8383 macrophages. NR8383 cells were seeded in 6-well plates (10^6 cells/well) and they were grown in Ham's F12K supplemented with 15% FBS. The next day, the medium was replaced with fresh medium without serum. A) C) E) and G). After 2 hours of incubation, vehicle or 10 μM of C1P were added and the cells were harvested at the indicated time points. The presence of p-Akt, p-ERK1-2, p-Paxillin and p-PAK1 proteins were detected by Western blotting, as described in *Materials and Methods*, using specific antibodies to p-Akt, p-ERK1-2, p-Paxillin and p-PAK1. Equal loading of protein was monitored using specific antibodies to Akt, ERK1-2, Paxillin, PAK1 and GAPDH, respectively. B) D) F) and H) Results of scanning densitometry of the exposed films. Data are expressed as arbitrary units of intensity of the p-Akt, p-ERK1-2, p-Paxillin and p-PAK1 proteins and are the mean ± SEM of 4-6 independent experiments (*p<0.05; **p<0.01; ***p<0.001).

2.4. Pertussis toxin does not reverse the inhibitory effect of C1P on cell migration in NR8383 macrophages

Our group previously demonstrated that the chemotactic effect of C1P in different cell types requires the interaction of C1P with a putative pertussis toxin (Ptx)-sensitive receptor [26]. Hence, we sought to determine whether the C1P receptor was involved

in the inhibitory effect of C1P in alveolar macrophage migration. In order to address this question, we performed Boyden chamber-based migration assays by pre-treating the cells with Ptx before adding C1P. Ptx did not reverse the inhibition of cell migration induced by C1P, suggesting that the putative receptor of C1P is not involved in this process (Figure 6).

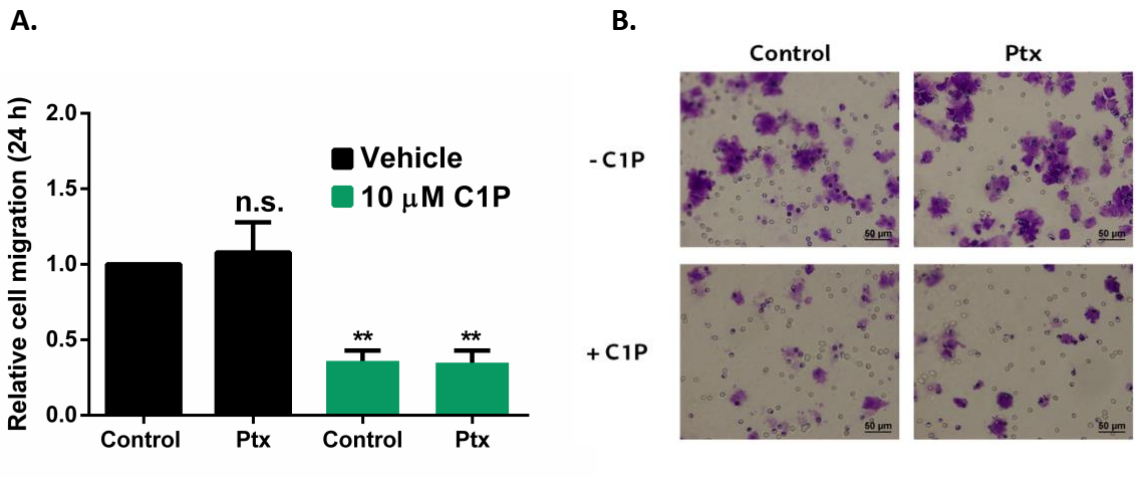

Figure 6. Pertussis toxin (Ptx) does not reverse the inhibitory effect of C1P on cell migration in NR8383 macrophages. Migration was measured using a Boyden chamber-based cell migration assay. Cells (10^5 cells/well) were seeded in the upper wells of 24-well chambers coated with fibronectin, and incubated for 2 hours. The cells were then preincubated for 4 hours with vehicle or with 0.1 µg/ml of Ptx. After this preincubation, either vehicle, Ptx or C1P were added to the cells and preincubated for 2 additional hours. The cells were then immersed in the lower compartments containing vehicle, 0.1 µg/ml Ptx or 10 µM of C1P. Cells were further incubated for 24 hours and cell migration was measured as described in *Materials and Methods*. A) Results are expressed as the number of migrated cells relative to the number of cells migrated in the control chamber and are the mean ± SEM of 3 independent experiments performed in duplicate (**p<0.01). B) Microscopic images of NR8383 migrated cells in chambers with 8 µm pore size.

2.5. Inflammatory granular nanosized silica induces NR8383 cell migration. Inhibition by C1P

Alveolar macrophages are the first line of defence against pathogenic microbes and pollutants that initiate an innate immune response in the lung. An important pollutant is silica dust, which could cause silicosis, a disease that is characterized by diffuse pulmonary interstitial inflammation and fibrosis. For this reason, we sought to

evaluate whether a granular nanosized silica-conditioned medium could induce alveolar macrophage migration, which might lead to an inflammatory state. To this purpose, we first stimulated NR8383 cells with granular nanosized silica and we then used the resultant conditioned medium to test if it could induce migration of the alveolar macrophages. We observed that the granular nanosized silica-conditioned medium did induce alveolar macrophage migration (Figure 7). We then tested to see whether C1P could inhibit the silica-conditioned medium-stimulated cell migration. Figure 7 shows that 10 µM C1P completely inhibited the silica-conditioned medium-stimulated migration of alveolar macrophages.

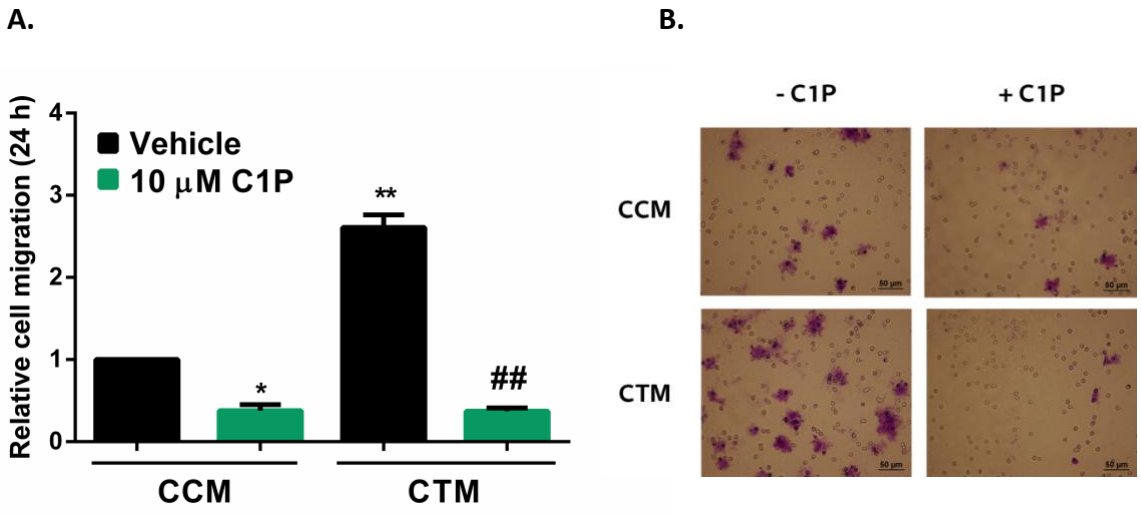

Figure 7. Conditioned-medium from NR8383 cells incubated with nanosized silica induce NR8383 cell migration. Inhibition by C1P. NR8383 macrophages were seeded in 6-well plates (2.3 x 10^6 cells/well) and were grown in Ham's F12K supplemented with 15% FBS. The next day, the medium was replaced with fresh medium without serum. After 2 hours of incubation, vehicle or 50 µg/ml of SiO_2 were added and cells were further incubated for 16 hours. Thereafter, the cells were removed by centrifugation at 400xg for 5 minutes and particles were removed by centrifugation at 15,000xg for 10 minutes at room temperature. The supernatants were immediately used for migration assays. A) Cell migration was measured using a Boyden chamber-based cell migration assay. Cells (10^5 cells/well) were seeded in the upper wells of 24-well chambers precoated with fibronectin, and incubated for 2 hours. The cells were then preincubated further for 1 hour with vehicle or with 10 µM C1P. After preincubation, cells were immersed in the lower compartments containing vehicle, 10 µM C1P, CCM (conditioned-control medium: supernatants not treated with SiO_2) or CTM (conditioned-treated medium: supernatants treated with SiO_2). The cells were further incubated for 24 hours and cell migration was measured as described in

Materials and Methods. Results are expressed as the number of migrated cells relative to the number of cells migrated in the control chamber and are the mean ± SEM of 3 independent experiments performed in duplicate (*p<0.05; **p<0.01; $^{\#\#}$p<0.01). B) Microscopic images of NR8383 migrated cells in chambers with 8 µm pore size.

2.6. Implication of the PI3K/Akt pathway in SiO_2 CTM-induced cell migration in NR8383 macrophages

Previous studies in our lab showed that the Phosphoinositide 3-kinase (PI3K)/Protein kinase B (PKB/Akt) and Mitogen activated protein kinase (MAPK)/Extracellular signal-regulated kinase (ERK1-2) pathways are implicated in the regulation of cell migration [26, 27, 30, 31]. Hence, we tested to evaluate whether the granular nanosized silica-conditioned medium might alter the phosphorylation state of AKT and ERK1-2 kinases. To this purpose, we incubated NR8383 cells with the granular nanosized silica-conditioned medium and measured the phosphorylation levels of these kinases at different time points. Also, we sought to evaluate whether C1P was able to alter the phosphorylation levels of both of these kinases. Figure 8 shows that the granular nanosized silica-conditioned medium phosphorylates AKT but not ERK1-2 and that C1P completely blocks Akt phosphorylation.

A.

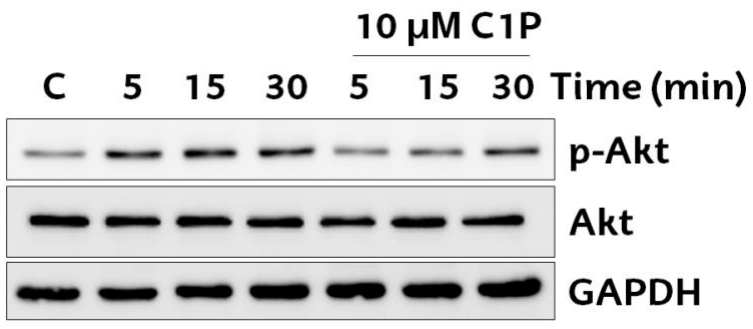

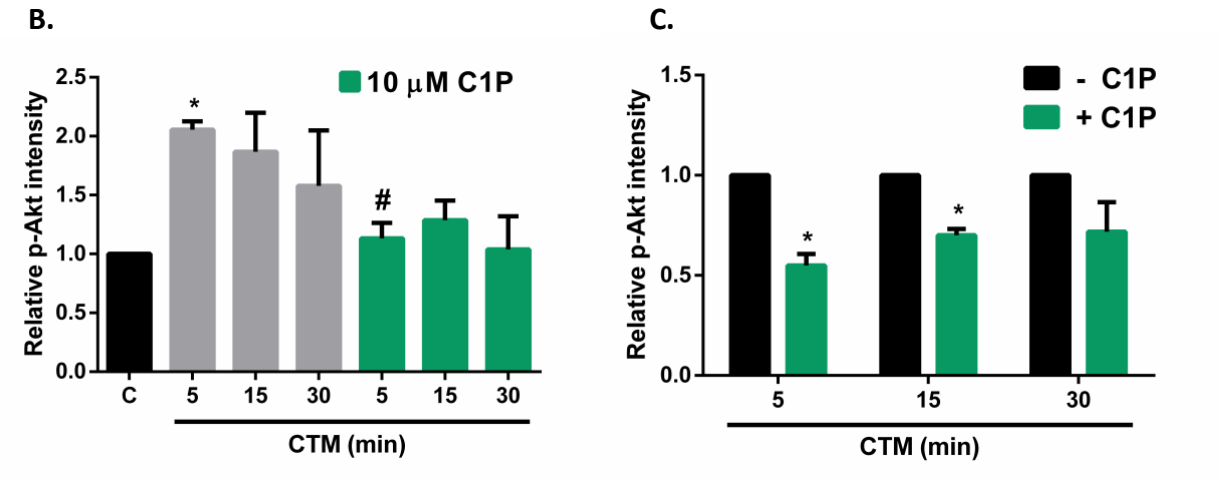
B.
10 µM C1P
Relative p-Akt intensity
2.5
2.0
1.5
1.0
0.5
0.0
*
#
C
5
15
30
5
15
30
CTM (min)
C.
- C1P
+ C1P
Relative p-Akt intensity
1.5
1.0
0.5
0.0
*
*
5
15
30
CTM (min)

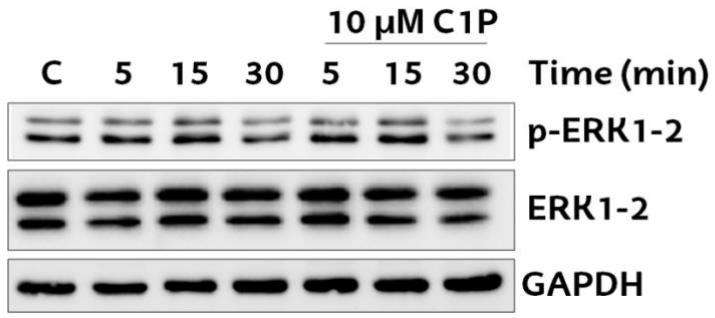
D.
10 µM C1P
C
5
15
30
5
15
30
Time (min)
p-ERK1-2
ERK1-2
GAPDH

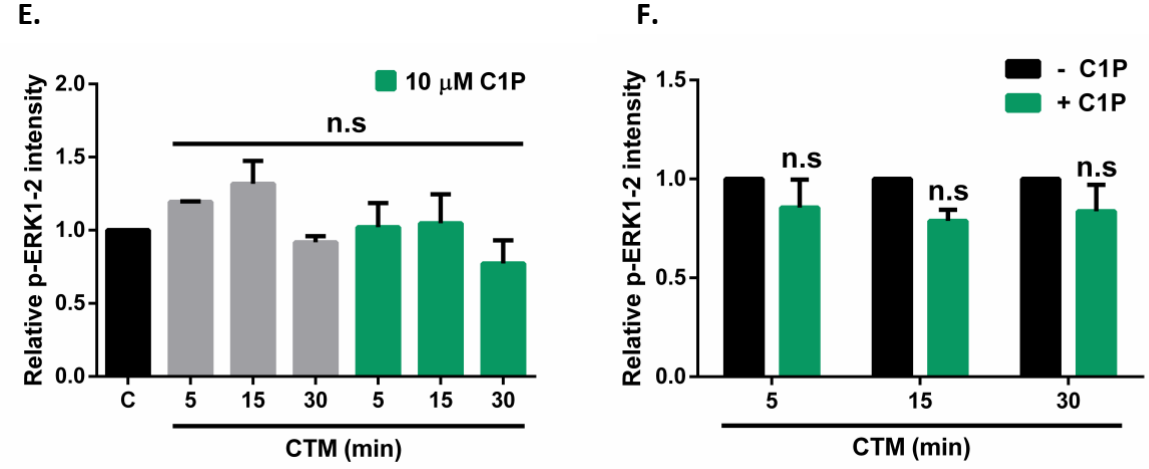
E.
10 µM C1P
n.s
Relative p-ERK1-2 intensity
2.0
1.5
1.0
0.5
0.0
C
5
15
30
5
15
30
CTM (min)
F.
- C1P
+ C1P
Relative p-ERK1-2 intensity
1.5
1.0
0.5
0.0
n.s
n.s
n.s
5
15
30
CTM (min)

Figure 8. Granular nanosized silica-conditioned medium (CTM) phosphorylates Akt but not ERK1-2 in NR8383 macrophages. Blockade of Akt phosphorylation by C1P. NR8383 macrophages were seeded in 6-well plates (2.3 x 10^6 cells/well) and grown in Ham's F12K supplemented with 15% FBS. The next day, the medium was replaced with fresh medium without serum. After 2 hours of incubation, vehicle or 50 µg/ml of SiO_2 were added and cells were further incubated for 16 hours. Thereafter, the cells were removed by centrifugation at 400 g for 5 minutes and particles were removed by centrifugation at 15,000 g for 10 minutes at room temperature. The supernatants (CTM) were immediately used in experiments. A) and D) Cells were preincubated for 1 hour with vehicle or 10 µM C1P. Then CTM was added and the cells were harvested at the indicated time points. The presence of p-Akt and p-ERK1-2 proteins were detected by Western blotting, as described in *Materials and Methods*, using specific antibodies to p-Akt and p-ERK1-2. Equal loading of protein was monitored using specific antibodies to total Akt and ERK1-2. B) C) E) and F) Results of scanning densitometry of exposed films. Data are expressed as arbitrary units of intensity of the p-Akt and p-ERK1-2 proteins and are the mean ± SEM of 2-3 independent experiments (*$p<0.05$; $^{\#}p<0.05$).

2.7. Pertussis toxin (Ptx) does not inhibit the SiO_2 CTM-induced cell migration in NR8383 macrophages

To evaluate if SiO_2 CTM-stimulated NR8383 macrophage migration involved activation of any Gi protein-coupled receptor, the cells were preincubated with Ptx prior to stimulation with the CTM. Figure 9 shows that the toxin did not inhibit this process, suggesting that no component of SiO_2 CTM was able to bind to any Gi protein-coupled receptor.

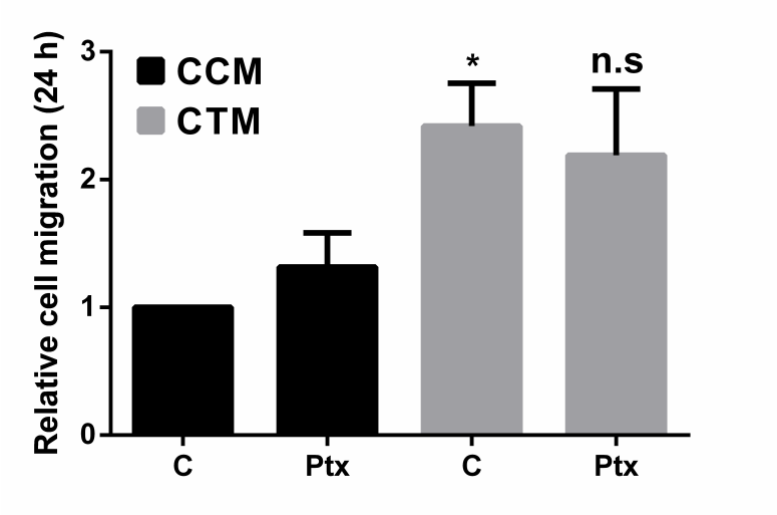

Figure 9. Pertussis toxin (Ptx) does not inhibit SiO_2 CTM-induced cell migration in NR8383 macrophages. NR8383 macrophages were seeded in 6-well plates (2.3 x 10^6 cells/well) and grown in Ham's F12K supplemented with 15% FBS. The next day, the medium was replaced with fresh medium without serum. After 2 hours of incubation, vehicle or 50 µg/ml of SiO_2 were added and cells were further incubated for 16 hours. Thereafter, the cells were removed by centrifugation at 400 g for 5 minutes and particles were removed by centrifugation at 15,000 g for 10 minutes at room temperature. The supernatants were immediately used for the migration assays. Cells (10^5 cells/well) were seeded in the upper wells of 24-well chambers precoated with fibronectin, and incubated for 2 hours. The cells were then preincubated for 4 hours with vehicle or with 0.1 µg/ml Ptx. After this preincubation, the cells were immersed in the lower compartments containing either CCM (conditioned-control medium: supernatants not treated with SiO_2) or CTM (conditioned-treated medium: supernatants treated with SiO_2). Cells were further incubated for 24 hours and cell migration was measured as described in *Materials and Methods*. Results are expressed as the number of migrated cells relative to the number of cells migrated in the control chamber and are the mean ± SEM of 7 independent experiments performed in duplicate (*$p<0.05$).

2.8. Lack of toxicity of the inhibitors used in experiments

All commonly used chemical inhibitors in cell signaling studies have been described to be toxic for cells at certain concentrations, also depending on the length of treatment or incubation times. To test if any of the inhibitors used in this work were toxic for the NR8383 macrophages at the indicated times and concentrations we performed cell viability assays (see *Materials and Methods*). We observed that none of the pharmacological inhibitors used in our studies caused any significant change on cell viability (Figure 11).

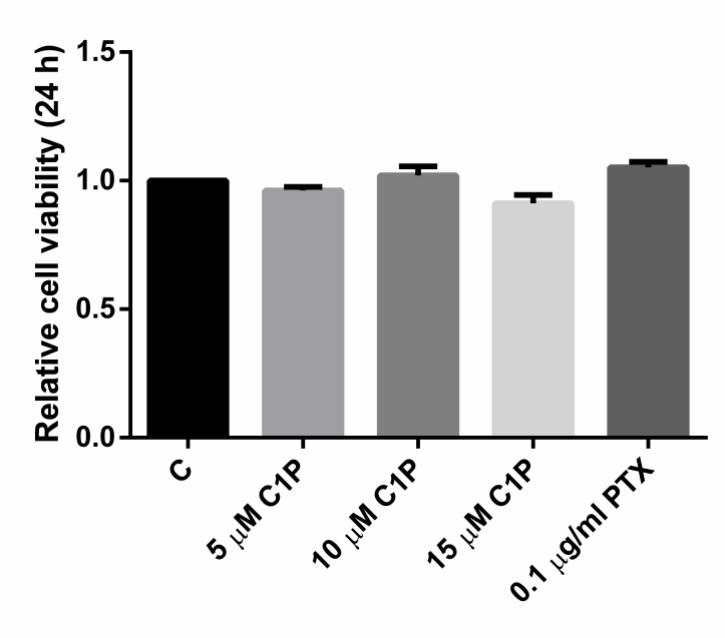

Figure 11. Cell viability after treatment with various chemical inhibitors in NR8383 macrophages. NR8383 cells were seeded in 96-well plates (20 x 10^3 cells/well) in serum-free Ham's F12K. After 2 hours of incubation, chemical inhibitors at the indicated concentrations were added and cell viability was measured after 24 hours of incubation. Cell viability was determined using the MTS-formazan assay as indicated in *Materials and Methods*. Results are the mean ± SEM of 3-4 independent experiments performed in triplicate.

3. Discussion

Alveolar macrophages are the most abundant innate immune cells in the distal lung, located on the luminal surface of the alveolar space. These cells are the first to encounter incoming pathogens and pollutants, so they orchestrate the initiation and

resolution of the immune response in the lungs [7]. Because of that, alveolar macrophages are built to respond rapidly to migratory stimuli. On this line, in this thesis we first observed that NR8383 alveolar macrophage cell line migrate spontaneously. Moreover, we demonstrated that protein kinase B (PKB/Akt), extracellular signal-regulated kinase (ERK1-2), PAK1 and Paxillin, which are important proteins involved in the regulation of cell migration that are activated by specific phosphorylations [26, 27, 30-35], were rapidly phosphorylated. This finding could explain why alveolar macrophages have the capacity of migrate spontaneously.

Concerning cell migration, our group previously established that the bioactive sphingolipid C1P induces migration of different cell types, including mouse (RAW264.7 and J774A.1) and human (THP-1) monocytes/macrophages, or human pancreatic cancer cells (PANC-1 and MIA PaCa-2) [26-28]. Also, in chapter 1 of this thesis we showed that C1P enhances the migration of 3T3-L1 preadipocytes. In this chapter, nevertheless, we have demonstrated that C1P not only does not enhance alveolar macrophage migration, but rather, it inhibits it. Moreover, we have observed that C1P dephosphorylates basal phosphorylated of PKB/Akt, ERK1-2, PAK1 and Paxillin, which suggests that the inhibition of cell migration by C1P is caused by the inhibition of those cell migration signaling cascades.

The implication of C1P in the regulation of alveolar macrophage migration suggests that the bioactive sphingolipid could play a role in the regulation of inflammation and immune response in the lungs. Indeed, it has been previously described that sphingolipids, such as sphingosine 1-phosphate (S1P) and C1P, have been implicated in the regulation of immune response during infections, as well as in inflammatory disorders associated with atherosclerosis, rheumatoid arthritis, asthma, acute respiratory distress syndrome or cystic fibrosis [36-40]. Interestingly, both pro- and anti-inflammatory behaviour of exogenous C1P has been described. For instance, C1P stimulates eicosanoid biosynthesis, migration of mouse macrophages from ascites and degranulation of mast cells [27, 38, 40]. Conversely, C1P inhibits Lipopolysaccharide (LPS)-triggered production of pro-inflammatory cytokine tumor necrosis factor α (TNF-αα) in bone marrow-derived macrophages [41]. Thus, it seems that C1P has pro- or anti-inflammatory properties depending on the cell or tissue type. The fact that C1P

has an inhibitory effect on NR8383 alveolar macrophage migration suggests that it could have an anti-inflammatory behaviour in the lungs. Indeed, previous studies have shown that C1P reduced cigarette smoke-induced acute and chronic lung inflammation and development of emphysema in mice by reducing nSMase and NF-κB activity in the lungs [17] and that C1P attenuates LPS-induced acute lung injury by preventing NF-κB activation and IL-8 production in human neutrophils [42].

Regarding chronic respiratory disorders, one of the most common is silicosis, which is caused by the inhalation of crystalline silicon dioxide (SiO_2) or silica dust. Chronic inhalation of silica into the lungs leads to activation of lung macrophages and lung inflammation. In fact, previous studies have demonstrated that silica increased some macrophage activation indicators, such as inducible nitric oxide synthase (iNOS), TNF-α, arginase-1 (Arg-1) and monocyte chemoattractant protein-1 (MCP1), as well as the expression of key glycolytic enzymes hexokinase-2 (HK2), pyruvate kinase M2 (PKM2) and lactate deshydrogenase A (LDHA) in NR8383 alveolar macrophages [43]. Noteworthy, the increased glycolysis induced by silica may be a vital metabolic feature of macrophage activation, which might contribute to lung inflammation. Indeed, it was shown that silencing LDHA inhibited the high levels of iNOS, TNF-α, Arg-1 and MCP1 [43].

In this thesis we have observed that granular nanosized silica-conditioned medium enhances NR8383 alveolar macrophage migration, which is in agreement with macrophage activation and lung inflammation. Moreover, we have observed that the silica-conditioned medium phosphorylates PKB/Akt, which suggests that the PI3K/Akt cascade may be a crucial pathway implicated in silica-induced inflammation. Our results support the notion that C1P may have anti-inflammatory properties in the lung through a mechanism involving the blockade of PKB/Akt phosphorylation.

Taken together, the results presented in this chapter demonstrated that silicon dioxide (SiO_2) activates alveolar macrophages by enhancing cell migration and that C1P has an anti-inflammatory effect by inhibiting that stimulated migration. These findings could be important for understanding the molecular mechanisms that regulate biological processes of alveolar macrophages, which could be a crucial step for

developing novel therapeutic strategies to control chronic respiratory disorders, such as silicosis. The scheme shown below emphasizes the new signaling pathways involved in alveolar macrophage migration and the effects of silica-conditioned medium and C1P.

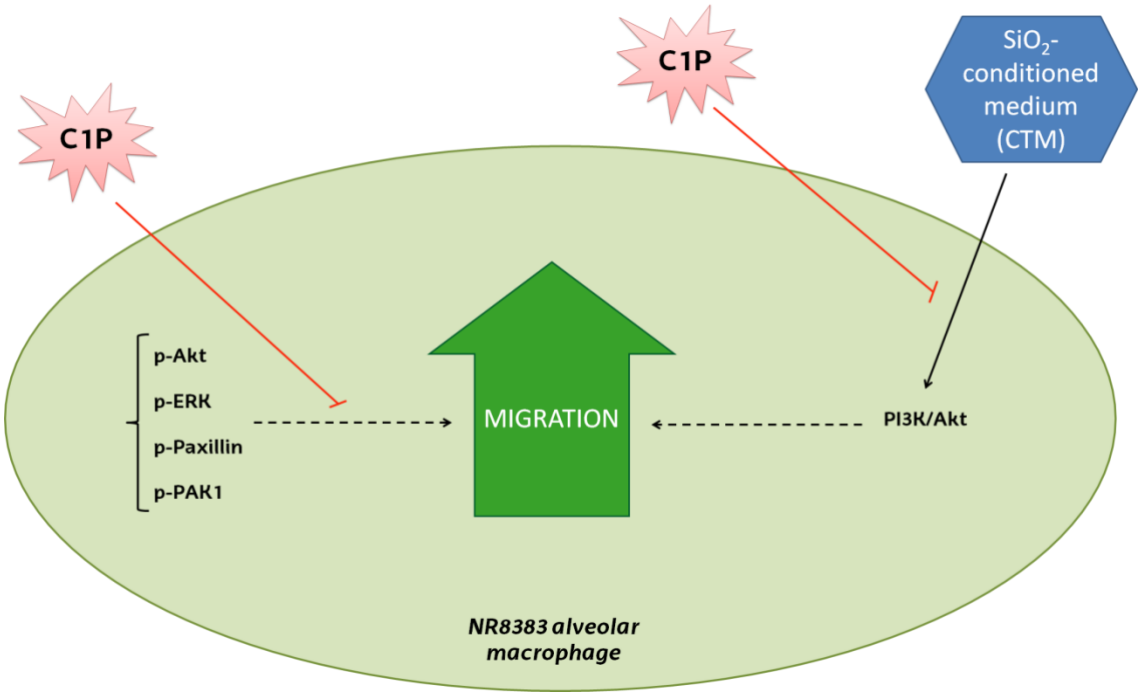

Figure 12. Working model for the implication of C1P and silica-conditioned medium in NR8383 alveolar macrophage migration.

4. References

1. Hussell T, Bell TJ. Alveolar macrophages: plasticity in a tissue-specific context. Nat Rev Immunol. 2014; 14(2): 81-93.
2. Misharin AV, Scott Budinger GR, Perlman H. The lung macrophage: a Jack of all trades. Am J Respir Crit Care Med. 2011; 184(5): 497-8.
3. Tan SYS, Krasnow MA. Developmental origin of lung macrophage diversity. Development. 2016; 143(8): 1318-27.
4. Schulz C, Gomez Perdiguero E, Chorro L, Szabo-Rogers H, Cagnard N, Kierdorf K, et al. A lineage of myeloid cells independent of Myb and hematopoietic stem cells. Science. 2012; 336(6077): 86-90.
5. Hashimoto D, Chow A, Noizat C, Teo P, Beasley MB, Leboeuf M, et al. Tissue-resident macrophages self-maintain locally throughout adult life with minimal contribution from circulating monocytes. Immunity. 2013; 38(4): 792-804.
6. Guilliams M, De Kleer I, Henri S, Post S, Vanhoutte L, De Prijck S, et al. Alveolar macrophages develop from fetal monocytes that differentiate into long-lived cells in the first week of life via GM-CSF. J Exp Med. 2013; 210(10): 1977-92.
7. Joshi N, Walter JM, Misharin AV. Alveolar macrophages. Cell Immunol. 2018; 330: 86-90.
8. Viola A, Munari F, Sánchez-Rodríguez R, Scolaro T, Castegna A. The metabolic signature of macrophage responses. Front Immunol. 2019; 10: 1462.

9. Xue J, Schmidt SV, Sander J, Draffehn A, Krebs W, Quester I, et al. Transcriptome-based network analysis reveals a spectrum model of human macrophage activation. Immunity. 2014; 40(2): 274-88.
10. Mosser DM, Edwards JP. Exploring the full spectrum of macrophage activation. Nat Rev Immunol. 2008; 8(12): 958-69.
11. Duffield JS, Lupher M, Thannickal VJ, Wynn TA. Host responses in tissue repair and fibrosis. Annu Rev Pathol. 2013; 8(1): 241-76.
12. Wynn TA, Vannella KM. Macrophages in tissue repair, regeneration, and fibrosis. Immunity. 2016; 44(3): 450-62.
13. Helmke RJ, German VF, Mangos JA. A continuous alveolar macrophage cell line: comparisons with freshly derived alveolar macrophages. In Vitro Cell Dev Biol. 1989; 25(1): 44-8.
14. Yiangou Y, Facer P, Durrenberger P, Chessell IP, Naylor A, Bountra C, et al. COX-2, CB2 and P2X7-immunoreactivities are increased in activated microglial cells/macrophages of multiple sclerosis and amyotrophic lateral sclerosis spinal cord. BMC Neurol. 2006; 6(1): 12.
15. Raherison C, Girodet P-O. Epidemiology of COPD. Eur Respir Rev. 2009; 18(114): 213-21.
16. Vestbo J, Hurd SS, Agustí AG, Jones PW, Vogelmeier C, Anzueto A, et al. Global strategy for the diagnosis, management, and prevention of chronic obstructive pulmonary disease: GOLD executive summary. Am J Respir Crit Care Med. 2013; 187(4): 347-65.
17. Baudiß K, Ayata CK, Lazar Z, Cicko S, Beckert J, Meyer A, et al. Ceramide-1-phosphate inhibits cigarette smoke-induced airway inflammation. Eur Respir J. 2015; 45(6): 1669-80.
18. Yang P, Song R, Li N, Sun K, Shi F, Liu H, et al. Silica dust exposure induces autophagy in alveolar macrophages through switching Beclin1 affinity from Bcl-2 to PIK3C3. Environ Toxicol. 2020; 35(7): 758-67.
19. Knight D, Ehrlich R, Fielding K, Jeffery H, Grant A, Churchyard G. Trends in silicosis prevalence and the healthy worker effect among gold miners in South Africa: a prevalence study with follow up of employment status. BMC Public Health. 2015; 15(1): 1258.

20. Jindal SK. Silicosis in India: Past and present. Curr Opin Pulm Med. 2013; 19(2): 163-8.
21. Hoy RF, Chambers DC. Silica-related diseases in the modern world. Allergy. 2020; 75(11): 2805-17.
22. Condeelis J, Pollard JW. Macrophages: obligate partners for tumor cell migration, invasion, and metastasis. Cell. 2006; 124(2): 263-6.
23. Friedl P, Weigelin B. Interstitial leukocyte migration and immune function. Nat Immunol. 2008; 9(9): 960-9.
24. Wynn TA, Chawla A, Pollard JW. Macrophage biology in development, homeostasis and disease. Nature. 2013; 496(7446): 445-55.
25. Beltman JB, Marée AFM, de Boer RJ. Analysing immune cell migration. Nat Rev Immunol. 2009; 9(11): 789-98.
26. Granado MH, Gangoiti P, Ouro A, Arana L, González M, Trueba M, et al. Ceramide 1-phosphate (C1P) promotes cell migration Involvement of a specific C1P receptor. Cell Signal. 2009; 21(3): 405-12.
27. Arana L, Ordoñez M, Ouro A, Rivera I-G, Gangoiti P, Trueba M, et al. Ceramide 1-phosphate induces macrophage chemoattractant protein-1 release: involvement in ceramide 1-phosphate-stimulated cell migration. Am J Physiol Endocrinol Metab. 2013; 304(11): E1213-26.
28. Rivera I-G, Ordoñez M, Presa N, Gangoiti P, Gomez-Larrauri A, Trueba M, et al. Ceramide 1-phosphate regulates cell migration and invasion of human pancreatic cancer cells. Biochem Pharmacol. 2016; 102: 107-19.
29. Cheng C-I, Chen P-H, Lin Y-C, Kao Y-H. High glucose activates Raw264.7 macrophages through RhoA kinase-mediated signaling pathway. Cell Signal. 2015; 27(2): 283-92.
30. Chalfant CE, Spiegel S. Sphingosine 1-phosphate and ceramide 1-phosphate: expanding roles in cell signaling. J Cell Sci. 2005; 118(Pt 20): 4605-12.
31. Gomez-Muñoz A, Gangoiti P, Arana L, Ouro A, Rivera I-G, Ordoñez M, et al. New insights on the role of ceramide 1-phosphate in inflammation. Biochim Biophys Acta. 2013; 1831(6): 1060-6.

32. López-Colomé AM, Lee-Rivera I, Benavides-Hidalgo R, López E. Paxillin: a crossroad in pathological cell migration. J Hematol Oncol. 2017; 10(1): 50.
33. Gagliardi PA, di Blasio L, Primo L. PDK1: A signaling hub for cell migration and tumor invasion. Biochim Biophys Acta. 2015; 1856(2): 178-88.
34. Matsuyama R, Okuzaki D, Okada M, Oneyama C. MicroRNA-27b suppresses tumor progression by regulating ARFGEF1 and focal adhesion signaling. Cancer Sci. 2016; 107(1): 28-35.
35. Huang C, Jacobson K, Schaller MD. MAP kinases and cell migration. J Cell Sci. 2004; 117(Pt 20): 4619-28.
36. Idzko M, Hammad H, van Nimwegen M, Kool M, Müller T, Soullié T, et al. Local application of FTY720 to the lung abrogates experimental asthma by altering dendritic cell function. J Clin Invest. 2006; 116(11): 2935-44.
37. Teichgräber V, Ulrich M, Endlich N, Riethmüller J, Wilker B, De Oliveira-Munding CC, et al. Ceramide accumulation mediates inflammation, cell death and infection susceptibility in cystic fibrosis. Nat Med. 2008; 14(4): 382-91.
38. Lamour NF, Chalfant CE. Ceramide-1-phosphate: the “missing” link in eicosanoid biosynthesis and inflammation. Mol Interv. 2005; 5(6): 358-67.
39. Matsusaka T, Fujikawa K, Nishio Y, Mukaida N, Matsushima K, Kishimoto T, et al. Transcription factors NF-IL6 and NF-kappa B synergistically activate transcription of the inflammatory cytokines, interleukin 6 and interleukin 8. Proc Natl Acad Sci U S A. 1993; 90(21): 10193-7.
40. Nixon GF. Sphingolipids in inflammation: pathological implications and potential therapeutic targets: Sphingolipids and inflammation. Br J Pharmacol. 2009; 158(4): 982-93.
41. Lamour NF, Wijesinghe DS, Mietla JA, Ward KE, Stahelin RV, Chalfant CE. Ceramide kinase regulates the production of tumor necrosis factor α (TNFα) via inhibition of TNFα-converting enzyme. J Biol Chem. 2011; 286(50): 42808-17.
42. Baudiß K, de Paula Vieira R, Cicko S, Ayata K, Hossfeld M, Ehrat N, et al. C1P attenuates lipopolysaccharide-induced acute lung injury by preventing NF-κB activation in neutrophils. J Immunol. 2016; 196(5): 2319-26.

43. Mao N, Yang H, Yin J, Li Y, Jin F, Li T, et al. Glycolytic reprogramming in silica-induced lung macrophages and silicosis reversed by Ac-SDKP treatment. Int J Mol Sci. 2021; 22(18): 10063.

Conclusions

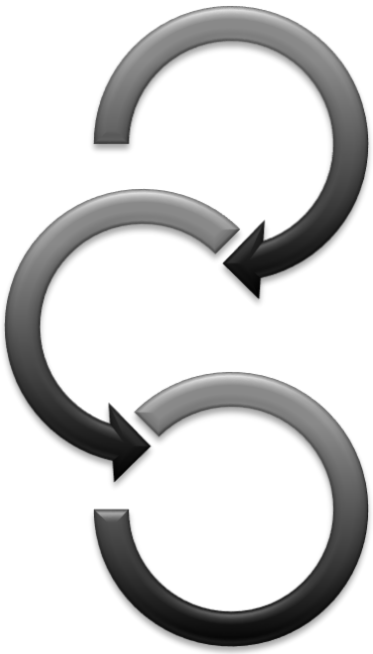

Conclusions

From the results obtained in this thesis, the following conclusions may be drawn.

1. C1P promotes cell survival and proliferation in 3T3-L1 preadipocytes. The mechanisms implicated in these biological actions involve activation of the PI3K/Akt, MEK/ERK1-2 and JAK/STAT3 pathways.

2. C1P enhances preadipocyte migration through activation of the PI3K/Akt, MEK/ERK1-2 and JAK/STAT3 pathways, likely in a receptor dependent manner, in which a GPCR may mediate stimulation of PI3K/Akt and MEK/ERK1-2, and a possible tyrosine kinase receptor might be implicated in the activation of JAK/STAT3 pathway.

3. C1P inhibits alveolar macrophage migration. The action may be caused by the blockade of PKB/Akt, ERK1-2, PAK1 and Paxillin activities, which are important proteins involved in the regulation of cell migration.

4. Granular nanosized silica (SiO_2)-conditioned medium enhances alveolar macrophage migration through activation of the PI3K/Akt signaling cascade. C1P inhibits this action by blocking PKB/Akt phosphorylation, thereby supporting the notion that this bioactive sphingolipid may have anti-inflammatory properties in lung cells.

Appendix

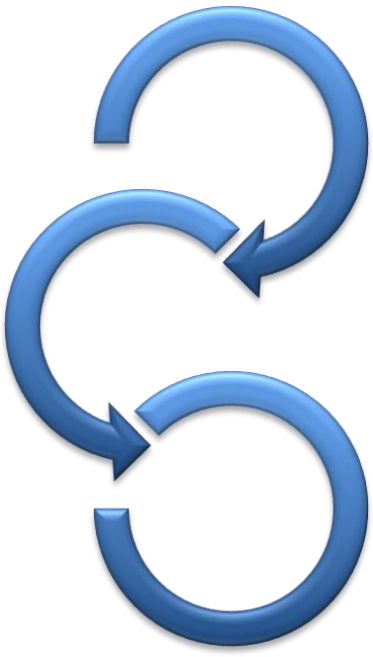

Scientific contributions

1

Regulation of adipogenesis by ceramide 1-phosphate.

Marta Ordoñez, Natalia Presa, **Asier Dominguez-Herrera**, Miguel Trueba, Antonio Gomez-Muñoz.

Exp Cell Res. 2018; 372(2): 150-7

Abstract

We showed previously that ceramide kinase (CerK) expression increases during adipogenesis pointing to a relevant role of intracellular C1P in this process. In the present work we demonstrate that administration of exogenous C1P inhibits the differentiation of 3T3-L1 pre-adipocytes into mature adipocytes through a mechanism involving activation of extracellularly regulated kinases (ERK) 1-2. Exogenous C1P reduced the accumulation of lipid droplets and the content of triacylglycerol in these cells, and potently inhibited the expression of the early and late adipogenic markers C/EBPβ and PPARγ, respectively. C1P also reduced the secretion of leptin, which is a crucial regulator of energy balance and appetite in the organism, and is considered to be a late marker of adipogenesis. Interestingly, all of these C1P actions were reversed by pertussis toxin, suggesting the intervention of a Gi protein-coupled receptor previously identified for C1P, in this process. Also, exogenous C1P significantly reduced CerK activity. Altogether, the data presented in this work suggest that exogenous C1P may balance adipogenesis, and that targeting CerK may be a novel way for potential applications in the treatment of obesity or other inflammation-associated diseases.

2

Novel signaling aspects of ceramide 1-phosphate.

Natalia Presa, Ana Gomez-Larrauri, **Asier Dominguez-Herrera**, Miguel Trueba, Antonio Gomez-Muñoz.

Biochim Biophys Acta Mol Cell Biol Lipids. 2020; 1865(4): 158630

Abstract

The bioactive sphingolipid ceramide 1-phosphate (C1P) regulates key physiologic cell functions and is implicated in a number of metabolic alterations and pathological processes. Initial studies using different types of fibroblasts and monocytes/macrophages revealed that C1P was mitogenic and that it promoted cell survival through inhibition of apoptosis. Subsequent studies implicated C1P in inflammatory responses with a specific role as pro-inflammatory agent. Specifically, C1P potently stimulated cytosolic phospholipase A2 (cPLA2) resulting in elevation of arachidonic acid and pro-inflammatory eicosanoid levels. However, increasing experimental evidence suggests that C1P can also exert anti-inflammatory actions in some cell types and tissues. Specifically, it has been demonstrated that C1P inhibits the release of pro-inflammatory cytokines and blocks activation of the pro-inflammatory transcription factor NF-κB in some cell types. Moreover, C1P was shown to increase the release of anti-inflammatory interleukin-10 in macrophages, and to overcome airway inflammation and reduce lung emphysema in vivo. Noteworthy, C1P stimulated cell migration, an action that is associated with diverse physiological cell functions, as well as with inflammatory responses and tumor dissemination. More recently, ceramide kinase (CerK), the enzyme that produces C1P in mammalian cells, has been shown to be upregulated during differentiation of pre-adipocytes into mature adipocytes, and that exogenous C1P, acting through a putative Gi protein-coupled receptor, negatively regulates adipogenesis. Although the latter actions seem to be contradictory, it is plausible that exogenous C1P may balance the adipogenic effects of intracellularly generated (CerK-derived) C1P in adipose tissue. The present review highlights novel signaling aspects of C1P and its impact in the regulation of cell growth and survival, inflammation and tumor dissemination.

3

Implication of phosphatidylethanolamine N-methyltransferase in adipocyte differentiation.

Natalia Presa, **Asier Dominguez-Herrera**, Jelske N van der Veen, Dennis E Vance, Antonio Gómez-Muñoz.

Biophys Acta Mol Basis Dis. 2020; 1866(10): 165853

Abstract

Phosphatidylethanolamine N-methyltransferase (PEMT) is a small integral membrane protein that converts phosphatidylethanolamine (PE) into phosphatidylcholine (PC). It has been previously reported that, unexpectedly, PEMT deficiency protected from high-fat diet (HFD)-induced obesity and insulin resistance, pointing to a possible role of this enzyme in the regulation of adipose cell metabolism. Using mouse 3T3-L1 preadipocytes as a biological system, we demonstrate that PEMT expression is strongly increased during the differentiation of preadipocytes into mature adipose cells. Knockdown of PEMT reduced the expression of early and late adipogenic markers, inhibited lipid droplet formation, reduced triacylglycerol content and decreased the levels of leptin release from the adipocytes, suggesting that PEMT is a novel and relevant regulator of adipogenesis. Investigation into the mechanisms whereby PEMT regulates adipocyte differentiation revealed that extracellularly regulated kinases (ERK1/2) and AKT are essential factors in this process. Specifically, the activities of ERK1/2 and AKT, which are decreased during adipocyte differentiation, were elevated upon Pemt knockdown. Moreover, treatment of cells with exogenous ceramide 1-phosphate (C1P), which we reported to be a negative regulator of adipogenesis, decreased PEMT expression, suggesting that PEMT is also a relevant factor in the anti-adipogenic action of C1P. Altogether, the data presented here identify PEMT as a novel regulator of adipogenesis and a mediator of the anti-adipogenic action of C1P.

4

Role of bioactive sphingolipids in physiology and pathology.

Ana Gomez-Larrauri, Natalia Presa, **Asier Dominguez-Herrera**, Alberto Ouro, Miguel Trueba, Antonio Gomez-Muñoz.

Essays Biochem. 2020; 64(3): 579–89

Abstract

Sphingolipids are a class of complex lipids containing a backbone of sphingoid bases, namely the organic aliphatic amino alcohol sphingosine (Sph), that are essential constituents of eukaryotic cells. They were first described as major components of cell membrane architecture, but it is now well established that some sphingolipids are bioactive and can regulate key biological functions. These include cell growth and survival, cell differentiation, angiogenesis, autophagy, cell migration, or organogenesis. Furthermore, some bioactive sphingolipids are implicated in pathological processes including inflammation-associated illnesses such as atherosclerosis, rheumatoid arthritis, inflammatory bowel disease (namely Crohn's disease and ulcerative colitis), type II diabetes, obesity, and cancer. A major sphingolipid metabolite is ceramide, which is the core of sphingolipid metabolism and can act as second messenger, especially when it is produced at the plasma membrane of cells. Ceramides promote cell cycle arrest and apoptosis. However, ceramide 1-phosphate (C1P), the product of ceramide kinase (CerK), and Sph 1-phosphate (S1P), which is generated by the action of Sph kinases (SphK), stimulate cell proliferation and inhibit apoptosis. Recently, C1P has been implicated in the spontaneous migration of cells from some types of cancer, and can enhance cell migration/invasion of malignant cells through interaction with a Gi protein-coupled receptor. In addition, CerK and SphK are implicated in inflammatory responses, some of which are associated with cancer progression and metastasis. Hence, targeting these sphingolipid kinases to inhibit C1P or S1P production, or blockade of their receptors might contribute to the development of novel therapeutic strategies to reduce metabolic alterations and disease.

5

Phosphatidic Acid Stimulates Myoblast Proliferation through Interaction with LPA1 and LPA2 Receptors.

Ana Gomez-Larrauri, Patricia Gangoiti, Natalia Presa, **Asier Dominguez-Herrera**, Chiara Donati, Paola Bruni, Miguel Trueba, Antonio Gomez-Muñoz, Alberto Ouro.

Int J Mol Sci. 2021; 22(3): 1452

Abstract

Phosphatidic acid (PA) is a bioactive phospholipid capable of regulating key biological functions, including neutrophil respiratory burst, chemotaxis, or cell growth and differentiation. However, the mechanisms whereby PA exerts these actions are not completely understood. In this work, we show that PA stimulates myoblast proliferation, as determined by measuring the incorporation of [3H]thymidine into DNA and by staining the cells with crystal violet. PA induced the rapid phosphorylation of Akt and ERK1/2, and pretreatment of the cells with specific small interferin RNA (siRNA) to silence the genes encoding these kinases, or with selective pharmacologic inhibitors, blocked PA-stimulated myoblast proliferation. The mitogenic effects of PA were abolished by the preincubation of the myoblasts with pertussis toxin, a Gi protein inhibitor, suggesting the implication of Gi protein-coupled receptors in this action. Although some of the effects of PA have been associated with its possible conversion to lysoPA (LPA), treatment of the myoblasts with PA for up to 60 min did not produce any significant amount of LPA in these cells. Of interest, pharmacological blockade of the LPA receptors 1 and 2, or specific siRNA to silence the genes encoding these receptors, abolished PA-stimulated myoblast proliferation. Moreover, PA was able to compete with LPA for binding to LPA receptors, suggesting that PA can act as a ligand of LPA receptors. It can be concluded that PA stimulates myoblast proliferation through interaction with LPA1 and LPA2 receptors and the subsequent activation of the PI3K/Akt and MEK/ERK1-2 pathways, independently of LPA formation.

6

Identification of Androgen Receptor Metabolic Correlome Reveals the Repression of Ceramide Kinase by Androgens.

Laura Camacho, Amaia Zabala-Letona, Ana R Cortazar, Ianire Astobiza, **Asier Dominguez-Herrera**, Amaia Ercilla, Jana Crespo, Cristina Viera, Sonia Fernández-Ruiz , Ainara Martinez-Gonzalez, Veronica Torrano, Natalia Martín-Martín, Antonio Gomez-Muñoz, Arkaitz Carracedo.

Cancers. 2021; 13(17): 4307

Abstract

Prostate cancer (PCa) is one of the most prevalent cancers in men. Androgen receptor signaling plays a major role in this disease, and androgen deprivation therapy is a common therapeutic strategy in recurrent disease. Sphingolipid metabolism plays a central role in cell death, survival, and therapy resistance in cancer. Ceramide kinase (CERK) catalyzes the phosphorylation of ceramide to ceramide 1-phosphate, which regulates various cellular functions including cell growth and migration. Here we show that activated androgen receptor (AR) is a repressor of CERK expression. We undertook a bioinformatics strategy using PCa transcriptomics datasets to ascertain the metabolic alterations associated with AR activity. CERK was among the most prominent negatively correlated genes in our analysis. Interestingly, we demonstrated through various experimental approaches that activated AR reduces the mRNA expression of CERK: (i) expression of CERK is predominant in cell lines with low or negative AR activity; (ii) AR agonist and antagonist repress and induce CERK mRNA expression, respectively; (iii) orchiectomy in wildtype mice or mice with PCa (harboring prostate-specific Pten deletion) results in elevated Cerk mRNA levels in prostate tissue. Mechanistically, we found that AR represses CERK through interaction with its regulatory elements and that the transcriptional repressor EZH2 contributes to this process. In summary, we identify a repressive mode of AR that influences the expression of CERK in PCa.